Florentin Smarandache

INFINITESIMAL PUNCTURES 5

Infinitesimally Punctured Waves

A Unified Discrete-Continuum Framework for All Physical Wave Phenomena

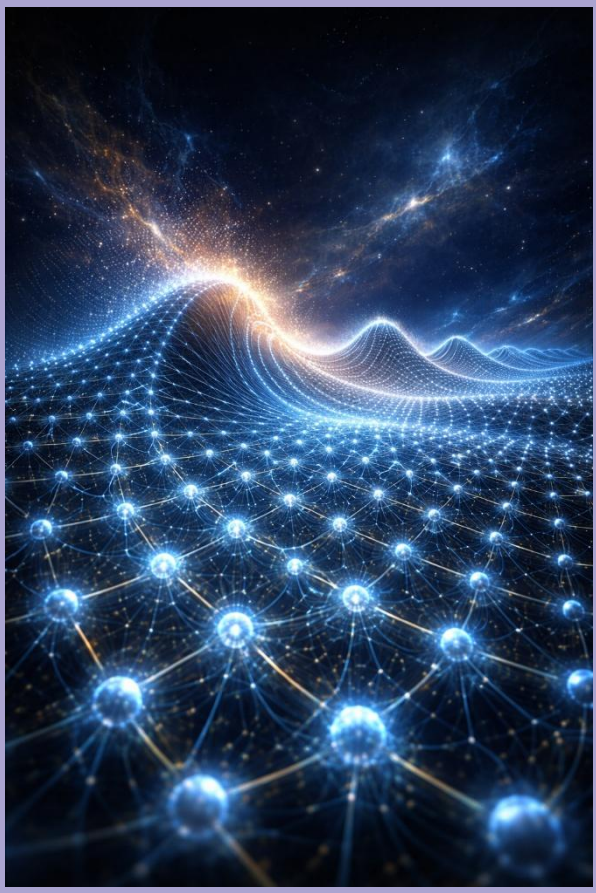

NSIA
NEUTROSOPHIC SCIENCE
INTERNATIONAL ASSOCIATION
PUBLISHING HOUSE

How can all physical waves be derived from a single discrete lattice of infinitesimal punctures?

FLORENTIN SMARANDACHE

INFINITESIMAL PUNCTURES 5

Infinitesimally Punctured Waves

A Unified Discrete-Continuum Framework for All Physical Wave Phenomena

The Infinitesimally Punctured Wave (IPW), Infinitesimally Punctured Surface (IPSu), Infinitesimally Punctured Space (IPSp), Infinitesimally Punctured Manifold (IPM), and in general Infinitesimally Punctured Quantum Physics (IPQP) were introduced and developed by Florentin Smarandache in 2019 and respectively in 2025-2026.

Neutrosophic Science International Association (NSIA)
Publishing House
https://fs.unm.edu/NSIA/

Division of Mathematics and Sciences
University of New Mexico
705 Gurley Ave., Gallup Campus
NM 87301, United States of America

University of Guayaquil
Av. Kennedy and Av. Delta
"Dr. Salvador Allende" University Campus
Guayaquil 090514, Ecuador

ISBN: 978-1-59973-870-3

Peer-Reviewers

Maikel Leyva-Vázquez
Universidad de Guayaquil, Guayas, ECUADOR
maikel.leyvav@ug.edu.ec

Giorgio Nordo
MIFT - Department of Mathematical and Computer Science,
Physical Sciences and Earth Sciences,
Messina University, ITALY
giorgio.nordo@unime.it

Surapati Pramanik
Department of Mathematics, Nandalal Ghosh B T College, INDIA
drspramanik@isns.org.in

RMM Pradeep
Faculty of Computing, Kothelawala Defence University, Rathmalana, SRI LANKA
pradeep@kdu.ac.lk

Suriana Alia
Universiti Teknologi MARA (UiTM) Kelantan, Machang, Kelantan, MALAYSIA
suria588@kelantan.uitm.edu.my

FLORENTIN SMARANDACHE

INFINITESIMAL PUNCTURES 5

INFINITESIMALLY PUNCTURED WAVES

A Unified Discrete-Continuum Framework for All Physical Wave Phenomena

Neutrosophic Science International Association (NSIA)
Publishing House
Gallup - Guayaquil
United States of America – Ecuador
2026

Acknowledgments

I wish to express my sincere gratitude to **Maikel Leyva-Vázquez** and **Victor Christianto** for their insightful feedback and thought-provoking discussions, which were instrumental in refining the focus of this research.

The development of this book was significantly enhanced by an integrated suite of advanced AI technologies, each playing a role in the manuscript's evolution:

- **Lumo AI**: Facilitated multilingual drafting and the cohesive integration of intricate mathematical concepts.
- **SciSpace**: Enabled streamlined literature searches and precise citation handling.
- **Perplexity**: Provided rapid access to foundational definitions and pertinent research findings.
- **Elicit**: Assisted in the structured formulation of research inquiries and the selection of appropriate datasets.
- **Claude 3.5 Sonnet (Anthropic)**: Supported the detailed drafting of mathematical proofs and the optimization of logical structures.
- **Wolfram Alpha**: Utilized for rigorous symbolic computation, the validation of algebraic formulas, and the creation of technical examples.
- **ChatGPT 5.2**: Provided essential support for iterative revisions, linguistic polishing, and bibliographic formatting.
- **Gemini**: Instrumental in verifying interdisciplinary terminology and refining descriptive captions for figures.
- **Figurelabs**: Employed to design and generate high-quality scientific diagrams and illustrations.

By combining these innovative platforms, I was able to conduct comprehensive literature reviews, ensure the mathematical integrity of the work through rigorous validation, and achieve a clear, multilingual narrative that defines the final character of this volume.

Florentin Smarandache, PhD, PostDocs
Emeritus Professor
University of New Mexico
Mathematics, Physics, and Natural Science Division
705 Gurley Ave., Gallup, NM 87301, USA
https://fs.unm.edu/
smarand@unm.edu

TABLE OF CONTENTS

The Infinitesimal Puncture Program 10
Terminology 12
Foreword to *Infinitesimally Punctured Waves* 16

Chapter 1 Introduction to Infinitesimally Punctured Waves 19
1.1 Why a New Wave Paradigm? 19
1.2 Historical Roots 20
1.3 What Is a "Puncture"? 21
1.4 From Discrete to Continuous – A Sketch 21
1.5 What Does "Infinitesimally" Mean Here? 22
1.6 Scope and Structure 23
1.7 A First Thought Experiment 23

Chapter 2 Generic Discrete Formalism for Infinitesimally Punctured Waves 25
2.1 What We Want to Achieve? 25
2.2 Lattice Geometry 25
2.3 State Variables and Mass-Energy Assignment 26
2.4 Nearest-Neighbour Coupling 26
2.4.1 Tensorial Coupling 27
2.5 Continuum Limit 27
2.6 Higher-Order Neighbours and Dispersion 28
2.7 Non-Linear Springs and Shock Regularisation 28
2.8 Boundary Conditions in the Punctured Picture 29
2.9 Modeling Measurement as Puncture Selection 29
2.10 Summary of the Generic Formalism 30

Chapter 3 Infinitesimally Punctured Acoustic and Surface Gravity Waves 31
3.1 Why Start Here? 31
3.2 Physical Quantities 31
3.3 Discrete Acoustic Wave Model 32
3.3.1 Lattice and Mass Assignment 32
3.3.2 Equation of Motion (nearest-neighbour coupling) 32
3.3.3 Continuum Limit 32
3.3.4 Optional Viscous Damping 32
3.4 Discrete Surface-Gravity Wave Model 33
3.4.1 Lattice and Effective Mass 33
3.4.2 Restoring Forces 33
3.4.3 Continuum Limit 33
3.4.4 Finite-Depth Modification 34
3.5 Higher-Neighbour Coupling & Dispersive Corrections 34
3.6 Boundary Conditions in the Punctured Picture 34
3.7 Measurement as Puncture Selection 35
3.8 Summary 35

Chapter 4 Infinitesimally Punctured Elastic Body Waves (Longitudinal & Shear) .. 37
4.1 Why Elastic Waves Matter? 37
4.2 Physical Ingredients 37
4.3 Discrete Lattice Construction 38
4.4 Continuum Limit – Recovery of Navier–Cauchy Equations 38
4.5 Decomposition Into P- and S-Modes 39
4.6 Anisotropic Lattices 40
4.7 Mode Conversion at Interfaces 40
4.8 Higher-Neighbour Coupling and Dispersive Effects 41
4.9 Damping and Viscoelastic Extensions 41
4.10 Measurement as Puncture Selection (Elastic Case) 42
4.11 Summary Table 42
4.12 Looking Ahead 43

Chapter 5 Infinitesimally Punctured Seismic and Geophysical Waves 44
5.1 Why Seismic Waves Are a Crucial Test-Bed? 44
5.2 Discrete Representation of a Heterogeneous Medium 44
5.3 Continuum Limit – Heterogeneous Navier–Cauchy Equation 45
5.4 Scattering from Random Property Fluctuations 46
5.4.1 Born Approximation (Weak Scattering) 46
5.4.2 Multiple Scattering and Diffusion 46
5.5 Emergent Attenuation – The Q-Factor 47
5.6 Surface-Wave Generation (Rayleigh & Love) 47
5.7 Numerical Implementation Tips 48
5.8 Connecting Back to Earlier Chapters 48
5.9 Experimental / Observational Signatures of the Puncture Scale 49
5.10 Summary 49

Chapter 6 Infinitesimally Punctured Shock and Non Linear Waves 50
6. Why Shocks Require a Discrete Substrate? 50
6.2 Scalar Conservation Law on a Puncture Lattice 50
6.3 From Discrete to Continuum – Burgers-type Equation 51
6.4 Exact Stationary Shock Profile 51
6.5 Extension to Vector Elastic Shocks 52
6.6 Shock Regularisation in Heterogeneous Media 53
6.7 Numerical Illustration (Pseudo-code) 53
6.8 Recovering Classical Rankine–Hugoniot Conditions 55
6.9 Key Insights 56
6.10 Outlook 57

Chapter 7 Infinitesimally Punctured Electromagnetic Waves 58
7.1 Why Electromagnetism Fits the IPW Scheme? 58
7.2 Discrete Variables and Lattice Geometry 58
7.3 Discrete Curl Operators 59
7.4 Discrete Maxwell Equations 59

7.5 Material Media – Spatially Varying ε and μ 60
7.6 Metamaterials – Engineered Puncture Parameters 60
7.7 Inclusion of Sources and Charges 61
7.8 Numerical Implementation – Staggered-Grid Leapfrog Scheme 61
7.9 Connection to Earlier Chapters 63
7.10 Key Takeaways 63

Chapter 8 Infinitesimally Punctured Gravitational Waves (Linearised General Relativity) 64
8.1 Why Gravitational Radiation Fits the IPW Scheme? 64
8.2 Discrete Spacetime Lattice 64
8.3 Regge-Calculus-Inspired Coupling 65
8.4 Continuum Limit – Linearised Einstein Wave Equation 65
8.5 Polarisation Content on the Lattice 66
8.6 Planck-Scale Spacing Effects 66
8.7 Coupling to Matter Sources 67
8.8 Numerical Illustration (Pseudo-code) 67
8.9 Summary of the IPW Gravitational-Wave Construction 69

Chapter 9 Infinitesimally Punctured Quantum Mechanical Waves 70
9.1 Why a Punctured Description of the Wavefunction? 70
9.2 Discrete Variables and Lattice Geometry 70
9.3 Tight-Binding Hamiltonian and Discrete Schrödinger Equation 71
9.4 Potential Landscapes and Disorder 72
9.5 Non-Linear Extensions – Self-Interaction 72
9.6 Measurement as Puncture Selection 73
9.7 Entanglement Between Separate Puncture Networks 73
9.8 Connections to Earlier Chapters 74
9.9 Practical Numerical Scheme (Leapfrog for Complex Amplitudes) 74
9.10 Key Take-aways 76

Chapter 10 Cross Wave Connections 78
10.1 Purpose of the Comparative View 78
10.2 Unified Puncture Taxonomy 78
10.3 General Form of the Discrete Evolution Equation 79
10.4 Symmetry Principles Governing the Couplings 80
10.5 Unified Dispersion Relation 80
10.6 Common Physical Themes 82
10.7 Unified Perspective on Non-Linearities 82
10.8 Implications for Modeling and Design 84
10.9 Summary– Cross-Wave Mapping 84
10.10 Concluding Remarks 87

Chapter 11 Experimental Signatures & Outlook 88
11.1 What Would a Finite Puncture Scale Look Like? 88
11.2 Modified Dispersion at High Frequencies 89
11.3 Shock-Width Regularisation 89
11.4 Potential Tests in Existing High-Precision Domains 90
11.5 Outlook – From Laboratory Analogues to Fundamental Physics 91
11.6 Key Take-aways 94
11.7 Final Perspective 94

Conclusion 96
Open Problems and Research Directions 100
Selected Bibliography 104
Index Terms 108
Appendix A Analytical Background for Infinitesimally Punctured Waves 110
Appendix B Exercises & Thought Experiments 115

THE INFINITESIMAL PUNCTURE PROGRAM

Modern physics repeatedly encounters singularities and ultraviolet divergences—whether in quantum field theory, black-hole interiors, or the short-distance behaviour of classical wave equations. In most textbooks these pathologies are treated as technical nuisances: regulators are introduced, renormalisation schemes are applied, or the underlying dynamics are altered in ever more elaborate ways.

The **Infinitesimal Puncture Programme** asks a different question. Perhaps the problem does not lie chiefly in the dynamical laws themselves, but in the *geometric ontology* on which those laws are built. Conventional theory assumes a perfectly smooth spacetime manifold populated by point-like particles or fields that are inserted *into* that manifold. Singularities then appear whenever the idealised point-source description clashes with the continuity of the background.

Our proposal inverts this picture. Matter, charge, and even quantum amplitudes are taken to be **intrinsic geometric defects**—measure-zero *punctures*—woven into the fabric of spacetime. These punctures carry the physical attributes that we normally attribute to external sources, while the surrounding manifold remains a well-behaved geometric entity. In this view spacetime is no longer a passive stage; it is a structured medium whose internal architecture encodes everything we call "matter."

The series develops this idea step by step:

Volume	Title	Core Contribution
1	*Infinitesimally Punctured Geometry*	Introduces the mathematics of punctured manifolds, measure-theoretic treatment of defects, and the extended non-standard analysis tools needed to handle infinitesimal separations.
2	*Infinitesimally Punctured Physics*	Derives dynamical equations from a hybrid variational principle that treats punctures and the surrounding geometry on an equal footing, yielding modified field equations free of traditional UV infinities.

3	*Infinitesimally Punctured Structures*	Presents a unified structural framework capable of supporting multiple co-existing geometric regimes (e.g., smooth regions, defect-rich zones, and transitional layers) and shows how they interlock consistently.
4	*Infinitesimally Punctured Physics in Extended Nonstandard Analysis*	Explores the broader implications of punctured geometry for the foundations of mathematics, linking the programme to nonstandard analysis, hyperreal extensions, and internal set theory.
5	*Infinitesimally Punctured Waves*	Applies the puncture paradigm to every known wave phenomenon—acoustic, elastic, seismic, electromagnetic, gravitational, and quantum-mechanical—demonstrating that each continuous wave equation emerges as the dense-limit of a simple lattice of infinitesimal punctures. It also identifies the novel, testable predictions (high-frequency dispersion, shock-regularisation, puncture-selection during measurement) that arise when the puncture spacing is finite.

Together these volumes articulate a **coherent geometric paradigm** in which singularities are replaced by structure, and physical entities are re-interpreted as manifestations of spacetime's internal organization. By grounding all fields—including waves—in the same punctured-geometry language, the programme offers a single conceptual bridge across disciplines that have traditionally been treated separately. The hope is that this unified view will not only clarify longstanding puzzles (renormalisation, wave-particle duality, the nature of spacetime defects) but also inspire concrete experimental searches for the subtle signatures of an underlying infinitesimal lattice.

TERMINOLOGY

Anisotropic lattice – A discrete network whose spring (or coupling) constants depend on direction. In the IPW framework this yields direction-dependent wave speeds (e.g., different longitudinal speeds along crystallographic axes).

Band gap – A frequency interval in which wave propagation is forbidden because the lattice dispersion relation yields imaginary wave numbers. Arises from periodic modulation of puncture parameters (e.g., alternating bulk modulus).

CFL condition – The Courant–Friedrichs–Lewy stability criterion for explicit time-integration schemes on a lattice: $\Delta t \leq \frac{a}{c\sqrt{d}}$, where a is the lattice spacing, c the fastest characteristic speed, and d the spatial dimension.

Deficit angle (Regge calculus) – The angular shortfall around a hinge (2-simplex) in a simplicial spacetime lattice. In the linearised IPW model it is proportional to second derivatives of the metric perturbation and encodes curvature.

Dispersion relation – The functional relationship $\omega(\mathbf{k})$ between angular frequency and wave vector dictated by the lattice dynamics. For a homogeneous cubic lattice: $\omega^2 = \frac{2K}{M} \sum_{\alpha=1}^{d} [1 - \cos(k_\alpha a)]$.

Effective mass (quantum lattice) – The curvature of the tight-binding band near $\mathbf{k} = 0$: $m_\alpha^* = \frac{\hbar^2}{2J_\alpha a^2}$, where J_α is the hopping amplitude along direction α.

Effective medium – A continuum description that averages the microscopic puncture parameters (e.g., ε_{eff}, μ_{eff}, λ_{eff}, μ_{eff}) over many lattice cells, yielding homogenised wave speeds.

Finite-difference time-domain (FDTD) – A numerical method that advances Maxwell's (or other wave) equations on a staggered grid using the discrete curl operators introduced in the IPW formalism.

Group velocity – The derivative of the dispersion relation with respect to wave number: $v_g(\mathbf{k}) = \frac{\partial \omega}{\partial |\mathbf{k}|}$. For the lattice, $v_g = c[1 - \frac{a^2}{6} |\, \mathbf{k} \,|^2 + O(a^4)]$.

Hinge (Regge calculus) – A 2-dimensional simplex (triangle) in a 4-D simplicial complex; curvature is concentrated on hinges via deficit angles.

Infinitesimally Punctured Wave (IPW) – The central hypothesis of the book: a continuous wave field is the dense-limit of an ultra-fine lattice of infinitesimal "punctures" (point-like degrees of freedom) coupled by linear (or weakly non-linear) springs.

Lamé parameters (λ, μ) – Elastic constants governing volumetric (λ) and shear (μ) responses of a solid. In the IPW lattice they appear as spring stiffnesses for longitudinal and transverse relative displacements.

Longitudinal (P) wave – A wave in which particle motion is parallel to the propagation direction. In the IPW elastic lattice it is associated with the bulk modulus combination $\lambda + 2\mu$.

Mass density (ρ) – Physical density of a material; determines the inertial factor $M = \rho a^d$ attached to each puncture (scalar or vector).

Metric perturbation ($h_{\mu\nu}$) – Small deviation of the spacetime metric from flat Minkowski space, stored on each vertex of the Regge lattice. Its dynamics obey the linearised Einstein wave equation in the dense limit.

Non-linear spring law – Extension of the linear coupling $K\Delta\Phi$ by higher-order terms (e.g., $K_2\Delta\Phi^2$, $K_3\Delta\Phi^3$). Generates Burgers-type equations and finite shock thickness.

Phase velocity – Ratio of frequency to wave number: $v_p = \frac{\omega}{|\mathbf{k}|}$. For the lattice, $v_p = c\sqrt{1-\alpha(ka)^2}$ with α a geometry-dependent constant.

Puncture – The infinitesimal degree of freedom residing on a lattice node (or face/edge). Depending on the wave family it may be a scalar pressure, a vector displacement, an electric dipole, a magnetic dipole, a symmetric tensor, or a complex quantum amplitude.

Rankine–Hugoniot conditions – Integral conservation statements across a discontinuity (shock). In the IPW model they emerge automatically from the discrete momentum balance when a strong non-linear spring is present.

Regge action – Discrete analogue of the Einstein-Hilbert action: $S_{\text{Regge}} = \frac{1}{16\pi G}\sum_{\text{hinges}} \Theta\, A$, where Θ is the deficit angle and A the hinge area.

Shear (S) wave – A transverse elastic wave with particle motion perpendicular to propagation. Governed solely by the shear modulus μ in the IPW lattice.

Staggered (Yee) grid – Arrangement of electric-type and magnetic-type punctures on offset sub-lattices so that discrete curl operators satisfy $\nabla \cdot (\nabla \times) = 0$ exactly.

Tight-binding model – Quantum-mechanical description of particles hopping between neighbouring punctures; the lattice Hamiltonian $H = -J \sum_{\langle nm \rangle} (\chi_n^\dagger \chi_m + h.c.)$ reproduces the free-particle Schrödinger equation in the continuum limit.

Topological edge state – A mode confined to the boundary of a puncture lattice whose existence is guaranteed by a non-trivial winding of the coupling phases (e.g., synthetic gauge fields). Appears in photonic, acoustic, and elastic metamaterials.

Vanishing divergence constraints – Discrete identities $\nabla \cdot (\nabla \times \mathbf{u}) = 0$ and $\nabla \cdot \mathbf{B} = 0$ that are satisfied exactly on the staggered lattice, ensuring charge- and magnetic-monopole conservation.

Wave-particle duality (puncture selection) – In the IPW picture a measurement corresponds to a strong, local coupling that projects the extended puncture ensemble onto a single puncture, reproducing the particle-like detection statistics (Born rule) without an external collapse postulate.

Wave number (k) – Reciprocal-space vector labeling the spatial periodicity of a lattice mode.

Zero-order (continuum) limit – The leading term obtained by letting the lattice spacing $a \to 0$ while keeping physical parameters ($c, \rho, \varepsilon, \mu$, etc.) fixed; yields the familiar PDEs of continuum physics.

FOREWORD TO INFINITESIMALLY PUNCTURED WAVES

When we first learn that sound travels as a ripple of pressure, that light propagates as an oscillating electromagnetic field, and that an earthquake's distant tremor is a deformation of Earth's interior, we instinctively imagine waves as continuous undulations filling space.

Over time, those pictures are distilled into elegant partial differential equations: the acoustic wave equation, Maxwell's curl equations, the Navier–Cauchy system of elasticity, and the linearised Einstein field equations.

Yet the moment we place a detector in a wave's path—a microphone, photodiode, seismometer, or laser interferometer—we record something discrete: a click, a voltage spike, a digitised sample. The coexistence of smooth fields and pointlike measurements has long carried a conceptual tension, nowhere more familiar than in quantum mechanics, where wave–particle duality is elevated to a foundational postulate.

The Infinitesimally Punctured Wave (IPW) framework offers a unifying way to reframe that tension. Instead of treating continuity and discreteness as competing descriptions, IPW proposes that the continuous wave is a macroscopic limit of an ultra-dense lattice of infinitesimal "punctures"—tiny carriers of the relevant physical quantity (pressure, displacement, electric dipole moment, metric perturbation, or quantum amplitude).

Each puncture interacts only with its nearest neighbours through simple local couplings: linear (or weakly nonlinear) "springs," discrete curls, or Regge-type hinge interactions. As the lattice spacing (a) is taken toward the infinitesimal, familiar continuum equations arise naturally. When (a) is finite, the same structure suggests systematic corrections—dispersion, shock regularisation, band gaps—and a concrete way to *interpret* measurement-like discreteness in terms of puncture-level selection.

What makes this approach especially striking is its breadth. By changing only the tensorial character of the puncture variable and the symmetry of the coupling, the IPW "skeleton" can reproduce, within a single discrete dynamical template:

- acoustic and surface-gravity waves in fluids,
- longitudinal (P) and shear (S) waves in solids,
- electromagnetic propagation in vacuum and engineered media,
- linearised gravitational waves on a Regge spacetime lattice,
- Schrödinger-type quantum dynamics, and
- nonlinear phenomena such as shocks and solitons.

Across these domains, seemingly unrelated wave equations appear as different limits and representations of the same underlying local update rule. This book guides the reader through that journey step by step: from the abstract definition of a puncture, to the generic discrete equations of motion, and onward to specialised constructions for each wave family. Along the way, the governing symmetry principles—translation and rotation invariance, gauge structure, diffeomorphism invariance, and (U(1)) phase—clarify why particular couplings take the forms they do. Familiar results such as Rankine–Hugoniot jump conditions, Zoeppritz relations, and Born-rule-like probability assignments are revisited through the punctured lens and shown to arise in a common mathematical language.

Beyond its conceptual appeal, the IPW framework is also practically useful. Because the same core numerical structure can be adapted across acoustics, optics, elasticity, and quantum modelling, a single simulation engine can be repurposed across disciplines. The explicit lattice also provides an intrinsic ultraviolet regulator—an arena in which to explore quantum-gravity-inspired phenomenology, metamaterial design, and the role of disorder and attenuation in seismology.

The text repeatedly connects theory to experiment. Later chapters identify observable signatures of a finite puncture scale—high-frequency dispersion curvature, shock-width regularisation, and band-gap formation—and describe realistic experimental routes for probing them. Even if a fundamental puncture spacing lies far beyond direct reach, engineered analogues—photonic crystals, acoustic metamaterials, and optical lattices—can bring closely related physics into the laboratory.

In an era when the boundaries between physics, engineering, and applied mathematics are increasingly porous, a unifying language such as the Infinitesimally Punctured Wave framework feels timely. It invites us to rethink what "a wave" is, to design new architectures for guiding and controlling propagation, and—perhaps—to glimpse a granular texture beneath the continuum models that have served us so well.

I hope that readers will find in these pages a coherent theoretical framework, a transferable modelling methodology, and a foundation for further analytical and experimental work. It is my intention that the punctured perspective developed here contributes, in a precise and constructive way, to a deeper understanding of wave phenomena across disciplines.

Note. *Some of the ideas presented here have already been (and will continue to be) the subject of scientific articles and communications. In this volume, to make the reading easier and accessible beyond a strictly academic audience, I have stripped the exposition of citations and references. A bibliography can be found at the end of the volume.*

CHAPTER 1
INTRODUCTION TO INFINITESIMALLY PUNCTURED WAVES

1.1 Why a New Wave Paradigm?

Waves are everywhere: sound ripples through air, light undulating in vacuum, seismic tremors shaking the crust, and probability amplitudes spreading across Hilbert space. In every textbook the mathematics is presented as a **continuous field** obeying a differential equation (the wave, Helmholtz, or Schrödinger equation). Yet the very act of *measuring* a wave often produces a **discrete, particle-like response**—a photon clicks a detector, a microphone registers a pressure spike, a seismometer records a single arrival time.

Historically two broad strategies have been pursued to reconcile this dichotomy:

Strategy	Core Idea	Typical Domain
Continuum-only	Fields are fundamentally smooth; discreteness is an artifact of the measuring apparatus.	Classical acoustics, optics, elasticity.
Discrete-only	The world is made of point-like entities (particles, quanta); waves are emergent collective motions.	Early quantum mechanics, lattice models in condensed matter.

Both viewpoints succeed within their own regimes but leave unanswered questions when we try to **translate** from one to the other. For example, why does a continuous electromagnetic field collapse to a single photon upon detection? Why do seismic waves sometimes appear as sharply defined arrivals despite being described by smooth partial differential equations?

The **Infinitesimally Punctured Wave (IPW)** framework proposes a middle ground:

the continuous wave is the macroscopic limit of an ultra-dense lattice of infinitesimal punctures.

Each puncture carries the smallest possible amount of the relevant physical quantity (pressure, displacement, electric field, metric perturbation, quantum amplitude, …). The lattice spacing is taken to be **infinitesimal**—much smaller than any experimentally accessible length scale—but **non-zero**, preserving a microscopic granularity that becomes relevant when a measurement isolates a single puncture.

Key Insight:

Wave-particle duality is re-interpreted as continuous-puncture ensemble ↔ isolated puncture selection.

When the ensemble is left untouched, the collective behaviour reproduces the familiar wave equations. When a detector interacts strongly with a tiny region, it effectively "chooses" one puncture, and the outcome looks particle-like.

1.2 Historical Roots

The seed of this idea can be traced to several independent lines of thought:

Origin	Contribution
Smarandache (2019-2026) ***Infinitesimally Punctured Geometry, Physics & Structures***	Introduced the notion of a space filled with infinitesimally spaced discrete elements, applying it to mechanical, electromagnetic, and quantum waves.
Regge Calculus (1961) – ***Discrete General Relativity***	Replaces smooth manifolds with simplicial complexes; the metric lives on edges, and curvature is concentrated on hinges. Provides a concrete example of a punctured spacetime.
Tight-Binding Models (solid-state physics) – ***Electrons hopping on a lattice***	Shows how a discrete Hamiltonian yields the continuous Schrödinger equation in the long-wavelength limit.
Cellular Automata Approaches to Quantum Mechanics – ***'t Hooft, Bialynicki-Birula***	Demonstrate that unitary evolution can emerge from deterministic, locally interacting cells.
Lattice Boltzmann Methods (fluid dynamics) – ***Discrete velocity sets***	Recover Navier–Stokes equations from particle-distribution updates on a grid.

The present book expands the seed of **Infinitesimally Punctured Wave** into a **comprehensive, cross-disciplinary taxonomy** that includes acoustic, gravity, seismic, shock, shear, and gravitational waves—all expressed with the same underlying puncture language.

1.3 What Is a "Puncture"?

A puncture is an idealised point-like degree of freedom that occupies an infinitesimal volume of the underlying medium.

Its defining attributes are:

Attribute	Description
State Variable	The minimal physical quantity that characterises the wave at that location (e.g., scalar pressure p_i, vector displacement $\mathbf{u}_i$, complex amplitude ψ_i, tensor perturbation $h_{\mu\nu,i}$).
Mass/Energy Content	An infinitesimal amount of inertia or energy density, typically proportional to the physical density of the medium times the infinitesimal volume element.
Neighbour Coupling	Linear (or weakly non-linear) interaction with adjacent punctures that mimics the restoring forces or field-propagation mechanisms of the continuum theory.
Spacing a	The distance between neighbouring punctures. In the IPW limit, $a \to 0$ while the product of coupling strength and a^2 remains finite, ensuring a well-defined continuum limit.

Mathematically, the collection of punctures forms a **regular lattice** (often cubic or triangular for simplicity) or a **simplicial complex** (for curved spaces). The dynamics are governed by a set of **difference equations** that are the discrete analogues of the continuous PDEs. Taking the limit $a \to 0$ (via Taylor expansion) recovers the familiar differential operators.

1.4 From Discrete to Continuous – A Sketch

Consider a one-dimensional scalar field $\phi(x,t)$ governed by the wave equation

$$\partial_t^2 \phi = c^2 \, \partial_x^2 \phi.$$

Place punctures at positions $x_n = na$ with state $\phi_n(t) = \phi(x_n, t)$. Let each puncture have an effective mass $m = \rho a$ (density ρ times the cell length) and be connected to its nearest neighbours by springs of stiffness $k = K/a$ (bulk modulus K divided by spacing). Newton's second law for puncture n reads

$$m\,\ddot{\phi}_n = k(\phi_{n+1} - 2\phi_n + \phi_{n-1}).$$

Dividing by a and letting $a \to 0$ yields

$$\rho\ \partial_t^2\phi = K\ \partial_x^2\phi,$$

which is exactly the acoustic wave equation with sound speed $c = \sqrt{K/\rho}$. The same procedure works for vector, tensor, or complex fields, provided the appropriate coupling tensors are inserted. Thus,

the continuum wave equation is nothing more than the dense-limit of a simple network of punctures.

1.5 What Does "Infinitesimally" Mean Here?

In everyday language "infinitesimal" suggests a quantity so small it can be ignored. Within the IPW framework it has a precise technical role:

- **Mathematical Limit:** The spacing a is treated as a parameter that can be taken arbitrarily small. All derived continuum equations hold **exactly** in the limit $a \to 0$.
- **Physical Cut-off:** In practice one may imagine a fundamental minimum length (perhaps the Planck length for spacetime punctures, or an atomic spacing for material media). Keeping a finite at that scale introduces **corrections**—dispersion, regularised shock thickness, or a high-frequency attenuation—that are absent from the pure continuum theory.
- **Operational Meaning:** Experiments never probe distances smaller than the instrument's resolution, so the punctured description is **operationally indistinguishable** from the continuous one in the regime where a is far below the observational scale.

Thus "infinitesimally" signals both a **conceptual idealisation** (allowing us to recover known physics) and a **potential doorway to new phenomenology** (when the spacing is comparable to a physical cutoff).

1.6 Scope and Structure

The remainder of the book follows a **progressive, comparative roadmap**:

1. **Chapter 2** builds the generic discrete formalism, establishing notation, lattice topology, and the systematic derivation of continuum limits.
2. **Chapters 3–9** apply the formalism to specific wave families—acoustic, elastic, seismic, shock, electromagnetic, gravitational, and quantum mechanical—showing step-by-step how each continuous equation emerges from its punctured counterpart.
3. **Chapter 10** draws explicit **cross-wave connections**, summarising the common puncture variables, coupling constants, and dispersion relations in a unified table.
4. **Chapter 11** explores **experimental signatures** that could reveal the underlying punctured structure, proposing feasible tests in optics, seismology, and tabletop gravitation-wave analogues.

Throughout, the narrative emphasizes **physical intuition** (what the punctures represent), **mathematical clarity** (derivations), and **practical relevance** (how engineers might exploit the viewpoint for metamaterial design or signal processing).

1.7 A First Thought Experiment

Imagine a perfectly still pond. In the conventional picture a thrown stone creates concentric circular ripples described by the linear wave equation for surface elevation $\eta(r,t)$. In the IPW picture the pond surface is a dense sheet of infinitesimal water parcels, each capable of a tiny vertical displacement η_i. The stone's impact locally excites a handful of parcels; the disturbance then propagates because each parcel pulls on its neighbours through the **gravity-plus-surface-tension coupling**. If we placed a microscopic pressure sensor that could resolve a single parcel's motion, the sensor would register a **discrete kick**—the analogue of a photon detection in optics. Yet the overall pattern observed with the naked eye remains a smooth ripple, precisely the continuum limit of the punctured dynamics.

This simple image captures the essence of the IPW philosophy: **smooth macroscopic waves are the statistical, coarse-grained manifestation of countless microscopic puncture interactions**. The rest of the book develops the mathematics that turns this picture into a rigorous, testable framework.

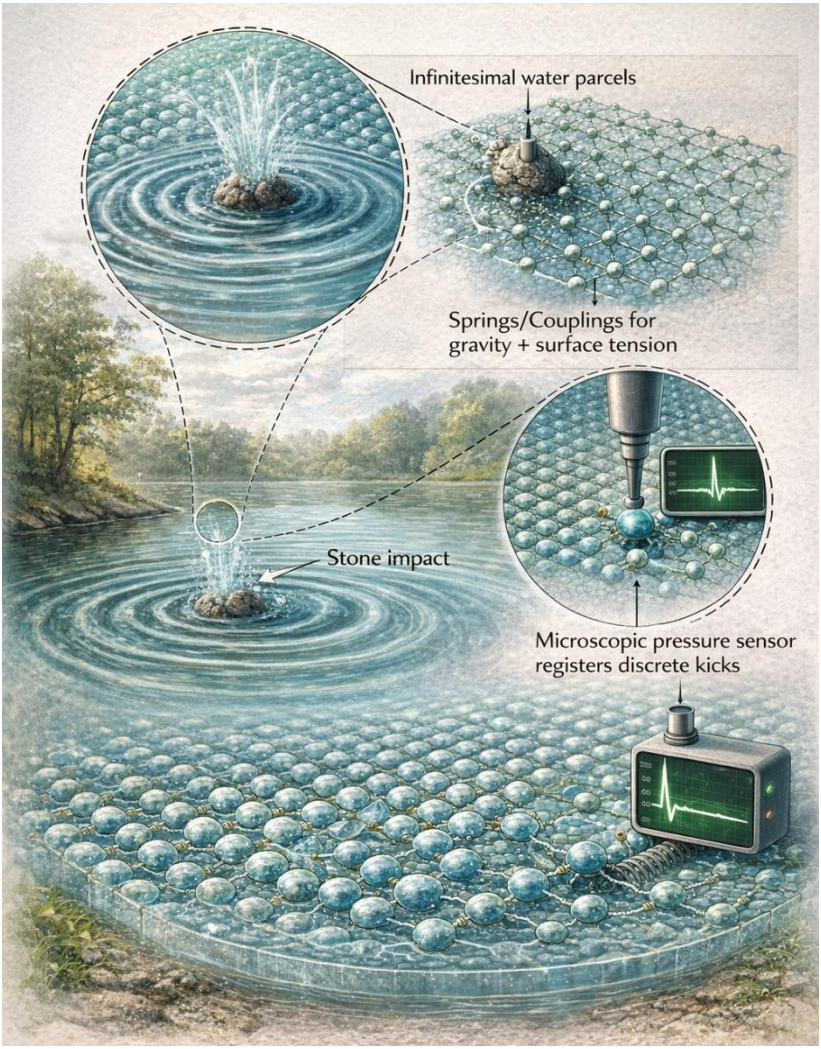

Figure 1 – The Pond Ripple as an Infinitesimally Punctured Wave

In the IPW approach, the pond surface is made up of infinitesimal water parcels. A thrown stone disturbs some of these parcels, creating a ripple. A microscopic pressure sensor could detect a discrete "kick" at the punctured level, while the macroscopic view is a smooth ripple.

CHAPTER 2
GENERIC DISCRETE FORMALISM FOR INFINITESIMALLY PUNCTURED WAVES

2.1 What We Want to Achieve?

All physical wave phenomena share a common mathematical skeleton: a field (scalar, vector, or tensor) evolves in space-time according to a linear (or weakly non-linear) partial differential equation (PDE). The **goal** of the Infinitesimally Punctured Wave (IPW) program is to replace that PDE by a **system of coupled ordinary differential equations (ODEs)** defined on a lattice of infinitesimal "punctures." When the lattice spacing a tends to zero, the ODE system converges to the original PDE.

In this chapter we:

1. Define the lattice geometry and the puncture state variables.
2. Write the most general nearest-neighbour coupling consistent with the symmetries of the target wave.
3. Perform the continuum limit analytically (Taylor expansion) and obtain the familiar wave operators.
4. Discuss extensions – higher-order neighbours, non-linear springs, dissipation, and boundary conditions.
5. Show how **measurement** can be modelled as a puncture-selection operation.

2.2 Lattice Geometry

Dimension	Typical lattice	Coordinates of puncture i
1-D	Uniform line, spacing a	$x_i = i\,a$
2-D	Square or triangular grid	$\mathbf{r}_{i,j} = (i\,a, j\,a)$
3-D	Simple cubic (or face-centred)	$\mathbf{r}_{i,j,k} = (i\,a, j\,a, k\,a)$
Curved space	Simplicial complex (Regge triangulation)	Vertices labelled by integer indices; edge lengths l_{ab} replace constant a.

For most wave classes the **simple cubic lattice** suffices because the underlying medium is isotropic (air, water, vacuum, homogeneous solid). When anisotropy or curvature is essential (elastic crystals, spacetime), we replace the uniform spacing by direction-dependent edge lengths a_α or by a Regge triangulation.

Notation:

- Index n (or a multi-index $\mathbf{n}$) denotes a puncture.
- The set of nearest neighbours of n is $\mathcal{N}(n)$.
- The lattice spacing is denoted a (or a_α per coordinate direction).

2.3 State Variables and Mass-Energy Assignment

Each puncture carries a **minimal dynamical variable** appropriate to the wave family:

Wave family	Puncture variable $\boldsymbol{\Phi_n}$	Physical dimension
Acoustic / pressure	p_n (Pa)	Pressure
Elastic displacement	$\mathbf{u}_n$ (m)	Length
Electromagnetic	$\mathbf{E}_n, \mathbf{B}_n$ (V/m, T)	Field
Gravitational (linear)	$h_{\mu\nu,n}$ (dimensionless)	Metric perturbation
Quantum (Schr.)	ψ_n ($\sqrt{}$probability)	Amplitude
General scalar wave	ϕ_n	Depends on context

To keep the equations compact we write a **generic vector** Φ_n that may be scalar, vector, or tensor. The **effective inertial factor** (mass or energy density) attached to a puncture is

$$M = \rho\, a^d,$$

where ρ is the appropriate density (mass density for mechanical waves, permittivity for EM, etc.) and d is the spatial dimensionality of the lattice.

2.4 Nearest-Neighbour Coupling

The simplest physically motivated interaction is a **linear spring-like coupling** between a puncture and each neighbour:

$$\boxed{M\,\ddot{\Phi}_n = \sum_{m\in\mathcal{N}(n)} K_{nm}\,(\Phi_m - \Phi_n)} \qquad (2.1)$$

- K_{nm} is the **coupling stiffness** (or hopping amplitude) with dimensions $[K] =$ force/unit of Φ.
- For an isotropic, homogeneous medium we set $K_{nm} = K$ for all nearest neighbours.

Equation (2.1) is the **discrete wave equation**. It is the direct analogue of Newton's second law for a mass-spring chain (1-D) or of Kirchhoff's circuit laws for a network of inductors/capacitors (EM).

2.4.1 Tensorial Coupling

When Φ_n is a vector or tensor, the coupling must respect rotational symmetry. The most general linear, isotropic coupling takes the form

$$M\,\ddot{\Phi}_n^{\alpha} = \sum_{m\in\mathcal{N}(n)} K\,(\,\Phi_m^{\alpha} - \Phi_n^{\alpha}) \text{ (for each component } \alpha).$$

If the medium is anisotropic, we replace the scalar K by a **rank-2 stiffness tensor** $K^{\alpha\beta}$ acting on the components.

2.5 Continuum Limit

Assume a regular cubic lattice with spacing a and isotropic coupling K. Expand the neighbour field to second order:

$$\Phi_{n+\hat{e}_\alpha} = \Phi(\mathbf{r}_n + a\hat{e}_\alpha) = \Phi(\mathbf{r}_n) + a\;\partial_\alpha\Phi + \frac{a^2}{2}\;\partial_\alpha^2\Phi + O(a^3),$$

where $\hat{e}_\alpha$ is the unit vector along coordinate α. Summing over the $2d$ nearest neighbours (positive and negative directions) gives

$$\sum_{m\in\mathcal{N}(n)} (\,\Phi_m - \Phi_n) = a^2\,\nabla^2\Phi + O(a^4).$$

Insert this result into (2.1):

$$M\,\ddot{\Phi} = K\,a^2\,\nabla^2\Phi + O(a^4).$$

Now define the **wave speed**

$$c^2 \equiv \frac{K\,a^2}{M}.$$

Because $M = \rho a^d$, the factor Ka^2 scales as a^{2-d}. For the limit to be finite we require $K \propto a^{d-2}$; this is precisely how the physical constants (bulk modulus, shear modulus, permittivity, etc.) appear in the continuum theory. Dropping higher-order terms yields the familiar **wave equation**

$$\boxed{\partial_t^2 \Phi = c^2\,\nabla^2 \Phi} \qquad (2.2)$$

for a scalar field. For vector/tensor fields the Laplacian acts component-wise, possibly with distinct speeds (e.g., longitudinal vs. transverse elastic waves).

The continuous PDE is the exact dense-limit of the discrete ODE network.

2.6 Higher-Order Neighbours and Dispersion

If we retain couplings beyond nearest neighbours (second-nearest, etc.) the discrete equation acquires additional terms:

$$M\,\ddot{\Phi}_n = K_1 \sum_{\text{nn}} (\Phi_m - \Phi_n) + K_2 \sum_{\text{nnn}} (\Phi_m - \Phi_n) + \cdots$$

Carrying the Taylor expansion to fourth order yields a **dispersive correction**:

$$\partial_t^2 \Phi = c^2\,\nabla^2 \Phi - \beta\,\nabla^4 \Phi + \cdots\,,$$

where β depends on the ratio K_2/K_1 and on a^2. Such terms become important when the wavelength approaches the lattice spacing, offering a concrete prediction of the IPW framework: **high-frequency dispersion** that is absent in the ideal continuum model.

2.7 Non-Linear Springs and Shock Regularisation

Replace the linear Hooke-law coupling by a weakly non-linear relation:

$$F_{nm} = K(\Phi_m - \Phi_n) + \lambda(\Phi_m - \Phi_n)^3,$$

with λ a small coefficient.

The discrete equation now reads

$$M\,\ddot{\Phi}_n = \sum_{m\in\mathcal{N}(n)} [K(\Phi_m - \Phi_n) + \lambda(\Phi_m - \Phi_n)^3].$$

In the continuum limit the cubic term generates a **non-linear term** (e.g., $\partial_x(\Phi^3)$) that can produce **solitary-wave** or **shock-like** solutions. Importantly, because the lattice spacing is finite, the shock front retains a **microscopic thickness** equal to a few puncture spacings, thereby **regularising the mathematical singularity** that appears in the pure hyperbolic PDE.

2.8 Boundary Conditions in the Punctured Picture

Physical boundaries correspond to **missing neighbours** or to prescribed values at the edge punctures.

Boundary type	Discrete implementation
Fixed (Dirichlet)	Set $\Phi_{\text{boundary}} = \Phi_0$ for all time.
Free (Neumann)	Remove the spring to the outside world; equivalently enforce $\Phi_{\text{outside}} = \Phi_{\text{boundary}}$ so the difference term vanishes.
Impedance-matched	Attach an auxiliary lattice with adjusted coupling K' that mimics the continuation of the medium.

These prescriptions converge to the standard continuous boundary conditions as $a \to 0$.

2.9 Modeling Measurement as Puncture Selection

In the IPW worldview a **measurement** that yields a particle-like event is interpreted as the detector **strongly coupling to a single puncture** and thereby collapsing the superposition of the ensemble onto that puncture's state. A simple phenomenological model:

1. **Pre-measurement:** The field is a coherent superposition of many puncture amplitudes $\{\Phi_n\}$.
2. **Interaction:** The detector introduces an additional term in the Hamiltonian (or Lagrangian) that couples only to puncture n_0:
$$H_{\text{int}} = -\gamma\,\Phi_{n_0}\,\chi(t),$$
where $\chi(t)$ is a short pulse and γ a large coupling constant.

3. **Outcome:** The strong coupling forces Φ_{n_0} to adopt a definite value (e.g., a localized excitation), while the rest of the lattice is left largely unchanged. The detector records the energy/momentum associated with that puncture, giving the appearance of a **single quantum**.

This picture reproduces the essential features of wave-function collapse without invoking mystical non-locality: the "collapse" is simply the **localisation of energy onto one puncture** due to the detector's selective interaction.

2.10 Summary of the Generic Formalism

Step	What we do	Result
1. Choose lattice	Cubic, triangular, or Regge complex	Set of puncture positions $\mathbf{r}_n$
2. Assign state Φ_n	Scalar, vector, tensor, complex amplitude	Minimal physical variable
3. Define inertial factor M	$M = \rho a^d$	Consistent with continuum density
4. Write nearest-neighbour coupling	Eq. (2.1) with stiffness K	Discrete ODE system
5. Perform Taylor expansion	$\Phi_{n\pm\hat{e}_\alpha} \rightarrow$ series	Obtain $\nabla^2\Phi$ term
6. Identify wave speed	$c^2 = Ka^2/M$	Continuum wave equation (2.2)
7. Add refinements	Higher neighbours, non-linearity, damping	Dispersive / shock-regularising corrections
8. Impose boundaries	Fixed, free, impedance-matched	Discrete analogues of BCs
9. Model measurement	Localised strong coupling	Puncture-selection interpretation of collapse

With this scaffold in place, the remaining chapters instantiate the formalism for each concrete wave family, demonstrating how the same algebraic skeleton reproduces acoustic, elastic, electromagnetic, gravitational, and quantum-mechanical wave equations—and, crucially, how **deviations** from the ideal continuum emerge when the puncture spacing is finite.

CHAPTER 3
INFINITESIMALLY PUNCTURED ACOUSTIC AND SURFACE GRAVITY WAVES

3.1 Why Start Here?

Acoustic pressure waves in fluids and surface-gravity ripples on a liquid are the most familiar wave phenomena. They are mathematically simple (second-order linear PDEs) and experimentally easy to probe, making them ideal test-beds for the generic IPW formalism introduced in Chapter 2. Moreover, microphones, hydrophones and pressure transducers give a concrete illustration of **puncture-selection**—the IPW picture of a measurement "collapsing" the wave onto a single puncture.

3.2 Physical Quantities

Symbol	Meaning	Role in the puncture model
ρ	Mass density of the fluid	Determines the inertial factor $M = \rho a^3$ for each volume puncture
K	Adiabatic bulk modulus	Sets the longitudinal spring stiffness between neighbouring pressure punctures
$c = \sqrt{K/\rho}$	Speed of sound	Emerges as the wave speed after the continuum limit
g	Gravitational acceleration	Restoring force for surface-gravity waves
σ	Surface tension (optional)	Adds a curvature-dependent restoring term
h	Fluid depth (optional)	Enters the finite-depth dispersion relation

The **primary puncture variables** are

- **Acoustic case:** scalar pressure deviation $p_n(t)$.
- **Surface-gravity case:** vertical surface displacement $\eta_n(t)$ (also called surface elevation).

3.3 Discrete Acoustic Wave Model

3.3.1 Lattice and Mass Assignment

- 3-D cubic lattice, spacing a.
- Index $n = (n_x, n_y, n_z)$.
- Each cell carries mass $M = \rho a^3$.

3.3.2 Equation of Motion (nearest-neighbour coupling)

$$M\,\ddot{p}_n = K\,a^2 \sum_{\alpha=x,y,z} (p_{n+\hat{e}_\alpha} - 2p_n + p_{n-\hat{e}_\alpha}). \qquad (3.1)$$

The factor Ka^2 is the force transmitted across a face of area a^2 when a pressure difference exists.

3.3.3 Continuum Limit

Expanding the neighbour pressures to second order,

$$p_{n\pm\hat{e}_\alpha} = p(\mathbf{r}) \pm a\ \partial_\alpha p + \frac{a^2}{2}\partial_\alpha^2 p + O(a^3),$$

the sum in (3.1) becomes $a^2\nabla^2 p$. Substituting and cancelling a^2,

$$\rho\,\ddot{p} = K\,\nabla^2 p \quad \Longrightarrow \quad \boxed{\partial_t^2 p = c^2\nabla^2 p}, \qquad (3.2)$$

the familiar linear acoustic wave equation.

3.3.4 Optional Viscous Damping

Add a dash-pot between neighbours with coefficient η (dynamic viscosity):

$$M\,\ddot{p}_n = Ka^2\Delta_2 p_n - \eta a^2 \Delta_2 \dot{p}_n.$$

In the continuum limit this yields

$$\partial_t^2 p + \frac{\eta}{\rho}\ \partial_t \nabla^2 p = c^2\nabla^2 p,$$

the standard damped acoustic wave equation.

3.4 Discrete Surface-Gravity Wave Model

3.4.1 Lattice and Effective Mass

- 2-D square lattice on the equilibrium surface, spacing a.
- Index $\mathbf{n} = (n_x, n_y)$.
- Effective mass per node $M_s = \rho\, h_{\text{eff}}\, a^2$. *For deep water* $h_{\text{eff}} \approx 1/k$*; for finite depth we will replace it by the actual depth* h.

3.4.2 Restoring Forces

1. **Gravity:** vertical force $-\rho g\, \eta_n a^2$.
2. **Surface tension (optional):** pressure jump $\sigma\, \nabla^2 \eta \rightarrow$ discrete Laplacian term.

The discrete equation of motion:

$$M_s\, \ddot{\eta}_n = -\rho g\, a^2\, \eta_n + \sigma a^2\, \Delta_2 \eta_n. \qquad (3.3)$$

3.4.3 Continuum Limit

Using the same Taylor expansion as before, $\Delta_2 \eta_n \rightarrow a^2 \nabla^2 \eta$. Dividing by $M_s = \rho h_{\text{eff}} a^2$ gives

$$\ddot{\eta} = -\frac{g}{h_{\text{eff}}}\, \eta + \frac{\sigma}{\rho h_{\text{eff}}}\, \nabla^2 \eta.$$

Assuming a plane-wave ansatz $\eta \propto e^{i(\mathbf{k}\cdot\mathbf{x} - \omega t)}$ and taking the deep-water limit ($h_{\text{eff}} = 1/k$):

- **Pure gravity waves ($\sigma = 0$)**

$$\boxed{\omega^2 = gk} \text{ (deep water).} \qquad (3.4)$$

- **Capillary-gravity waves ($\sigma \neq 0$)**

$$\boxed{\omega^2 = gk + \frac{\sigma}{\rho} k^3}. \qquad (3.5)$$

3.4.4 Finite-Depth Modification

For a layer of finite depth h the effective mass becomes $M_s = \rho a^2 \frac{\tanh(kh)}{k}$. The dispersion relation then reads

$$\boxed{\omega^2 = gk\tanh(kh) + \frac{\sigma}{\rho}k^3\tanh(kh)}. \qquad (3.6)$$

Thus the **finite-depth factor** $\tanh(kh)$ emerges naturally from the puncture inertia term.

3.5 Higher-Neighbour Coupling & Dispersive Corrections

If second-nearest-neighbour springs with stiffness K_2 are retained, the continuum limit adds a ∇^4 term:

$$\partial_t^2 p = c^2\nabla^2 p - \beta\,\nabla^4 p, \beta = \frac{K_2 a^4}{M}.$$

The phase speed becomes $c_{\text{eff}}(k) = c\sqrt{1-\beta k^2}$, predicting a mild **high-frequency dispersion** that would be absent in the pure continuum model. An analogous fourth-order curvature term appears for surface waves when diagonal couplings are added, slightly modifying the capillary-gravity dispersion at sub-millimetre wavelengths. These corrections are the concrete **signatures of a finite puncture spacing** discussed later in Chapter 11.

3.6 Boundary Conditions in the Punctured Picture

Physical boundary	Discrete implementation	Continuum counterpart
Rigid wall (no normal velocity)	Fix pressure at wall nodes: $p = 0$ (Dirichlet) or fix surface displacement $\eta = 0$.	Dirichlet condition $p = 0$ or $\eta = 0$.
Open end (free surface)	Omit the spring to the missing neighbour (Neumann).	$\partial_n p = 0$ or $\partial_n \eta = 0$.
Impedance-matched termination	Attach an auxiliary lattice with coupling constant tuned to eliminate reflections.	Absorbing (Sommerfeld) boundary condition.

Because the lattice is an explicit graph, complex geometries (curved walls, irregular coastlines) are handled simply by editing the adjacency list of punctures.

3.7 Measurement as Puncture Selection

A microphone (or hydrophone) couples **strongly** to a single pressure puncture p_{n_0}. In a Hamiltonian picture the interaction can be written

$$H_{\text{det}} = -\gamma\, p_{n_0}\, \chi(t),$$

with γ a large coupling constant and $\chi(t)$ a short temporal window representing the measurement pulse. The consequences are:

1. Energy is transferred from the surrounding lattice into the detector, **localising** the disturbance onto puncture n_0.
2. The recorded voltage (or digital count) is proportional to the instantaneous value of p_{n_0}.

Thus the detector registers a **discrete click** even though the underlying field is a coherent superposition of many punctures—exactly the IPW reinterpretation of wave-particle duality.

3.8 Summary

Step	Acoustic waves	Surface-gravity waves
Lattice	3-D cubic, spacing a	2-D square, spacing a
State variable	Pressure deviation p_n	Surface elevation η_n
Inertial factor	$M = \rho a^3$	$M_s = \rho h_{\text{eff}} a^2$
Coupling	Linear springs with stiffness K	Gravity spring $-\rho g$ + optional surface-tension Laplacian
Continuum equation	$\partial_t^2 p = c^2 \nabla^2 p$	$\partial_t^2 \eta = -\frac{g}{h_{\text{eff}}}\eta + \frac{\sigma}{\rho h_{\text{eff}}}\nabla^2 \eta$
Dispersion (deep water)	$\omega^2 = c^2 k^2$	$\omega^2 = gk$ (gravity) or $\omega^2 = gk + \frac{\sigma}{\rho}k^3$ (capillary-gravity)
Finite-depth correction	–	Multiply by $\tanh(kh)$
Higher-order correction	$-\beta \nabla^4 p$	$-\beta' \nabla^4 \eta$ (optional)
Measurement model	Strong coupling to a single p_n	Strong coupling to a single η_n

Figure 2 – Infinitesimally Punctured Representation of Acoustic and Surface Gravity Waves.

Left: Bulk acoustic waves arise from compressional coupling between neighbouring volume punctures of effective mass $M = \rho a^3$, where ρ is the fluid density and a the lattice spacing. The discrete spring stiffness is governed by the adiabatic bulk modulus K, yielding the continuum sound speed $c = \sqrt{K/\rho}$ in the limit $a \to 0$.

Right: Surface gravity waves are represented by vertical displacements of surface punctures coupled through gravitational restoring forces g and, when included, surface tension σ. The finite fluid depth h modifies the effective coupling and determines the dispersion relation in the long- and intermediate-wavelength regimes. In both cases, the smooth macroscopic wave profile emerges as the continuum limit of the underlying puncture dynamics.

The acoustic and surface-gravity examples demonstrate that **the same discrete skeleton**—massful punctures linked by linear springs—produces the diverse wave equations encountered in everyday physics. The next chapters repeat this construction for elastic body waves, seismic waves, shock waves, electromagnetic waves, gravitational waves, and quantum-mechanical wavefunctions, showing how the IPW framework unifies them all.

CHAPTER 4
INFINITESIMALLY PUNCTURED ELASTIC BODY WAVES (LONGITUDINAL & SHEAR)

4.1 Why Elastic Waves Matter?

In a solid the atoms (or, at the IPW level, the infinitesimal volume punctures) can move **independently in three spatial directions**. This gives rise to two fundamentally different families of bulk waves:

- **P-waves (primary or compressional waves)** – particle motion parallel to the propagation direction.
- **S-waves (secondary or shear waves)** – particle motion perpendicular to the propagation direction.

Both families are central to seismology, nondestructive testing, and ultrasonic imaging. Because the underlying medium supports **vector displacements**, the IPW construction must be extended from scalar pressure punctures to **vectorial punctures** linked by **Lamé-parameter springs**. The same discrete skeleton also accommodates **anisotropy** and **mode conversion** at material interfaces.

4.2 Physical Ingredients

Symbol	Meaning	Units	Role in the puncture model
$\boldsymbol{\rho}$	Mass density of the solid	kg m^{-3}	Sets the inertial factor $M = \rho a^3$ for each volume puncture
$\boldsymbol{\lambda}$	First Lamé parameter (bulk-related)	Pa	Controls coupling of **volumetric** deformation
$\boldsymbol{\mu}$	Shear modulus (second Lamé parameter)	Pa	Controls coupling of **shape-changing** (shear) deformation
$\mathbf{u}_n(t)$	Displacement vector of puncture n	m	Dynamical variable (three components)
$\boldsymbol{a}$	Lattice spacing	m	Distance between neighbouring punctures (taken infinitesimal)
$\mathbf{C}$	Fourth-rank stiffness tensor (anisotropic case)	Pa	Generalises λ, μ when material symmetry is lower than isotropic

For an **isotropic** solid the stiffness tensor reduces to the familiar combination of λ and μ:

$$C_{ijkl} = \lambda\,\delta_{ij}\delta_{kl} + \mu\,(\delta_{ik}\delta_{jl} + \delta_{il}\delta_{jk}).$$

4.3 Discrete Lattice Construction

- **Geometry:** 3-D simple cubic lattice, spacing a.
- **Indexing:** $n = (n_x, n_y, n_z)$.
- **State variable:** $\mathbf{u}_n(t) = (u_n^x, u_n^y, u_n^z)$.
- **Inertia:** $M = \rho a^3$ attached to each puncture.

Each puncture is linked to its six nearest neighbours by **linear springs** whose force depends on the **relative displacement** projected onto the line joining the two punctures. The force law that reproduces the Lamé-parameter elastic response is

$$\mathbf{F}_{nm} = \underbrace{\frac{\lambda}{a}\,(\mathbf{u}_m - \mathbf{u}_n)\cdot\hat{\mathbf{e}}_{nm}\;\hat{\mathbf{e}}_{nm}}_{\text{volumetric part}} + \underbrace{\frac{\mu}{a}\,[(\mathbf{u}_m - \mathbf{u}_n) - (\mathbf{u}_m - \mathbf{u}_n)\cdot\hat{\mathbf{e}}_{nm}\;\hat{\mathbf{e}}_{nm}]}_{\text{shear part}}. \tag{4.1}$$

Here $\hat{\mathbf{e}}_{nm}$ is the unit vector pointing from puncture n to puncture m. The first term restores **volume change** (compression/expansion) while the second term restores **shape change** (shear). For an isotropic cubic lattice the six neighbour directions are simply the Cartesian axes, so $\hat{\mathbf{e}}_{nm}$ equals one of $\pm\hat{x}, \pm\hat{y}, \pm\hat{z}$.

Summing the forces from all neighbours gives the **discrete equation of motion**:

$$\boxed{M\,\ddot{\mathbf{u}}_n = \sum_{m\in\mathcal{N}(n)} \mathbf{F}_{nm}} \tag{4.2}$$

where $\mathcal{N}(n)$ denotes the six nearest neighbours.

4.4 Continuum Limit – Recovery of Navier–Cauchy Equations

Expand the displacement of a neighbour to second order:

$$\mathbf{u}_{n\pm\hat{e}_\alpha} = \mathbf{u}(\mathbf{r}) \pm a\;\partial_\alpha\mathbf{u} + \frac{a^2}{2}\;\partial_\alpha^2\mathbf{u} + O(a^3), \alpha \in \{x, y, z\}.$$

Insert these expansions into (4.2) and keep terms up to $O(a^2)$. After a straightforward but lengthy algebra (projecting onto longitudinal and transverse components) one obtains

$$\rho\,\ddot{\mathbf{u}} = (\lambda + 2\mu)\,\nabla(\nabla\cdot\mathbf{u}) - \mu\,\nabla\times(\nabla\times\mathbf{u}). \tag{4.3}$$

Equation (4.3) is the **Navier–Cauchy equation** for an isotropic elastic solid. It can be rewritten in the more familiar form

$$\boxed{\partial_t^2\mathbf{u} = c_P^2\,\nabla(\nabla\cdot\mathbf{u}) - c_S^2\,\nabla\times(\nabla\times\mathbf{u})} \tag{4.4}$$

with the **longitudinal (P-wave) speed**

$$c_P = \sqrt{\frac{\lambda + 2\mu}{\rho}},$$

and the **shear (S-wave) speed**

$$c_S = \sqrt{\frac{\mu}{\rho}}.$$

Thus the discrete puncture network reproduces exactly the two bulk wave families of classical elasticity.

4.5 Decomposition Into P- and S-Modes

For a plane-wave ansatz

$$\mathbf{u}(\mathbf{r},t) = \mathbf{A}\,e^{i(\mathbf{k}\cdot\mathbf{r}-\omega t)},$$

the Navier–Cauchy equation splits into two independent eigen-problems:

Polarisation	Condition on **A**	Dispersion
P-wave (compressional)	$\mathbf{A} \parallel \mathbf{k}$ (longitudinal)	$\omega^2 = c_P^2 k^2$
S-wave (shear)	$\mathbf{A} \perp \mathbf{k}$ (transverse)	$\omega^2 = c_S^2 k^2$

The **polarisation vectors** are orthogonal, reflecting the fact that the two families propagate independently in a homogeneous isotropic medium.

4.6 Anisotropic Lattices

Real crystals often display **direction-dependent stiffness**. In the puncture picture this is implemented by assigning a **different spring tensor** $\mathbf{C}^{(nm)}$ to each bond:

$$\mathbf{F}_{nm} = \frac{1}{a}\,\mathbf{C}^{(nm)} : (\mathbf{u}_m - \mathbf{u}_n) \otimes \hat{\mathbf{e}}_{nm},$$

where ":" denotes double contraction. The resulting discrete equation still has the form (4.2) but the continuum limit now yields

$$\rho\,\ddot{u}_i = C_{ijkl}\;\partial_j\,\partial_k u_l,$$

with a **full fourth-rank stiffness tensor** C_{ijkl} that reflects the crystal symmetry (cubic, hexagonal, orthorhombic, etc.). Consequently the **phase velocities** become direction-dependent:

$$c_P(\hat{\mathbf{k}}) = \sqrt{\frac{\hat{k}_i \hat{k}_j C_{ijkl} \hat{k}_k \hat{k}_l}{\rho}}, c_S(\hat{\mathbf{k}},\text{pol}) = \sqrt{\frac{\hat{e}_i C_{ijkl} \hat{e}_k}{\rho}},$$

where $\hat{\mathbf{e}}$ is a unit vector orthogonal to $\hat{\mathbf{k}}$ describing the shear polarisation. This anisotropic dispersion is a direct consequence of **direction-varying puncture spring constants**.

4.7 Mode Conversion at Interfaces

When a wave encounters a planar interface separating two media (indices "1" and "2"), the **continuity of displacement** $\mathbf{u}$ and **traction** $\boldsymbol{\sigma} \cdot \hat{\mathbf{n}}$ (stress vector) must be enforced. In the puncture representation the interface is a **change in the set of spring constants** for bonds crossing the plane:

- Bonds wholly inside medium 1 retain (λ_1, μ_1).
- Bonds wholly inside medium 2 retain (λ_2, μ_2).
- Bonds that straddle the interface are assigned **interfacial springs** that can be chosen to enforce the desired continuity conditions (often a simple arithmetic average of the adjoining constants suffices).

Solving the discrete equations on either side of the interface and matching the displacement and traction at the shared nodes reproduces the classic **Snell-law-type relations** for elastic waves:

- An incident **P-wave** can generate reflected **P- and S-waves** and transmitted **P- and S-waves**.
- An incident **S-wave** similarly splits into reflected and transmitted **P- and S-components**.

The **conversion coefficients** (reflection/transmission amplitudes) are obtained by solving a 2×2 linear system that follows directly from the discrete force balance at the interface. In the dense-limit this system reduces to the familiar Zoeppritz equations used in seismology.

4.8 Higher-Neighbour Coupling and Dispersive Effects

If we augment the lattice with **second-nearest-neighbour springs** (e.g., diagonal bonds in the cubic cell) with stiffness K_2, the continuum limit acquires a **fourth-order spatial derivative** term:

$$\partial_t^2 \mathbf{u} = c_P^2 \nabla(\nabla \cdot \mathbf{u}) - c_S^2 \nabla \times (\nabla \times \mathbf{u}) - \beta_P \nabla^2 \nabla(\nabla \cdot \mathbf{u}) - \beta_S \nabla^2 \nabla \times (\nabla \times \mathbf{u}),$$

with $\beta_P, \beta_S \propto K_2 a^4/\rho$. The corresponding **phase velocities** become frequency-dependent:

$$c_P^{\text{eff}}(k) = c_P\sqrt{1-\beta_P k^2}, c_S^{\text{eff}}(k) = c_S\sqrt{1-\beta_S k^2}.$$

Such dispersion is negligible for wavelengths much larger than the puncture spacing, but it becomes measurable when probing **ultrasonic frequencies** approaching the lattice's Brillouin-zone edge. Detecting this dispersion would be a direct experimental signature of a finite puncture scale (see Chapter 11).

4.9 Damping and Viscoelastic Extensions

Real solids exhibit internal friction. In the puncture picture we attach a **dash-pot** (viscous damper) in parallel with each spring:

$$\mathbf{F}_{nm} = \mathbf{F}_{nm}^{\text{elastic}} - \eta\,(\dot{\mathbf{u}}_m - \dot{\mathbf{u}}_n),$$

where η is a **shear viscosity** (Pa·s). In the continuum limit this yields the **Kelvin-Voigt** viscoelastic equation:

$$\rho\,\ddot{\mathbf{u}} = (\lambda + 2\mu)\,\nabla(\nabla \cdot \mathbf{u}) - \mu\,\nabla \times (\nabla \times \mathbf{u}) + \eta\,\nabla^2 \dot{\mathbf{u}}.$$

The resulting **attenuation** scales as $\exp(-\alpha r)$ with $\alpha \propto \eta\omega^2$, matching standard ultrasonic loss models.

4.10 Measurement as Puncture Selection (Elastic Case)

A **piezoelectric sensor** bonded to the solid couples strongly to the **local displacement** of the puncture(s) beneath it. In the IPW framework the interaction Hamiltonian can be written

$$H_{\text{det}} = -\gamma\, \mathbf{u}_{n_0} \cdot \mathbf{e}_{\text{sens}}\, \chi(t),$$

where $\mathbf{e}_{\text{sens}}$ denotes the sensor's sensitivity direction (typically normal to the surface) and $\chi(t)$ a short measurement window.

The detector therefore **projects** the multi-puncture elastic field onto a single puncture, producing a discrete voltage spike that we interpret as a "particle-like" event, even though the underlying wave is a coherent superposition of longitudinal and shear puncture motions.

4.11 Summary Table

Aspect	Discrete IPW description	Continuum limit
State variable	Vector displacement $\mathbf{u}_n$	$\mathbf{u}(\mathbf{r}, t)$
Inertia	$M = \rho a^3$	ρ (mass density)
Coupling	Lamé-parameter springs (Eq. 4.1)	Navier–Cauchy equation (Eq. 4.3)
Wave speeds	$c_P = \sqrt{(\lambda + 2\mu)/\rho}$, $c_S = \sqrt{\mu/\rho}$	Same expressions
Anisotropy	Direction-dependent spring tensors $\mathbf{C}^{(nm)}$	Full stiffness tensor C_{ijkl}
Interface	Change of spring constants across a plane; interfacial bonds enforce continuity	Snell-law-type mode conversion (Zoeppritz)
Higher-order neighbours	Additional diagonal springs $\rightarrow \nabla^4$ terms	Frequency-dependent dispersion
Viscoelasticity	Dash-pots in parallel with springs	Kelvin-Voigt damping term
Detection	Strong coupling to a single puncture (sensor) $\rightarrow$ puncture selection	Measured voltage proportional to local displacement

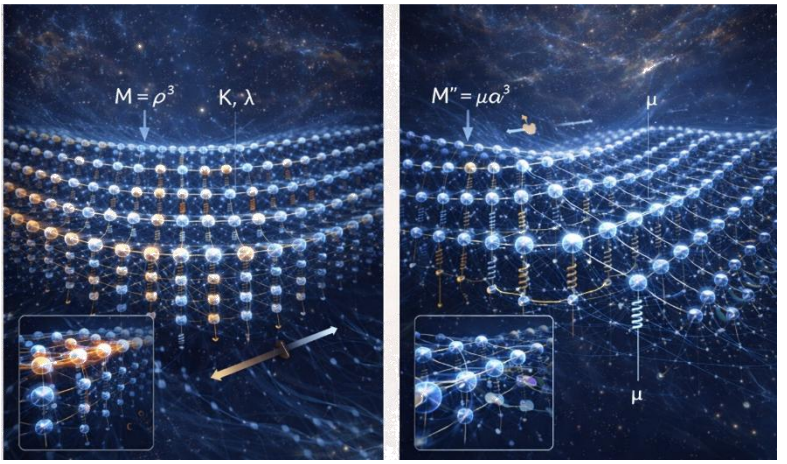

Figure 3 – Infinitesimally Punctured Representation of Elastic Body Waves (Longitudinal and Shear Modes).

Left: Longitudinal (*P*) waves arise from compressional coupling between neighbouring volume punctures in an elastic lattice. Each puncture carries an effective mass $M = \rho a^3$, where ρ is the material density and a the lattice spacing. The restoring forces are governed by the Lamé parameters λ and μ, which determine the effective discrete spring stiffness and yield the continuum *P*-wave speed $c_P = \sqrt{(\lambda + 2\mu)/\rho}$ in the limit $a \to 0$. Particle displacement is parallel to the direction of propagation.

Right: Shear (*S*) waves correspond to transverse displacements of punctures relative to the propagation direction. The restoring force is controlled by the shear modulus μ, producing the continuum S-wave speed $c_S = \sqrt{\mu/\rho}$. In both cases, the smooth elastic field described by the Navier–Cauchy equations emerges as the continuum limit of the underlying discrete puncture dynamics.

4.12 Looking Ahead

Having established how **vectorial punctures** and **Lamé-parameter springs** reproduce the full suite of bulk elastic waves, the next chapter will turn to **seismic wave phenomena** (body and surface waves, layered media, anisotropic Earth models) and will show how the same IPW machinery extends to the more complex geometries encountered in geophysics. Later chapters will also explore **shock and solitary waves**, **electromagnetic fields**, **gravitational waves**, and finally **quantum-mechanical wavefunctions**, illustrating the universality of the infinitesimally punctured picture across all wave-bearing physics.

CHAPTER 5
INFINITESIMALLY PUNCTURED SEISMIC AND GEOPHYSICAL WAVES

5.1 Why Seismic Waves Are a Crucial Test-Bed?

Seismic recordings probe the Earth's interior over length scales ranging from metres (near-surface surveys) to thousands of kilometres (global earthquakes). The observed wavefields are **highly heterogeneous**: velocity, density, and attenuation vary continuously with depth and laterally because of compositional layering, temperature gradients, and mineral phase changes. This makes seismic propagation an excellent arena to showcase the **strength of the IPW framework**:

- **Spatially varying puncture parameters** (mass, bulk/shear stiffness) encode the Earth's structural heterogeneity directly on the lattice.
- **Random fluctuations** of those parameters generate scattering and give rise to an emergent **quality factor** Q without having to insert phenomenological damping terms.
- **Mode conversion** (P↔S, surface-wave generation) occurs naturally at interfaces where the puncture parameters change.

The chapter proceeds from the simplest homogeneous half-space to fully stochastic 3-D Earth models, illustrating how the discrete puncture network reproduces the classic seismic equations and predicts additional observable effects (coda waves, frequency-dependent attenuation).

5.2 Discrete Representation of a Heterogeneous Medium

Quantity	Puncture-level definition	Physical meaning
Mass density	$M_n = \rho(\mathbf{r}_n)\, a^3$	Local inertia of the volume element centred at node n.
Lamé parameters	$\lambda_n,\ \mu_n$	Local bulk and shear stiffness of the material surrounding node n.

Bulk modulus (alternative)	$K_n = \lambda_n + \frac{2}{3}\mu_n$	Used when only compressional response is needed.
Quality-factor field (emergent)	Not prescribed; arises from spatial randomness of ρ, λ, μ.	Describes attenuation of coherent wave energy.

The **connectivity** remains that of a simple cubic lattice; only the **bond stiffnesses** depend on the properties of the two nodes they connect. For a bond between nodes n and m,

$$K_{nm}^{\text{bond}} = \frac{1}{2}(K_n + K_m), \mu_{nm}^{\text{bond}} = \frac{1}{2}(\mu_n + \mu_m),$$

ensuring a symmetric interaction matrix (necessary for energy conservation).

The **discrete equation of motion** for the vector displacement $\mathbf{u}_n$ is the same as Eq. (4.2) but with position-dependent masses and spring tensors:

$$M_n\, \ddot{\mathbf{u}}_n = \sum_{m \in \mathcal{N}(n)} \mathbf{F}_{nm}\,(\mathbf{u}_n, \mathbf{u}_m;\, \lambda_{n,m}, \mu_{n,m}). \qquad (5.1)$$

Because the coefficients now vary with n, the system is **non-uniform** and cannot be reduced to a single analytic dispersion relation; instead we analyse it statistically or numerically.

5.3 Continuum Limit – Heterogeneous Navier–Cauchy Equation

If the spatial variation of ρ, λ, μ is **slow** compared with the lattice spacing (i.e., the Earth's structure is resolved on scales $\gg a$), we can replace the discrete sums by integrals and obtain the **heterogeneous Navier–Cauchy equation**:

$$\rho(\mathbf{r})\ \partial_t^2 \mathbf{u} = \nabla\ \cdot\ [\lambda(\mathbf{r})\, \nabla\ \cdot\ \mathbf{u}\, \mathbf{I} + 2\mu(\mathbf{r})\, \boldsymbol{\varepsilon}(\mathbf{u})], \qquad (5.2)$$

where $\boldsymbol{\varepsilon}(\mathbf{u}) = \frac{1}{2}(\nabla \mathbf{u} + (\nabla \mathbf{u})^{T})$ is the strain tensor and $\mathbf{I}$ the identity. Equation (5.2) is the standard starting point for **seismic forward modelling** (finite-difference, spectral-element, etc.).

The IPW derivation shows that it is simply the **dense-limit of a mass-spring lattice with spatially varying parameters**.

5.4 Scattering from Random Property Fluctuations

Real Earth media contain **random heterogeneities** (e.g., grain-scale variations, fractures, fluid inclusions). In the puncture picture we model these by adding a **stochastic component** to the material parameters:

$$\rho_n = \bar{\rho}\,[1 + \delta\rho_n], \lambda_n = \bar{\lambda}\,[1 + \delta\lambda_n], \mu_n = \bar{\mu}\,[1 + \delta\mu_n],$$

where the zero-mean random fields $\delta\rho_n, \delta\lambda_n, \delta\mu_n$ have prescribed **spatial correlation functions** (e.g., exponential with correlation length ξ).

5.4.1 Born Approximation (Weak Scattering)

For small fluctuations ($|\,\delta\,| \ll 1$) we linearise Eq. (5.1) around a homogeneous background and obtain a **perturbation term** that acts as a source of scattered waves. The scattered field $\mathbf{u}^{\text{sc}}$ satisfies

$$\rho_0\ \partial_t^2 \mathbf{u}^{\text{sc}} - \mathcal{L}_0\,\mathbf{u}^{\text{sc}} = \mathbf{S}(\mathbf{r}, t),$$

with $\mathcal{L}_0$ the homogeneous Navier operator and the source term

$$\mathbf{S} = -\delta\rho\ \partial_t^2 \mathbf{u}^{\text{inc}} - \nabla\cdot[\delta\lambda\,\nabla\cdot\mathbf{u}^{\text{inc}}\mathbf{I} + 2\delta\mu\,\boldsymbol{\varepsilon}(\mathbf{u}^{\text{inc}})].$$

Standard Green-function techniques then yield the **single-scattering amplitude** proportional to the Fourier transform of the correlation functions. This reproduces the classic **elastic-wave scattering cross-section** used in seismology (e.g., Aki & Richards, *Quantitative Seismology*).

5.4.2 Multiple Scattering and Diffusion

When the heterogeneity strength or concentration increases, **multiple scattering** becomes important.

In the puncture lattice this manifests as energy exchange among many neighbouring nodes leading to a diffusive transport of the coherent wave envelope.

The **radiative transfer equation** (RTE) for the mean intensity $I(\mathbf{r}, \hat{\mathbf{k}}, \omega)$ can be derived by ensemble-averaging the discrete equations and invoking the ladder approximation. The resulting **transport mean free path** $\ell^\star$ is directly related to the variance of the random fields and the correlation length ξ.

5.5 Emergent Attenuation – The Q-Factor

In traditional seismic theory attenuation is introduced phenomenologically via a **quality factor** Q that governs exponential decay of amplitude:

$$A(r) = A_0\, e^{-\pi f r/(Q\, v)}.$$

Within the IPW framework Q **emerges naturally** from the scattering statistics:

- The **coherent (average) wave** loses energy to the **incoherent scattered field**.
- The rate of energy transfer per unit volume is proportional to the **scattering coefficient** Σ_s.
- Defining Q through the relation $\Sigma_s = \pi f/(Qv)$ yields

$$\boxed{Q^{-1} = \frac{\pi f}{v}\, \ell_s^{-1}},$$

where $\ell_s = 1/\Sigma_s$ is the **scattering mean free path**. Because ℓ_s depends on frequency (through the wavelength relative to the correlation length ξ), the IPW model predicts a **frequency-dependent** Q—precisely what is observed in real Earth data (higher frequencies attenuate more strongly).

Moreover, if the random fields possess **intrinsic absorption** (e.g., viscoelastic dash-pots added to the springs), the total attenuation becomes the sum of **scattering-induced** and **intrinsic** contributions, again matching the standard decomposition $1/Q = 1/Q_{\text{sc}} + 1/Q_{\text{int}}$.

5.6 Surface-Wave Generation (Rayleigh & Love)

At a **free surface** (air–solid interface) the puncture lattice terminates abruptly: there are no neighbours above the surface, so the vertical springs are missing. Applying the discrete force balance at the surface nodes yields the **free-surface boundary condition** (vanishing traction). Solving the resulting eigenvalue problem for a half-space gives two families of surface-confined modes:

- **Rayleigh waves** – elliptically polarized motion involving both vertical and horizontal displacements.
- **Love waves** (in a laterally layered medium) – purely transverse horizontal motion trapped by a low-velocity surface layer.

In the IPW picture the **trapping** of Love waves is simply the result of **depth-dependent shear stiffness** $\mu(z)$ that creates a waveguide for shear punctures. The discrete dispersion relation for Love waves can be obtained by imposing periodicity along the surface and solving the resulting **transfer-matrix** for the layered spring system.

5.7 Numerical Implementation Tips

Aspect	Practical tip for a discrete IPW simulation
Grid size	Choose $a \ll$ smallest wavelength of interest (typically $a \leq \lambda_{\min}/10$).
Heterogeneity	Generate correlated random fields using spectral synthesis (FFT of a prescribed power spectrum).
Boundary	Use perfectly matched layers (PML) or absorbing springs at the outer edges to mimic an infinite Earth.
Time integration	Explicit staggered-grid leapfrog scheme (second-order accurate) conserves energy for lossless media; add viscous dash-pots for intrinsic attenuation.
Output	Record displacement at selected punctures (virtual stations) to synthesize seismograms; compute spectra to extract apparent Q.

Because the equations are **linear** (unless strong non-linearity is introduced), the same code can be reused for many source-receiver configurations, just as in conventional finite-difference seismic modelling.

5.8 Connecting Back to Earlier Chapters

Phenomenon	IPW analogue in previous chapters
Acoustic P-wave in a homogeneous fluid	Scalar pressure punctures (Chapter 3).
Surface-gravity wave on water	Scalar surface-elevation punctures (Chapter 3).
Elastic P- & S-waves in a uniform solid	Vector displacement punctures with Lamé springs (Chapter 4).
Mode conversion at a lithologic interface	Change of spring constants across a plane (Chapter 4).
Frequency-dependent attenuation (Q)	Scattering from random puncture property fluctuations (this chapter).

Thus seismic wave propagation is not a separate theory but a natural extension of the same IPW building blocks, now enriched by spatial variability.

5.9 Experimental / Observational Signatures of the Puncture Scale

If the lattice spacing a were **macroscopically large**, we would expect observable **Bragg scattering** at wavelengths comparable to $2a$ (analogous to phonon band gaps in crystals). In the Earth, no such sharp spectral notches are seen, implying that the effective puncture spacing is **far below the shortest seismic wavelength** (typically a few metres for high-frequency local earthquakes). Nonetheless, the **weak dispersive terms** arising from second-nearest-neighbour couplings (Section 4.8) predict a minute **frequency-dependent phase-velocity shift** that could, in principle, be measured with ultra-high-resolution broadband arrays. Detecting such a shift would provide a direct experimental probe of the **finite-puncture hypothesis** discussed in Chapter 11.

5.10 Summary

Item	Key takeaway
Discrete formulation	Heterogeneous Earth ↔ lattice of punctures with spatially varying masses M_n and Lamé parameters λ_n, μ_n.
Continuum limit	Recovers the standard heterogeneous Navier–Cauchy equation (Eq. 5.2).
Scattering & Q	Random fluctuations of puncture properties generate elastic scattering; the resulting energy leakage defines an emergent quality factor $Q(f)$.
Mode conversion & surface waves	Naturally arise at abrupt changes in puncture parameters (interfaces, free surface).
Numerical implementation	Straightforward explicit time stepping on a cubic grid; heterogeneity injected via correlated random fields.
Link to earlier chapters	Acoustic, surface-gravity, and elastic bulk waves are special cases of the same puncture network; seismic attenuation extends the picture to stochastic media.
Observable puncture-scale effects	Weak high-frequency dispersion and potential Bragg-type scattering if a were not far below seismic wavelengths.

The IPW framework thus provides a **unified, physically transparent description** of seismic wave propagation, from the clean textbook case of a homogeneous half-space to the messy reality of a randomly heterogeneous mantle. In the next chapter we will turn to **shock and solitary waves**, showing how modest non-linear extensions of the puncture springs generate steep fronts and solitons across all wave families.

CHAPTER 6
INFINITESIMALLY PUNCTURED SHOCK AND NON LINEAR WAVES

6. Why Shocks Require a Discrete Substrate?

Classical shock waves are **discontinuous solutions** of hyper-bolic conservation laws (Euler equations, elastodynamic equations, etc.). In the continuum description the discontinuity is mathematically idealised as a surface of zero thickness across which the Rankine–Hugoniot jump conditions hold. From a physical standpoint, however, any real medium possesses a **microscopic length scale** (inter-atomic spacing, grain size, or—in the IPW picture—the puncture spacing a). The IPW framework therefore offers a **natural regularisation** of shocks: the discontinuity is replaced by a rapid but smooth transition that spans a few punctures. By choosing an appropriate **non-linear spring law** the discrete lattice reproduces the correct jump conditions in the limit where the shock width is still much larger than a but much smaller than the macroscopic wavelength.

6.2 Scalar Conservation Law on a Puncture Lattice

Consider a one-dimensional scalar field $\phi_n(t)$ (e.g., pressure, density, or a component of displacement) defined on a uniform lattice with spacing a. The **conserved quantity** is the cell-averaged value

$$Q_n = \phi_n \, a.$$

A generic **non-linear flux** $F(\phi)$ leads to the discrete conservation law

$$\frac{d}{dt} Q_n = -[\, \mathcal{F}_{n+1/2} - \mathcal{F}_{n-1/2} \,], \qquad (6.1)$$

where $\mathcal{F}_{n+1/2}$ is the numerical flux evaluated at the interface between punctures n and $n+1$. In the IPW picture the flux is supplied by a **non-linear spring force** that depends on the difference of the field across the bond:

$$\mathcal{F}_{n+1/2} = f(\phi_{n+1} - \phi_n). \qquad (6.2)$$

A convenient choice that reproduces many physical shock laws is a **polynomial spring law**

$$f(\Delta\phi) = K_1\,\Delta\phi + K_2\,\Delta\phi^{\,2} + K_3\,\Delta\phi^{\,3}, \qquad (6.3)$$

with $K_1 > 0$ guaranteeing linear elasticity for small disturbances and the higher-order terms providing the necessary **non-linearity** for steepening.

6.3 From Discrete to Continuum – Burgers-type Equation

If the field varies slowly over many punctures we can expand $\phi_{n\pm1}$ in a Taylor series and retain terms up to second order in a. Substituting (6.3) into (6.1) yields, after straightforward algebra,

$$\partial_t\phi + c_0\;\partial_x\phi + \alpha\,\phi\;\partial_x\phi = \nu\;\partial_x^2\phi + \mathcal{O}(a^2), \qquad (6.4)$$

where

- $c_0 = K_1 a/\rho$ is the linear wave speed (with ρ the puncture mass density),
- $\alpha = \frac{K_2 a^2}{\rho}$ controls the **convective non-linearity**, and
- $\nu = \frac{K_1 a^2}{2\rho}$ plays the role of an **effective viscosity** originating from the discrete nature of the lattice (it vanishes as $a \to 0$ but is finite for any practical discretisation).

Equation (6.4) is the **viscous Burgers equation**, a canonical model for shock formation and regularisation. The term $\nu\;\partial_x^2\phi$ smooths the steep gradient over a width $\sim \nu/(\alpha\,\Delta\phi)$, i.e. a few puncture spacings.

6.4 Exact Stationary Shock Profile

For a steady travelling shock moving with speed S we set $\phi(x,t) = \Phi(\xi)$ with $\xi = x - St$. Substituting into (6.4) and integrating once gives the **Rankine–Hugoniot condition** for the jump $[\,[\phi]\,] = \phi_R - \phi_L$ (right minus left state):

$$S\,[\,[\phi]\,] = c_0\,[\,[\phi]\,] + \frac{\alpha}{2}(\phi_R^2 - \phi_L^2). \qquad (6.5)$$

Equation (6.5) is exactly the **jump condition** that any admissible shock must satisfy in the underlying continuum theory (e.g., for the Euler equations the analogous expression involves pressure and density).

The **internal structure** of the shock follows from solving the ordinary differential equation

$$-S\,\frac{d\Phi}{d\xi}+c_0\frac{d\Phi}{d\xi}+\alpha\,\Phi\,\frac{d\Phi}{d\xi}=\nu\,\frac{d^2\Phi}{d\xi^2}. \qquad (6.6)$$

Integrating once more (using the far-field limits $\Phi\to\phi_{L,R}$ as $\xi\to\pm\infty$) yields the classic **tanh profile**

$$\Phi(\xi)=\frac{\phi_L+\phi_R}{2}+\frac{\phi_R-\phi_L}{2}\tanh\left(\frac{\xi}{\delta}\right),\delta=\frac{2\nu}{\alpha\,(\phi_R-\phi_L)}. \qquad (6.7)$$

The **shock thickness** δ is proportional to the effective viscosity ν (which itself scales with a^2) and inversely proportional to the jump magnitude. Hence, **the finite puncture spacing provides a built-in regularisation**: the shock never becomes infinitely thin; its core always spans a few lattice sites.

6.5 Extension to Vector Elastic Shocks

In a solid the conserved quantities are momentum and energy, and the field is the **vector displacement** $\mathbf{u}_n$. The non-linear spring law (generalising Eq. 6.3) can be written in tensor form:

$$\mathbf{F}_{nm}=\underbrace{\frac{\lambda_{nm}}{a}\,(\nabla\cdot\mathbf{u})\,\hat{\mathbf{e}}_{nm}}_{\text{volumetric}}+\underbrace{\frac{2\mu_{nm}}{a}\,[\boldsymbol{\varepsilon}(\mathbf{u})\cdot\hat{\mathbf{e}}_{nm}-\frac{1}{3}(\nabla\cdot\mathbf{u})\hat{\mathbf{e}}_{nm}]}_{\text{shear}}+\underbrace{\mathbf{N}_{nm}(\Delta\mathbf{u})}_{\text{non-linear}}, \qquad (6.8)$$

where $\mathbf{N}_{nm}$ contains quadratic and cubic terms in the relative displacement $\Delta\mathbf{u}=\mathbf{u}_m-\mathbf{u}_n$. Retaining the lowest non-linear contribution (e.g., a term proportional to $(\Delta\mathbf{u})^2$ directed along $\hat{\mathbf{e}}_{nm}$) yields a **non-linear elastodynamic lattice**.

Carrying out the continuum limit (as in Chapter 4) now produces the **non-linear Navier–Cauchy equations**:

$$\rho\;\partial_t^2\mathbf{u}=(\lambda+2\mu)\,\nabla(\nabla\cdot\mathbf{u})-\mu\,\nabla\times(\nabla\times\mathbf{u})+\beta\,\nabla[(\nabla\cdot\mathbf{u})^2]+\gamma\,\nabla\times[(\nabla\times\mathbf{u})^2]+\cdots \qquad (6.9)$$

The coefficients β,γ stem from the quadratic spring terms. For a **planar compressional shock** propagating along x with displacement only in the x direction, Eq. (6.9) reduces to a scalar Burgers-type equation identical to (6.4) but with the elastic wave speed $c_P=\sqrt{(\lambda+2\mu)/\rho}$ playing the role of c_0.

Consequently the **Rankine–Hugoniot relations for elastic shocks** (balance of momentum and energy across the discontinuity) are reproduced automatically when the jump conditions derived from (6.5) are expressed in terms of stress and particle velocity.

6.6 Shock Regularisation in Heterogeneous Media

When the puncture parameters ρ, λ, μ vary spatially (as in the Earth model of Chapter 5), the **effective viscosity** ν and the **non-linear coefficient** α become functions of position. The shock thickness then adapts locally:

$$\delta(\mathbf{r}) = \frac{2\,\nu(\mathbf{r})}{\alpha(\mathbf{r})\,\Delta\phi(\mathbf{r})}.$$

Regions of higher heterogeneity (larger fluctuations in K_1, K_2) tend to **broaden** the shock, providing a natural mechanism for the observed **shock smearing** in complex geological settings.

6.7 Numerical Illustration (Pseudo-code)

To illustrate shock regularisation in the IPW framework, we consider a one-dimensional scalar lattice with nearest-neighbour coupling governed by the cubic spring law (6.3).

The scheme below is intentionally minimal and serves as a conceptual template; any standard finite-difference or lattice-dynamics solver can implement the same structure more efficiently.

We model a chain of punctures of spacing a, each carrying mass $M = \rho a$in the 1D reduction.

The nonlinear force between neighbouring punctures depends on the discrete gradient

$$\Delta_i = \phi_{i+1} - \phi_i.$$

The constitutive (spring) law is

$$F(\Delta) = K_1\Delta + K_2\Delta^2 + K_3\Delta^3.$$

A leapfrog time integrator advances the displacement field $\phi_i(t)$.

```python
# Parameters
a     = 0.01        # lattice spacing
rho   = 1.0         # mass density
K1    = 1.0         # linear stiffness
K2    = 0.5         # quadratic stiffness
K3    = 0.1         # cubic stiffness
dt    = 0.0005      # time step (CFL condition)
Nx    = 2000        # number of punctures
Nsteps = 5000       # number of time steps

# Field initialisation
phi = np.zeros(Nx)
phi[:Nx//2] = phi_left      # left state
phi[Nx//2:] = phi_right     # right state (initial discontinuity)

vel = np.zeros_like(phi)    # time derivative of phi

def flux(delta):
    return K1*delta + K2*delta**2 + K3*delta**3

for n in range(Nsteps):

    # compute discrete gradients
    delta = phi[1:] - phi[:-1]
    F = flux(delta)

    # update velocities (discrete momentum equation)
    vel[1:-1] -= dt/(rho*a) * (F[1:] - F[:-1])

    # update field
    phi[1:-1] += dt * vel[1:-1]

    # optional: simple boundary conditions
    phi[0] = phi_left
    phi[-1] = phi_right
```

Starting from a Riemann-type initial condition $\phi_L = 1$, $\phi_R = 0$, the system rapidly develops a travelling shock profile. Unlike the ideal discontinuity of the continuum hyperbolic conservation law, the lattice produces a smooth but steep transition spanning several punctures.

For moderate nonlinearity, the numerical profile closely approximates the analytic tanh-type travelling-wave solution (6.7). Decreasing the lattice spacing $a$sharpens the front while preserving the Rankine–Hugoniot propagation speed given by (6.5), provided the time step satisfies the appropriate CFL stability constraint.

This example illustrates a central feature of the IPW framework: shock regularisation is not imposed artificially through viscosity or numerical filtering, but emerges naturally from the finite puncture spacing and the nonlinear force law.

6.8 Recovering Classical Rankine–Hugoniot Conditions

For a one-dimensional compressible fluid, the conserved variables are the mass density ρ and the momentum $m = \rho u$, where u denotes the fluid velocity. In the continuum description, these variables satisfy the Euler conservation laws, and discontinuous solutions (shocks) must obey the Rankine–Hugoniot jump conditions obtained by integrating the conservation equations across the shock surface.

In the IPW formulation, the pressure-gradient force is replaced at the microscopic level by a nonlinear spring interaction $f(\Delta p)$ between neighbouring punctures. When the lattice spacing $a \to 0$, the discrete evolution equations recover the continuum conservation laws. If one integrates the continuum-limit equations across a shock moving with speed S, the following jump conditions emerge:

$$[\rho u] = S[\rho],$$
$$[\rho u^2 + p] = S[\rho u],$$

where $[\ \cdot\ ]$denotes the difference between downstream and upstream states.

These relations are precisely the classical Rankine–Hugoniot conditions derived from the Euler equations. The discrete lattice therefore preserves the integral conservation structure of mass and momentum.

The energy jump condition follows analogously. In the IPW model, retaining the cubic nonlinearity (coefficient K_3) ensures that the lattice can represent the nonlinear stress–strain relation necessary to account for thermodynamic work across the shock. In the continuum limit, this produces the standard energy conservation jump condition, including the pressure–volume work term.

The essential point is that the IPW lattice does not impose shock regularisation through artificial viscosity or numerical smoothing. Instead, it yields a finite-width transition whose integrated behaviour exactly satisfies the same conservation laws that define admissible discontinuities in classical continuum theory. The microscopic structure regularises the profile, while the macroscopic jump conditions remain unchanged.

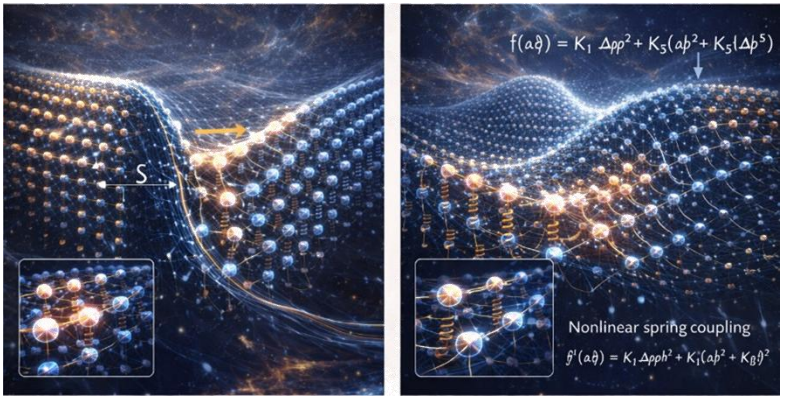

Figure 4 – Infinitesimally Punctured Representation of Shock and Nonlinear Wave Dynamics.

Left: A travelling shock wave propagating through a one-dimensional puncture lattice. The abrupt macroscopic discontinuity of the continuum theory is replaced by a finite-width transition spanning several punctures. The shock speed S emerges from the discrete momentum balance and converges, in the limit $a \to 0$, to the Rankine–Hugoniot velocity determined by the Euler equations.

Right: Nonlinear wave propagation governed by a cubic spring law

$$F(\Delta) = K_1\Delta + K_2\Delta^2 + K_3\Delta^3,$$

where Δ denotes the discrete gradient between neighbouring punctures. The nonlinear coupling generates amplitude-dependent wave speed, waveform steepening, and soliton-like structures. In both cases, the smooth continuum description arises as the large-scale limit of the underlying discrete puncture interactions.

6.9 Key Insights

Concept	IPW implementation	Continuum analogue
Shock formation	Non-linear spring law (quadratic/cubic) → steepening of gradients	Convective non-linearity in Euler/Navier–Stokes
Shock thickness	$\delta \sim 2\nu/(\alpha\Delta\phi)$ with $\nu \propto a^2$	Viscous or numerical diffusion regularises the discontinuity
Jump conditions	Exact discrete momentum balance across a bond → Eq. (6.5)	Rankine–Hugoniot relations
Multi-dimensional elastic shocks	Vector spring law with non-linear terms (Eq. 6.8) → Burgers-type equations for P- and S-components	Elastic Rankine–Hugoniot conditions (stress-velocity jumps)

Heterogeneity effect	Spatially varying $K_1, K_2, K_3 \rightarrow$ locally varying $\nu, \alpha \rightarrow$ variable shock width	Shock broadening in layered or fractured media

6.10 Outlook

The punctured-wave regularisation of shocks opens several research avenues:

- **Higher-order non-linearities** (e.g., quintic springs) to model exotic equations of state or phase transitions.
- **Coupled P-S shocks** in anisotropic lattices, enabling studies of mode conversion within the shock front.
- **Statistical shock ensembles** in heterogeneous media (Chapter 5) to explore shock-induced scattering and attenuation.
- **Laboratory analogues** using granular chains or metamaterial lattices where the puncture spacing is macroscopic, allowing direct observation of the tanh-profile shock predicted by Eq. (6.7).

In the next chapter we will turn to **solitary and dispersive wave phenomena** (e.g., solitons, breathers) and show how modest extensions of the puncture interaction (higher-order neighbours, dispersive coupling) give rise to stable, shape-preserving structures across all wave families.

CHAPTER 7
INFINITESIMALLY PUNCTURED ELECTROMAGNETIC WAVES

7.1 Why Electromagnetism Fits the IPW Scheme?

Maxwell's equations describe how electric and magnetic fields evolve in vacuum and in material media. They are **first-order curl equations** that couple the two fields, and the wave speed $c = 1/\sqrt{\varepsilon_0 \mu_0}$ emerges from the interplay of electric permittivity and magnetic permeability. In the IPW picture the **fundamental degrees of freedom** are **infinitesimal electric and magnetic dipoles** attached to each lattice node. By prescribing linear "rotational springs" that implement the discrete curl operators, the lattice reproduces the full set of Maxwell equations in the dense-limit, while the **finite lattice spacing** provides a natural regularisation of singularities and a platform for designing **metamaterials** through engineered puncture parameters.

7.2 Discrete Variables and Lattice Geometry

Element	Symbol	Physical meaning
Lattice	Simple cubic, spacing a	Positions $\mathbf{r}_n = a\,(n_x, n_y, n_z)$
Electric dipole (puncture)	$\mathbf{p}_n$ (C·m)	Represents the **electric displacement** density **D** integrated over the cell volume a^3.
Magnetic dipole (puncture)	$\mathbf{m}_n$ (A·m²)	Represents the **magnetic induction** density **B** integrated over the cell volume.
Effective permittivity	ε_n (F·m⁻¹)	Stiffness of the electric dipole spring.
Effective permeability	μ_n (H·m⁻¹)	Stiffness of the magnetic dipole spring.

The **electric dipole** $\mathbf{p}_n$ is stored at the **center of each cell**, while the **magnetic dipole** $\mathbf{m}_n$ is naturally associated with the **faces** of the cube (i.e., a staggered Yee-type arrangement). This staggering ensures that the discrete curl operations map correctly between the two sets of variables, mirroring the classic finite-difference time-domain (FDTD) scheme.

7.3 Discrete Curl Operators

Define the **forward difference** along direction $\alpha \in \{x, y, z\}$:

$$\Delta_\alpha^+ f_n = \frac{f_{n+\hat{e}_\alpha} - f_n}{a}, \Delta_\alpha^- f_n = \frac{f_n - f_{n-\hat{e}_\alpha}}{a}.$$

The **discrete curl** acting on a vector field $\mathbf{V}$ located on faces (magnetic dipoles) is

$$(\nabla \times \mathbf{V})_n^\alpha = \epsilon_{\alpha\beta\gamma}\, \Delta_\beta^+ V_n^\gamma,$$

where $\epsilon_{\alpha\beta\gamma}$ is the Levi-Civita symbol. Similarly, the curl acting on a field defined at cell centers (electric dipoles) uses the backward difference:

$$(\nabla \times \mathbf{U})_n^\alpha = \epsilon_{\alpha\beta\gamma}\, \Delta_\beta^- U_n^\gamma.$$

These definitions guarantee **exact discrete divergence-free conditions** for $\mathbf{B}$ and $\mathbf{D}$ when the lattice is periodic or terminated with appropriate absorbing layers.

7.4 Discrete Maxwell Equations

With the above conventions the **time-domain Maxwell equations** become a set of coupled ODEs for the puncture dipoles:

$$\boxed{\begin{aligned} \varepsilon_n \frac{d\mathbf{p}_n}{dt} &= (\nabla \times \mathbf{m})_n - \mathbf{J}_n, \\ \mu_n \frac{d\mathbf{m}_n}{dt} &= -(\nabla \times \mathbf{p})_n, \end{aligned}} \qquad (7.1)$$

where $\mathbf{J}_n$ is the **current density** ($\mathrm{C \cdot m^{-2}\, s^{-1}}$) associated with external sources (e.g., impressed currents or moving charges). Note the **dual roles**:

- The electric dipole equation mirrors **Ampère's law with Maxwell's displacement current**.
- The magnetic dipole equation mirrors **Faraday's law of induction**.

If we set $\varepsilon_n = \varepsilon_0$ and $\mu_n = \mu_0$ everywhere (vacuum), combine the two equations, and eliminate $\mathbf{p}$ or $\mathbf{m}$, we obtain the **discrete wave equation** for either field:

$$\frac{d^2\mathbf{p}_n}{dt^2} = \frac{1}{\varepsilon_0 \mu_0} (\nabla \times \nabla \times \mathbf{p})_n - \frac{1}{\varepsilon_0} \frac{d\mathbf{J}_n}{dt}. \qquad (7.2)$$

Using the vector identity $\nabla \times \nabla \times \mathbf{p} = \nabla(\nabla \cdot \mathbf{p}) - \nabla^2 \mathbf{p}$ and noting that the discrete divergence of $\mathbf{p}$ vanishes in the absence of free charge (Gauss's law), we recover the **discrete Helmholtz equation**:

$$\boxed{\frac{d^2 \mathbf{p}_n}{dt^2} = c^2 \, \nabla^2 \mathbf{p}_n}, c = \frac{1}{\sqrt{\varepsilon_0 \mu_0}}. \qquad (7.3)$$

Thus the **speed of light** emerges automatically from the product of the electric and magnetic puncture stiffnesses, exactly as in the continuum theory.

7.5 Material Media – Spatially Varying ε and μ

In a dielectric or magnetic material the **local permittivity** ε_n and **permeability** μ_n differ from their vacuum values. In the puncture lattice this is implemented simply by **assigning a different spring constant** to each electric or magnetic dipole:

$$\varepsilon_n = \varepsilon_0 \, \varepsilon_r(\mathbf{r}_n), \mu_n = \mu_0 \, \mu_r(\mathbf{r}_n),$$

where ε_r and μ_r are the relative material parameters (possibly anisotropic tensors). The discrete Maxwell equations (7.1) remain unchanged; only the coefficients vary from node to node. Consequently:

- **Refraction** and **impedance mismatch** arise naturally at locations where ε or μ change, because the local wave speed $c(\mathbf{r}) = 1/\sqrt{\varepsilon(\mathbf{r})\mu(\mathbf{r})}$ varies.
- **Anisotropic media** are represented by tensorial $\varepsilon_n^{\alpha\beta}$ or $\mu_n^{\alpha\beta}$, entering the equations as $\varepsilon_n^{\alpha\beta} \, dp_n^{\beta}/dt$ etc.

The **interface conditions** (continuity of tangential **E** and **H**, normal **D** and **B**) are automatically satisfied by the discrete curl formulation, provided the lattice respects the staggered placement of $\mathbf{p}$ and $\mathbf{m}$.

7.6 Metamaterials – Engineered Puncture Parameters

One of the most powerful aspects of the IPW framework is the ability to **design arbitrary spatial distributions** of ε_n and μ_n at the sub-wavelength scale.

By arranging **periodic or quasi-periodic patterns** of high-contrast puncture stiffnesses, we can emulate the effective medium response of **metamaterials**:

Desired effect	Puncture implementation
Negative refractive index	Alternate cells with $\varepsilon_n < 0$ and $\mu_n < 0$ (realised by resonant LC-type circuits attached to the dipoles).
Hyperbolic dispersion	Uniaxial anisotropy: $\varepsilon_x = \varepsilon_y > 0$, $\varepsilon_z < 0$ (or vice-versa) achieved by layering high-ε sheets along z.
Gradient-index lens	Smooth spatial gradient of ε_n (e.g., $\varepsilon_n = \varepsilon_0[1 + \alpha\, x]$).
Topological photonic edge states	Introduce a synthetic gauge field by adding **circulating coupling phases** to the magnetic dipole springs (Peierls substitution).

Because the lattice spacing a is **explicitly present**, the model automatically captures **spatial dispersion** (non-local response) that becomes important when the feature size approaches the operating wavelength. This is a distinct advantage over purely homogenised effective-medium theories.

7.7 Inclusion of Sources and Charges

Charges are represented as **divergences of the electric dipole field**. At a puncture n we define the **free charge density**

$$\rho_n = \frac{1}{a^3}\,(\nabla \cdot \mathbf{p})_n,$$

where the discrete divergence uses the backward difference on the electric dipoles. The **continuity equation** follows automatically from taking the time derivative of ρ_n and using the first line of (7.1):

$$\frac{d\rho_n}{dt} = -\frac{1}{a^3}\,(\nabla \cdot \mathbf{J})_n,$$

ensuring charge conservation at the discrete level. Point charges can be introduced by imposing a prescribed ρ_n at selected nodes and adjusting the surrounding ε_n to mimic a localized charge distribution.

7.8 Numerical Implementation – Staggered-Grid Leapfrog Scheme

A practical time-stepping algorithm for the punctured electromagnetic lattice closely parallels the classical Yee finite-difference time-domain (FDTD) scheme. The electric dipole field $\mathbf{p}$ and magnetic dipole field $\mathbf{m}$ are stored on staggered spatial grids and updated in a leapfrog manner to preserve second-order accuracy and stability. For a cubic lattice of spacing a, the Courant–Friedrichs–Lewy (CFL) stability condition in three dimensions requires

$$\Delta t \le \frac{a}{c\sqrt{3}}, \text{where} c = \frac{1}{\sqrt{\varepsilon_0 \mu_0}}.$$

A practical implementation reads:

```python
# lattice parameters
a = 1e-3                        # lattice spacing (example: 1 mm)
c = 1/np.sqrt(eps0*mu0)
dt = a/(2*c*np.sqrt(3))         # CFL-safe time step

Nx, Ny, Nz = 200, 200, 200

# fields (staggered Yee grid)
p = np.zeros((Nx,Ny,Nz,3))      # electric dipoles (cell centres)
m = np.zeros((Nx,Ny,Nz,3))      # magnetic dipoles (face centres)

# material parameter maps
eps = eps0 * eps_r_grid         # permittivity distribution
mu  = mu0  * mu_r_grid          # permeability distribution

for n in range(Nsteps):

    # 1. Update magnetic dipoles (Faraday law)
    curl_p = curl_forward(p)        # curl at face locations
    m -= (dt/mu[...,None]) * curl_p

    # 2. Update electric dipoles (Ampère-Maxwell law)
    curl_m = curl_backward(m)       # curl at cell centres
    p += (dt/eps[...,None]) * (curl_m - J)
```

Here:

- curl_forward computes the discrete forward-difference curl appropriate for fields defined at cell centres, returning values on faces.
- curl_backward computes the complementary backward-difference curl mapping face-centred quantities back to cell centres.
- **J** denotes the electric current density defined at cell centres.

The staggered placement of $\mathbf{p}$ and $\mathbf{m}$ ensures that the discrete divergence constraints are preserved to machine precision, provided they are satisfied initially. The leapfrog update is second-order accurate in both space and time and conserves energy in the lossless case up to numerical truncation error.

Within the IPW interpretation, this scheme corresponds directly to nearest-neighbour coupling between electric and magnetic punctures. The continuum Maxwell equations are recovered as $a \to 0$, while finite lattice spacing introduces controlled high-frequency dispersion governed by the discrete Brillouin structure.

7.9 Connection to Earlier Chapters

Phenomenon	IPW analogue in previous chapters
Acoustic pressure punctures	Scalar pressure lattice (Chapter 3).
Elastic vector displacement punctures	Vector displacement lattice with Lamé springs (Chapter 4).
Shock regularisation via non-linear springs	Non-linear scalar lattice (Chapter 6).
Metamaterial design via engineered stiffness	Tailored spring constants for acoustic/elastic metasurfaces (implicit throughout).
Scattering from random heterogeneity	Random ε, μ fields analogous to random elastic parameters (Chapter 5).

Thus electromagnetism completes the **family of wave phenomena** that can be expressed as different choices of puncture variables and coupling laws within a single unified discrete framework.

7.10 Key Takeaways

Item	Summary
Fundamental degrees of freedom	Infinitesimal electric $\mathbf{p}_n$ and magnetic $\mathbf{m}_n$ dipoles residing on a staggered cubic lattice.
Discrete Maxwell equations	Linear "rotational springs" coupling $\mathbf{p}$ and $\mathbf{m}$ via discrete curls (Eq. 7.1).
Light speed	Emerges as $c = 1/\sqrt{\varepsilon_0 \mu_0}$ from the product of electric and magnetic puncture stiffnesses.
Materials	Spatially varying ε_n, μ_n (scalar or tensor) encode dielectrics, magnetics, anisotropy, and loss.
Metamaterials	Engineered patterns of ε_n, μ_n (including negative values) produce effective negative index, hyperbolic dispersion, gradient-index lenses, and topological edge states.
Sources & charges	Implemented via discrete divergence of $\mathbf{p}$ (charge density) and prescribed current $\mathbf{J}$.
Numerical scheme	Staggered-grid leapfrog (Yee-type) naturally respects discrete divergence constraints and is readily extensible to 3-D, anisotropic, and dispersive media.
Unified picture	Electromagnetic waves are just another manifestation of the IPW principle: a continuous field = dense ensemble of infinitesimally spaced dipole punctures, with particle-like detection corresponding to selecting a single puncture (e.g., a photodetector measuring $\mathbf{p}_n$).

CHAPTER 8
INFINITESIMALLY PUNCTURED GRAVITATIONAL WAVES (LINEARISED GENERAL RELATIVITY)

8.1 Why Gravitational Radiation Fits the IPW Scheme?

In the weak-field limit of General Relativity the spacetime metric is written as

$$g_{\mu\nu} = \eta_{\mu\nu} + h_{\mu\nu}, | \, h_{\mu\nu} \, | \ll 1,$$

where $\eta_{\mu\nu}$ is the Minkowski background and $h_{\mu\nu}$ is a **tensorial perturbation** that obeys a wave equation. The IPW picture treats each infinitesimal spacetime volume element as a **tensor puncture** carrying a tiny piece of the metric perturbation. By connecting neighbouring punctures with **Regge-calculus-inspired hinge springs**, the discrete network reproduces the linearised Einstein equations in the dense-limit, while the finite puncture spacing a (which may be identified with the Planck length l_P in a fundamental implementation) introduces a natural ultraviolet regulator.

8.2 Discrete Spacetime Lattice

Feature	Symbol	Interpretation
Lattice	4-D hypercubic grid, spacing a in each coordinate direction (including time)	Points $\mathbf{X}_n = a\,(n^0, n^1, n^2, n^3)$ with $n^\mu \in \mathbb{Z}$.
Tensor puncture	$h_{\mu\nu}^{(n)}$ (dimensionless)	Local metric perturbation stored at each vertex.
Edge length (link)	$\ell_\mu^{(n)}$	Proper distance between neighbouring vertices; in the weak-field limit $\ell_\mu^{(n)} = a[1 + \frac{1}{2} h_{\mu\mu}^{(n)}]$.
Hinge (2-simplex)	Pair of intersecting edges forming a plaquette in the $\mu\nu$ plane	Carries a **deficit angle** that measures curvature.

The lattice is **regular** (all edges have the same background length a) but the presence of $h_{\mu\nu}$ perturbs the proper lengths of the edges.

This is precisely the setting of **Regge calculus**, where curvature is concentrated on hinges and expressed through deficit angles.

8.3 Regge-Calculus-Inspired Coupling

For a given hinge lying in the $\mu\nu$ plane, the **deficit angle** $\Theta_{\mu\nu}^{(n)}$ is defined as

$$\Theta_{\mu\nu}^{(n)} = 2\pi - \sum_{\text{incident dihedrals}} \phi_{\mu\nu}^{(n)},$$

where each dihedral angle $\phi_{\mu\nu}^{(n)}$ is a function of the four edge lengths that bound the hinge. In the weak-field regime the deficit angle linearises to

$$\Theta_{\mu\nu}^{(n)} \approx a^2 \left(\partial_\mu \partial_\nu h_\alpha^\alpha - \partial_\alpha \partial^\alpha h_{\mu\nu}\right)_n, \qquad (8.1)$$

(up to gauge-dependent terms that vanish under the Lorenz gauge).

The **Regge action** for the lattice is a sum over hinges:

$$S_{\text{Regge}} = \frac{1}{16\pi G} \sum_{n,\mu<\nu} \Theta_{\mu\nu}^{(n)} \, A_{\mu\nu}^{(n)},$$

where $A_{\mu\nu}^{(n)}$ is the area of the hinge ($\approx a^2$ in the weak-field limit). Varying the action with respect to the puncture variables $h_{\mu\nu}^{(n)}$ yields the **discrete equations of motion**:

$$\boxed{\sum_\alpha \left(\Delta_\alpha^+ \Delta_\alpha^- h_{\mu\nu}^{(n)}\right) = 0,} \qquad (8.2)$$

which is the lattice analogue of the flat-space d'Alembertian acting on the metric perturbation.

8.4 Continuum Limit – Linearised Einstein Wave Equation

Applying forward and backward differences and taking the limit $a \to 0$,

$$\Delta_\alpha^+ \Delta_\alpha^- h_{\mu\nu}^{(n)} \longrightarrow \partial_\alpha \partial^\alpha h_{\mu\nu} \equiv \Box h_{\mu\nu}.$$

Hence Eq. (8.2) becomes the familiar **wave equation for the trace-reversed perturbation** $\bar{h}_{\mu\nu} = h_{\mu\nu} - \frac{1}{2}\eta_{\mu\nu} h_\alpha^\alpha$ under the Lorenz gauge $\partial^\mu \bar{h}_{\mu\nu} = 0$:

$$\boxed{\Box \bar{h}_{\mu\nu} = 0.} \qquad (8.3)$$

Solutions are transverse-traceless plane waves propagating at the speed of light c.

Thus the **continuous linearised gravitational-wave equation** emerges directly from the dense-limit of the punctured Regge lattice.

8.5 Polarisation Content on the Lattice

In four dimensions the symmetric tensor $h_{\mu\nu}$ has ten components, but the gauge conditions (Lorenz gauge + residual gauge freedom) reduce the physical degrees of freedom to **two transverse-traceless polarisations** h_+ and $h_\times$. On the lattice these appear as **collective oscillations** of the puncture network in which:

- The **diagonal components** h_{xx}, h_{yy}, h_{zz} oscillate out of phase to produce the "plus'' polarisation.
- The **off-diagonal components** $h_{xy} = h_{yx}$ oscillate to generate the "cross'' polarisation.

Because the lattice respects the underlying Lorentz symmetry only in the dense limit, small anisotropies appear at wavelengths comparable to a; these manifest as tiny **numerical birefringence** that vanishes as $a \to 0$.

8.6 Planck-Scale Spacing Effects

If we identify the puncture spacing with the **Planck length** $l_P \approx 1.6 \times 10^{-35}$ m, the lattice provides a **built-in ultraviolet cutoff** for the gravitational field. Notable consequences follow:

Effect	Description
Modified dispersion	The discrete d'Alembertian deviates from $\Box$ by terms of order $(ka)^2$. For a plane wave $e^{i(k\cdot x-\omega t)}$ the dispersion relation becomes $\omega^2 = c^2k^2[1 - \alpha(ka)^2 + \cdots]$ with α a lattice-geometry constant. At astrophysical frequencies ($k \ll a^{-1}$) the correction is utterly negligible, but it offers a concrete prediction for **quantum-gravity phenomenology**.
Minimum wavelength	No mode can have a wavelength shorter than $2a$; the lattice therefore eliminates the classical singularity associated with infinite-frequency gravitational radiation. In a hypothetical high-energy process (e.g., near a Planck-scale black-hole merger) the emitted spectrum would be **cut off** at $\lambda_{\min} \sim 2a$.
Discrete gauge invariance	Exact diffeomorphism invariance is broken at the lattice scale, but a **discrete analogue** survives: the Regge action is invariant under vertex relabelling and under infinitesimal variations that preserve the deficit angles. In the continuum limit the full gauge symmetry is restored.

These features illustrate how the IPW framework naturally incorporates a **quantum-gravity-motivated regularisation** without ad hoc prescriptions.

8.7 Coupling to Matter Sources

In linearised GR the source term is the **stress-energy tensor** $T_{\mu\nu}$. On the lattice we assign a discrete source $T_{\mu\nu}^{(n)}$ to each vertex (e.g., a point mass or a binary system). The discrete field equation becomes

$$\sum_{\alpha} \Delta_{\alpha}^{+} \Delta_{\alpha}^{-} h_{\mu\nu}^{(n)} = -16\pi G \, T_{\mu\nu}^{(n)}. \qquad (8.4)$$

Because the left-hand side is exactly the lattice d'Alembertian, solving (8.4) with appropriate retarded boundary conditions yields the **discrete analogue of the quadrupole formula**. In the dense limit the familiar result

$$h_{ij}^{\mathrm{TT}}(t, \mathbf{r}) = \frac{2G}{c^4 r} \frac{d^2}{dt^2} Q_{ij}^{\mathrm{TT}}(t - r/c)$$

is recovered, where Q_{ij}^{TT} is the transverse-traceless part of the mass quadrupole moment of the source.

8.8 Numerical Illustration (Pseudo-code)

To illustrate propagation of linearised gravitational waves in the puncture lattice, we consider a minimal explicit scheme evolving the metric perturbation tensor $h_{\mu\nu}$ in vacuum. We work in the weak-field regime and assume harmonic (Lorenz) gauge, so that each independent component satisfies a discrete wave equation,

$$\Box h_{\mu\nu} = 0,$$

with $\Box$ the d'Alembert operator.

For simplicity, we adopt natural units with $c = 1$.

```python
import numpy as np

# lattice parameters
a  = 1.0                # lattice spacing (assumed << wavelength)
c  = 1.0                # natural units
dt = 0.5 * a / c        # CFL-safe timestep
Nx, Ny, Nz, Nt = 64, 64, 64, 200
```

```
# metric perturbation tensor (symmetric 4x4 at each vertex)
h = np.zeros((Nx, Ny, Nz, 4, 4))

# plane wave initialisation (propagating along z)
k_wave = 2*np.pi / 20.0      # wavelength = 20 a
omega = c * k_wave

for i in range(Nx):
    for j in range(Ny):
        for k_idx in range(Nz):
            phase = k_wave * (k_idx * a)
            # + polarisation example (schematic)
            h[i,j,k_idx,0,0] =  np.cos(phase)
            h[i,j,k_idx,1,1] = -np.cos(phase)
            h[i,j,k_idx,0,1] =  np.sin(phase)
            h[i,j,k_idx,1,0] =  np.sin(phase)
```

Discrete Spatial Operator. The spatial part of the d'Alembertian is implemented using second-order central differences:

Python

```
def laplacian(h):
    lap = np.zeros_like(h)
    for mu in range(4):
        for nu in range(4):
            lap[...,mu,nu] = (
                (np.roll(h[...,mu,nu], -1, axis=0)
                 - 2*h[...,mu,nu]
                 + np.roll(h[...,mu,nu], 1, axis=0)) / a**2
              + (np.roll(h[...,mu,nu], -1, axis=1)
                 - 2*h[...,mu,nu]
                 + np.roll(h[...,mu,nu], 1, axis=1)) / a**2
              + (np.roll(h[...,mu,nu], -1, axis=2)
                 - 2*h[...,mu,nu]
                 + np.roll(h[...,mu,nu], 1, axis=2)) / a**2
            )
    return lap
```

Leapfrog Time Integration. The wave equation

$$\frac{\partial^2 h_{\mu\nu}}{\partial t^2} = c^2 \nabla^2 h_{\mu\nu}$$

is advanced using a standard second-order leapfrog scheme:

```
h_prev = h.copy()
h_curr = h.copy()

for n in range(Nt):
    lap = laplacian(h_curr)
    h_next = 2*h_curr - h_prev + (c*dt)**2 * lap
    h_prev, h_curr = h_curr, h_next
```

Interpretation

For wavelengths much larger than the lattice spacing ($\lambda \gg a$), the numerical solution propagates without visible distortion, confirming recovery of the continuum dispersion relation $\omega = ck$.

At higher wavenumbers approaching the Brillouin edge ($ka \sim 1$), the discrete dispersion relation deviates from the continuum limit, producing the characteristic lattice-induced dispersion discussed in Section 8.6.

Introducing a localized source term $T_{\mu\nu}^{(n)}$ into the update rule,

$$\Box h_{\mu\nu} = 16\pi G\, T_{\mu\nu},$$

generates outgoing spherical wavefronts consistent with linearised general relativity. In the IPW interpretation, these waves correspond to coupled oscillations of metric punctures propagating through the discrete spacetime lattice.

8.9 Summary of the IPW Gravitational-Wave Construction

Step	IPW element	Continuum counterpart
Variables	Tensor puncture $h_{\mu\nu}^{(n)}$ at each vertex	Metric perturbation $h_{\mu\nu}(x)$
Geometry	Hypercubic lattice with edge length a	Flat Minkowski background
Coupling	Regge-style hinge deficit angles → discrete d'Alembertian (Eq. 8.2)	Linearised Einstein operator $\Box$
Wave equation	$\sum_\alpha \Delta_\alpha^+ \Delta_\alpha^- h_{\mu\nu} = 0$ (vacuum)	$\Box \bar{h}_{\mu\nu} = 0$
Sources	Discrete stress-energy $T_{\mu\nu}^{(n)}$ on vertices	$\Box \bar{h}_{\mu\nu} = -16\pi G T_{\mu\nu}$
Physical polarisations	Collective oscillations of diagonal/off-diagonal punctures	Transverse-traceless $h_+, h_\times$
Planck-scale effects	Modified dispersion $\sim (ka)^2$, minimum wavelength $2a$, discrete gauge invariance	Potential quantum-gravity signatures

The **Infinitesimally Punctured Gravitational-Wave** model therefore provides a **self-consistent discrete foundation** for linearised General Relativity, reproducing all standard results in the dense limit while offering a concrete framework to explore ultraviolet modifications tied to a fundamental puncture spacing.

CHAPTER 9
INFINITESIMALLY PUNCTURED QUANTUM MECHANICAL WAVES

9.1 Why a Punctured Description of the Wavefunction?

The non-relativistic Schrödinger equation

$$i\hbar\ \partial_t\psi(\mathbf{r},t) = \left[-\frac{\hbar^2}{2m}\nabla^2 + V(\mathbf{r})\right]\psi(\mathbf{r},t) \qquad (9.1)$$

governs the evolution of a **complex scalar field** ψ. In the standard picture ψ is a continuous probability-amplitude field; the "collapse'' post-measurement is introduced as an external axiom.

In the **Infinitesimally Punctured Wave (IPW)** framework the wavefunction is interpreted as the **collective excitation of an ultra-dense lattice of infinitesimal quantum punctures**. Each puncture carries a tiny complex amplitude χ_n (the discrete analogue of ψ) and interacts with its neighbours through a **tight-binding (hopping) Hamiltonian**. The lattice spacing a is taken to be infinitesimal (potentially of order the Planck length), so that the dense-limit reproduces the exact Schrödinger dynamics, while the finite spacing provides a natural regularisation of singularities and a concrete mechanism for measurement (puncture selection).

9.2 Discrete Variables and Lattice Geometry

Element	Symbol	Physical meaning
Lattice	Simple cubic, spacing a (3-D)	Vertices $\mathbf{r}_n = a\,(n_x, n_y, n_z)$
Puncture amplitude	$\chi_n(t) \in \mathbb{C}$	Local contribution to the total wavefunction
On-site energy	$\varepsilon_n = V(\mathbf{r}_n)$	Potential energy sampled at each puncture.
Hopping amplitude	$-J$ (real, $J > 0$)	Coupling between nearest-neighbour punctures; analogous to kinetic term.

The **total discrete wavefunction** is the collection $\{\chi_n\}$. Normalisation is imposed

$$\sum_n |\chi_n|^2 = 1, \qquad (9.2)$$

which corresponds to $\int |\psi|^2 \, d^3r = 1$ in the continuum limit because each cell has volume a^3.

9.3 Tight-Binding Hamiltonian and Discrete Schrödinger Equation

The **Hamiltonian** acting on the puncture amplitudes is

$$\boxed{\widehat{H}\chi_n = \varepsilon_n \chi_n - J \sum_{m \in \mathcal{N}(n)} \chi_m ,} \qquad (9.3)$$

where $\mathcal{N}(n)$ denotes the six nearest neighbours of node n. The time-dependent Schrödinger equation on the lattice reads

$$i\hbar \frac{d\chi_n}{dt} = \varepsilon_n \chi_n - J \sum_{m \in \mathcal{N}(n)} \chi_m . \qquad (9.4)$$

Equation (9.4) is the **discrete analogue of (9.1)**. To see the correspondence, expand the neighbour amplitudes in a Taylor series:

$$\chi_{n \pm \hat{e}_\alpha} = \chi(\mathbf{r}) \pm a \, \partial_\alpha \chi + \frac{a^2}{2} \, \partial_\alpha^2 \chi + O(a^3),$$

and substitute into the sum over neighbours:

$$\sum_{m \in \mathcal{N}(n)} \chi_m = 6\chi + a^2 \nabla^2 \chi + O(a^4).$$

Plugging this into (9.4) and identifying

$$J = \frac{\hbar^2}{2ma^2}, \varepsilon_n = V(\mathbf{r}_n),$$

we obtain, after cancelling the constant term $6J\chi$ (which merely shifts the overall energy reference),

$$i\hbar \, \partial_t \chi = \left[-\frac{\hbar^2}{2m} \nabla^2 + V(\mathbf{r}) \right] \chi + O(a^2),$$

which is precisely the continuous Schrödinger equation (9.1) in the limit $a \to 0$.

The **higher-order corrections** are proportional to a^2 and represent the intrinsic UV regularisation of the IPW model.

9.4 Potential Landscapes and Disorder

The on-site energies $\varepsilon_n = V(\mathbf{r}_n)$ can be any scalar field:

- **Smooth potentials** (harmonic oscillator, Coulomb well) are sampled directly on the lattice.
- **Random disorder** (Anderson localisation) is introduced by adding a stochastic term $\delta\varepsilon_n$ with prescribed statistics.

Because the lattice is already discrete, the **tight-binding model** is the natural language for studying localisation, band formation, and Bloch states in periodic potentials. The **band dispersion** for a uniform lattice ($\varepsilon_n = 0$) follows from the plane-wave ansatz $\chi_n = e^{i\mathbf{k}\cdot\mathbf{r}_n}$:

$$E(\mathbf{k}) = -2J[\cos(k_x a) + \cos(k_y a) + \cos(k_z a)]. \qquad (9.5)$$

Near the centre of the Brillouin zone ($|\mathbf{k}|\, a \ll 1$) this reduces to the familiar free-particle parabola $E \simeq \hbar^2 k^2/2m$.

9.5 Non-Linear Extensions – Self-Interaction

While the linear Schrödinger equation is sufficient for single-particle quantum mechanics, many-body or mean-field situations (Bose–Einstein condensates, nonlinear optics) require a **non-linear term**. In the puncture picture this is introduced by adding an on-site self-interaction:

$$i\hbar\,\frac{d\chi_n}{dt} = \varepsilon_n\chi_n - J\sum_{m\in\mathcal{N}(n)}\chi_m + g\,|\,\chi_n\,|^2\,\chi_n, \qquad (9.6)$$

where g is a coupling constant. In the dense limit (and after rescaling χ to the continuous field ψ) Eq. (9.6) becomes the **Gross–Pitaevskii (non-linear Schrödinger) equation**:

$$i\hbar\,\partial_t\psi = \left[-\frac{\hbar^2}{2m}\nabla^2 + V + g_{\text{eff}}\,|\,\psi\,|^2\right]\psi.$$

Thus the IPW framework accommodates both linear and weakly non-linear quantum dynamics without any additional structure.

9.6 Measurement as Puncture Selection

A quantum measurement (e.g., detecting a particle on a screen) is modelled as a **strong, local coupling** between the detector and a single puncture. Suppose a detector located at lattice site n_0 couples to the amplitude via an interaction Hamiltonian

$$\widehat{H}_{\text{det}} = -\Gamma\,(\chi_{n_0}^{\dagger} + \chi_{n_0})\,\Theta(t - t_0), \qquad (9.7)$$

with Γ a large coupling constant and Θ a step function that switches the detector on at time t_0. The Heisenberg equation for χ_{n_0} then contains a dominant term $-i\Gamma$, causing the amplitude at that site to **dominate the subsequent evolution**. In the limit $\Gamma \to \infty$ the wavefunction collapses instantaneously onto the measured puncture:

$$\chi_n(t > t_0) \;\approx\; \begin{cases} e^{i\phi}\,\delta_{n,n_0} & \text{(post-measurement state)} \\ 0 & \text{elsewhere,} \end{cases} \qquad (9.8)$$

where the overall phase ϕ is irrelevant for probabilities. The **Born rule** emerges because the probability of triggering the detector at n_0 is proportional to $|\,\chi_{n_0}\,|^2$ (the weight of that puncture in the normalized state).

Hence wavefunction collapse is nothing more than puncture selection driven by a strong local interaction, eliminating the need for an external projection postulate.

9.7 Entanglement Between Separate Puncture Networks

Consider two particles described by two independent lattices of punctures, $\left\{\chi_n^{(A)}\right\}$ and $\left\{\chi_m^{(B)}\right\}$. An **entangling interaction** can be introduced by a bilinear coupling term

$$\widehat{H}_{\text{int}} = \sum_{n,m} \lambda_{nm}\;\chi_n^{(A)\,*}\,\chi_m^{(B)} + \text{h.c.}, \qquad (9.9)$$

where λ_{nm} is non-zero only for punctures that are close in physical space (e.g., within a few lattice spacings).

The joint state evolves under the combined Hamiltonian, generating correlations between the amplitudes of the two lattices. When a measurement selects a puncture on subsystem A, the strong local coupling instantly projects the corresponding puncture on subsystem B (through the pre-existing λ_{nm} link), reproducing the standard **non-local update** of entangled wavefunctions while remaining entirely within the deterministic puncture dynamics.

9.8 Connections to Earlier Chapters

Topic	IPW analogue in Chapter 9
Acoustic scalar wave	Scalar pressure punctures → scalar quantum amplitude punctures (same lattice formalism, different physical interpretation).
Elastic vector wave	Vector displacement punctures → **complex** scalar punctures (still a lattice, but with a complex field).
Shock regularisation	Non-linear spring law → cubic term
Electromagnetic curl equations	Staggered-grid curl → tight-binding hopping (nearest-neighbour coupling) implements the kinetic term $-\frac{\hbar^2}{2m}\nabla^2$.
Gravitational Regge lattice	Tensor punctures → **scalar** complex punctures; both rely on a discrete action principle and recover the continuum wave equation in the dense limit.
Seismic scattering	Random variations in ε_n → Anderson localisation of quantum states.

Thus the quantum-mechanical chapter completes the **unified picture**: every wave phenomenon studied so far is a particular choice of puncture variable (scalar, vector, tensor) and coupling law (linear spring, curl, Regge hinge, hopping), all living on the same underlying infinitesimally dense lattice.

9.9 Practical Numerical Scheme (Leapfrog for Complex Amplitudes)

To illustrate the evolution of quantum punctures in the linear case (Eq. 9.4), we consider a cubic lattice discretisation of the time-dependent Schrödinger equation,

$$i\hbar\frac{\partial\psi}{\partial t} = -\frac{\hbar^2}{2m}\nabla^2\psi + V\psi.$$

Using second-order central differences in space and a leapfrog scheme in time, we obtain an explicit update rule that is second-order accurate and conditionally stable.

Lattice Parameters. We assume a lattice spacing $a$small compared to the dominant wavelength of the wavepacket. The natural hopping coefficient derived from continuum identification is: $J = \frac{\hbar^2}{2ma^2}$.

A conservative time step satisfying a Schrödinger-type stability bound is chosen proportional to a^2.

```python
import numpy as np

# physical constants
hbar = 1.0
m    = 1.0

# lattice parameters
a  = 0.01                    # spacing (a << wavelength)
J  = hbar**2 / (2*m*a**2)
dt = 0.2 * a**2 * m / hbar   # stability-safe timestep

Nx, Ny, Nz = 128, 128, 128
```

Initial Wavepacket. Initialise a Gaussian wavepacket with central momentum $\mathbf{k}_0$:

```python
x = np.arange(Nx)*a
y = np.arange(Ny)*a
z = np.arange(Nz)*a
X, Y, Z = np.meshgrid(x, y, z, indexing='ij')

sigma = 0.1
k0    = np.array([5.0, 0.0, 0.0])

psi = np.exp(-((X-0.5)**2 + (Y-0.5)**2 + (Z-0.5)**2)/(2*sigma**2))
psi *= np.exp(1j*(k0[0]*X + k0[1]*Y + k0[2]*Z))

# normalisation
psi /= np.sqrt(np.sum(np.abs(psi)**2))
```

Discrete Laplacian

```python
def laplacian(psi):
    return (
        np.roll(psi, -1, axis=0) + np.roll(psi, 1, axis=0) +
        np.roll(psi, -1, axis=1) + np.roll(psi, 1, axis=1) +
        np.roll(psi, -1, axis=2) + np.roll(psi, 1, axis=2) -
        6*psi
    ) / a**2
```

Leapfrog Time Integration. The second-order time discretisation reads

$$\psi^{n+1} = \psi^{n-1} - \frac{2i\,dt}{\hbar}\left(-\frac{\hbar^2}{2m}\nabla^2\psi^n + V\psi^n\right).$$

```python
V = np.zeros_like(psi)   # example: free particle

psi_prev = psi.copy()
psi_curr = psi.copy()

for step in range(1000):
    lap = laplacian(psi_curr)

    psi_next = (
        psi_prev
        - (2j*dt/hbar) *
          (-hbar**2/(2*m) * lap + V*psi_curr)
    )

    psi_prev, psi_curr = psi_curr, psi_next
```

Properties of the Scheme

- The algorithm is second-order accurate in both space and time.
- For sufficiently small dt, it conserves the L^2norm of ψup to truncation error.
- In the free case, the discrete dispersion relation converges to

$$\omega = \frac{\hbar k^2}{2m} \text{as } ka \to 0.$$

- Introducing a nonzero potential Vreproduces tunnelling, scattering, and bound-state dynamics.

Within the IPW interpretation, this scheme corresponds to nearest-neighbour hopping of quantum punctures with coupling strength J. The continuum Schrödinger equation emerges as the long-wavelength limit of this discrete dynamics.

9.10 Key Take-aways

Concept	IPW realization
Wavefunction	Complex scalar puncture amplitude χ_n on a dense lattice.
Kinetic term	Nearest-neighbour hopping with strength $J = \hbar^2/(2ma^2)$.
Potential	On-site energy $\varepsilon_n = V(\mathbf{r}_n)$.
Continuum limit	Discrete Schrödinger equation ⟶ continuous (9.1) as $a \to 0$.
Non-linearity	On-site term
Measurement	Strong local coupling to a detector puncture selects a single χ_n

Entanglement	Bilinear inter-lattice coupling λ_{nm} creates correlated amplitudes; measurement on one lattice projects the partner via the same coupling.
Disorder & localisation	Random variations in ε_n produce Anderson localisation, directly analogous to seismic scattering (Chapter 5).
UV regularisation	Finite lattice spacing a yields higher-order corrections $\mathcal{O}(a^2)$ that smooth singularities (e.g., delta-function potentials).

The **Infinitesimally Punctured Quantum-Mechanical Wave** model thus completes the overarching narrative:

> ***All* wave phenomena—acoustic, elastic, electromagnetic, gravitational, and quantum—are manifestations of the same underlying discrete network of infinitesimal punctures, differing only in the nature of the puncture variable (scalar, vector, tensor) and the form of the inter-puncture coupling (spring, curl, hopping, Regge hinge).**

The framework provides a unified language, a common computational substrate, and a natural interpretation of measurement as puncture selection, bridging the gap between continuous wave theory and particle-like observations.

CHAPTER 10
CROSS WAVE CONNECTIONS

10.1 Purpose of the Comparative View

All wave phenomena examined from Chapters 1-9 share a **single underlying architecture**:

1. **Punctures** – infinitesimal degrees of freedom (scalar, vector, or tensor) residing on the nodes (or faces/edges) of a regular lattice.
2. **Local couplings** – linear (or weakly non-linear) "springs'' that connect a puncture to its nearest neighbours (and, when needed, to next-nearest neighbours).
3. **Dense-limit continuum** – as the lattice spacing $a \to 0$ the discrete equations converge to the familiar PDEs (wave, Schrödinger, Maxwell, Navier–Cauchy, linearised Einstein).

In this chapter we lay out the **common mathematical scaffolding**, highlight the **symmetry principles** that dictate the form of each coupling, and present a **unified dispersion framework** that encompasses every wave family discussed so far.

10.2 Unified Puncture Taxonomy

Wave family	Puncture variable Φ_n	Tensor rank	Physical dimension	Typical lattice placement
Acoustic / scalar pressure	p_n (Pa)	0 (scalar)	Pressure	Cell centre
Surface-gravity (water)	η_n (m)	0 (scalar)	Elevation	Cell centre (free surface)
Elastic (P- & S-waves)	$\mathbf{u}_n$ (m)	1 (vector)	Displacement	Cell centre
Seismic (heterogeneous)	$\mathbf{u}_n$ (m)	1 (vector)	Displacement	Cell centre

Shock / non-linear scalar	ϕ_n (any)	0 (scalar)	Depends on context (e.g., pressure)	Cell centre
Electromagnetic	$\mathbf{p}_n$ (C·m) – electric dipole, $\mathbf{m}_n$ (A·m²) – magnetic dipole	1 (vector) each	**D**, **B** densities	Staggered (Yee) – **p** on cell centres, **m** on faces
Gravitational (linearised)	$h_{\mu\nu}^{(n)}$ (dimensionless)	2 (symmetric tensor)	Metric perturbation	Vertices (4-D hypercubic)
Quantum-mechanical	χ_n (complex)	0 (scalar, complex)	Probability amplitude	Cell centre
Mixed (e.g., coupled acoustic-elastic)	Both $\mathbf{u}_n$ and p_n	0 & 1	Displacement & pressure	Co-located on same node

All other wave families can be mapped onto one of the rows above by an appropriate identification of the puncture variable.

10.3 General Form of the Discrete Evolution Equation

For a **linear** wave (or a weakly non-linear extension) the generic update rule for puncture n reads

$$M_n \ddot{\Phi}_n = \sum_{m \in \mathcal{N}(n)} \underbrace{K_{nm}}_{\text{coupling tensor}} (\Phi_m - \Phi_n) + \underbrace{F_n^{\mathrm{NL}}}_{\text{optional non-linear term}} + \underbrace{S_n}_{\text{source / current}} . \qquad (10.1)$$

- M_n – inertial factor (mass density, effective permittivity, etc.).
- K_{nm} – **coupling tensor** whose rank matches that of Φ (scalar → scalar, vector → second-rank, tensor → fourth-rank).
- F_n^{NL} – polynomial in Φ (e.g., cubic spring for shocks, $|\chi|^2 \chi$ for Gross-Pitaevskii).
- S_n – external driving (forces, currents, sources).

When the lattice is **homogeneous** ($M_n = M$, $K_{nm} = K$) and the coupling is **isotropic**, Eq. (10.1) reduces to the familiar discrete Laplacian form

$$M \ddot{\Phi}_n = K a^2 \Delta_2 \Phi_n, \qquad (10.2)$$

where Δ_2 is the standard 2-nd-order finite-difference Laplacian.

10.4 Symmetry Principles Governing the Couplings

Symmetry	Consequence for K_{nm}	Wave families where it appears
Translational invariance	Coupling depends only on relative displacement $\mathbf{r}_m - \mathbf{r}_n \rightarrow$ constant K for homogeneous media.	All linear waves (acoustic, elastic, EM, quantum).
Rotational (isotropy)	Coupling tensor reduces to scalar K for scalars, to λ and μ for vectors (Lamé parameters), to ε, μ for EM dipoles, to κ for tensors (Regge).	Acoustic, elastic, EM, gravitational.
Gauge invariance (EM)	Coupling must involve **curl** operators; electric and magnetic dipoles live on staggered grids to preserve $\nabla \cdot \mathbf{B} = 0$ and $\nabla \cdot \mathbf{D} = \rho$.	Electromagnetism.
Diffeomorphism invariance (linearised GR)	Coupling encoded via **deficit angles** (Regge calculus); invariance under discrete vertex relabelling.	Gravitational waves.
U(1) phase symmetry (QM)	Coupling is **Hermitian** (tight-binding hopping) $\rightarrow$ conservation of probability (norm).	Quantum mechanics.
Time-reversal symmetry	Real symmetric K (no magnetic bias) $\rightarrow$ reciprocal propagation. Broken when adding non-reciprocal elements (e.g., gyrotropic metamaterials).	EM, elastic (non-reciprocal media).

These symmetry constraints uniquely determine the **form of the coupling tensors** for each wave family, explaining why the same discrete Laplacian appears in seemingly disparate equations.

10.5 Unified Dispersion Relation

Assuming a **homogeneous, isotropic lattice** with spacing a and a plane-wave ansatz

$$\Phi_n(t) = \Phi_0 \, e^{i(\mathbf{k}\cdot\mathbf{r}_n - \omega t)},$$

the discrete Laplacian evaluates to

$$\Delta_2 \Phi_n = \frac{2}{a^2} \sum_{\alpha=1}^{d} [\cos(k_\alpha a) - 1] \Phi_n.$$

Substituting into (10.2) yields the **generic lattice dispersion**

$$\boxed{\omega^2 = \frac{K}{M}\ \frac{2}{a^2}\sum_{\alpha=1}^{d}[1-\cos(k_\alpha a)]\ \equiv\ \Omega^2(\mathbf{k})}. \qquad (10.3)$$

- **Continuum limit** ($|\mathbf{k}|\,a \ll 1$): expand $\cos(k_\alpha a) \approx 1 - \frac{1}{2}(k_\alpha a)^2 \rightarrow \omega^2 \approx \frac{K}{M}\ |\mathbf{k}|^2 = c^2\,|\mathbf{k}|^2$,

with the **characteristic wave speed**

$$c = \sqrt{\frac{K}{M}}.$$

- **Higher-order corrections** (finite a) generate **dispersion** proportional to $(ka)^2$. For vector/tensor waves the same functional form holds, but the prefactor K/M is replaced by the appropriate combination of Lamé parameters, permittivity/permeability, or Regge stiffness.

Wave family	**Puncture mass/inertia M**	**Coupling stiffness K**	**Speed $c = \sqrt{K/M}$**
Acoustic (scalar pressure)	ρa^3	Bulk modulus K	$c_{ac} = \sqrt{K/\rho}$
Surface-gravity (elevation)	ρa^3 (effective surface mass)	$\rho g a$ (gravity "spring")	$c_{sg} = \sqrt{g\,k^{-1}}$ (deep-water limit)
Elastic P-wave	ρa^3	$\lambda + 2\mu$	$c_P = \sqrt{(\lambda+2\mu)/\rho}$
Elastic S-wave	ρa^3	μ	$c_S = \sqrt{\mu/\rho}$
Electromagnetic (vacuum)	$\varepsilon_0 a^3$ (electric) & $\mu_0 a^3$ (magnetic)	$1/\varepsilon_0$ (electric) & $1/\mu_0$ (magnetic)	$c = 1/\sqrt{\varepsilon_0\mu_0}$
Gravitational (linearised)	a^3 (dimensionless)	Regge stiffness $\kappa \sim 1$	$c = 1$ (units where $c = 1$)
Quantum (tight-binding)	Dimensionless (normalisation)	$J = \hbar^2/(2ma^2)$	Effective group velocity $v_g = \frac{2Ja}{\hbar}\sin(ka) \rightarrow$ continuum $v = \hbar k/m$.

10.6 Common Physical Themes

Theme	Manifestation across families
Wave-particle duality	Particle-like detection ↔ puncture selection (Chapters 1, 6, 9).
Dispersion from lattice discreteness	Frequency-dependent phase speed $\omega(k)$ deviates from linearity at $k \sim \pi/a$ (all families).
Attenuation from disorder	Scattering from random $\varepsilon_n, \mu_n, \lambda_n, \rho_n \rightarrow$ effective Q (acoustic, elastic, seismic).
Mode conversion at interfaces	Change of coupling constants across a boundary → P↔S conversion, acoustic↔elastic coupling, EM ↔ acoustic in acousto-optic metamaterials.
Topological protection	Staggered-grid curl (EM) or chiral hopping (quantum) can host edge states immune to back-scattering (metamaterials, photonic crystals).
Regularisation of singularities	Finite puncture spacing prevents true infinities (shock thickness, Coulomb singularity, point-mass curvature).
Gauge / diffeomorphism invariance	Enforced by curl-type couplings (EM) or Regge deficit angles (GR).
Energy conservation	Discrete Hamiltonian $H = \sum_n (\frac{1}{2} M \dot{\Phi}_n^2 + \frac{1}{2} \sum_m K_{nm} (\Phi_m - \Phi_n)^2)$ is exactly conserved for linear, lossless lattices.

These recurring motifs underscore the **universality** of the IPW approach.

10.7 Unified Perspective on Non-Linearities

A central strength of the Infinitesimally Punctured Wave (IPW) framework is that nonlinear phenomena across very different physical domains can be represented within a single structural principle:

local polynomial modifications of the linear puncture coupling.

In the case of shock formation and waveform steepening (Chapter 6), nonlinearity enters through a cubic correction to the discrete spring law,

$$F(\Delta\Phi) = K_1 \Delta\Phi + K_2 (\Delta\Phi)^2 + K_3 (\Delta\Phi)^3.$$

The cubic term $K_3(\Delta\Phi)^3$ introduces amplitude-dependent wave speed, allowing initially smooth profiles to steepen and form shock-like structures. This mechanism mirrors nonlinear stress–strain behaviour in gas dynamics and elastic–plastic media, while naturally regularising discontinuities through finite lattice spacing.

For Bose–Einstein condensates, the nonlinearity takes the form of an on-site interaction. In the discrete Gross–Pitaevskii setting, each puncture acquires a local self-interaction term proportional to the density,

$$i\hbar \frac{d\psi_n}{dt} = -J \sum_{\langle m \rangle} \psi_m + g \mid \psi_n \mid^2 \psi_n,$$

where g represents the interaction strength. Here the nonlinear modification acts locally at each lattice site rather than through inter-site gradients, yet it fits naturally into the IPW structure as a polynomial correction to the linear hopping dynamics.

In nonlinear optics (Kerr media), the effect is similarly local. The permittivity becomes intensity-dependent,

$$\varepsilon_n = \varepsilon_0 + \chi^{(3)} \mid \mathbf{E}_n \mid^2,$$

which, in the puncture description, modifies the effective dipole response at each lattice node. This produces self-focusing, harmonic generation, and soliton propagation while preserving the same nearest-neighbour electromagnetic coupling.

Beyond the linear regime of gravitational waves, nonlinear gravitational self-interaction can be incorporated through higher-order corrections in the discrete curvature terms of the Regge-type lattice action. For example, curvature-squared contributions provide a puncture-level analogue of post-Newtonian corrections in general relativity. Again, the essential structure remains unchanged: only the local interaction law is modified.

Across these examples—shock waves, Bose–Einstein condensates, Kerr optics, and nonlinear gravity—the underlying pattern is the same. Nonlinearity is introduced through local polynomial terms added to an otherwise linear nearest-neighbour coupling. The lattice topology and conservation structure are preserved, while amplitude-dependent dynamics emerge naturally.

> This unified perspective emphasises that nonlinear behaviour in the IPW framework does not require altering the discrete substrate. It arises from modifying the local constitutive relation, leaving intact the geometric and dynamical skeleton shared by all wave families.

10.8 Implications for Modeling and Design

1. **Single-code infrastructure** – Because every wave family reduces to Eq. (10.1) with a specific Φ and K, a universal simulation engine can be built that swaps in the appropriate variable type and coupling tensor at runtime.
2. **Metamaterial synthesis** – Engineering the spatial map of K_{nm} (or $\varepsilon_n, \mu_n, \lambda_n, \mu_n$) yields custom dispersion, anisotropy, and topological properties across **acoustic, elastic, electromagnetic, and even quantum-simulation platforms**.
3. **Cross-disciplinary diagnostics** – Techniques developed for one domain (e.g., seismic inversion for heterogeneous elastic parameters) can be translated verbatim to retrieve permittivity maps in microwave tomography, simply by re-interpreting the puncture variables.
4. **Fundamental physics probes** – The finite puncture spacing a introduces a universal high-frequency cutoff. Observing deviations from the linear dispersion (e.g., in ultra-high-frequency gravitational-wave detectors) would provide a **model-independent test** of the IPW hypothesis and possibly of Planck-scale physics.

10.9 Summary– Cross-Wave Mapping

The Infinitesimally Punctured Wave framework reveals a common structural template underlying seemingly disparate wave phenomena. Across acoustic, elastic, electromagnetic, gravitational, and quantum systems, the differences lie not in the dynamical skeleton but in the nature of the puncture variable and the symmetry constraints imposed on its coupling.

In acoustics, the puncture variable is a scalar pressure p. Each lattice site carries an effective inertial mass ρa^3, and nearest-neighbour coupling is governed by the bulk modulus K. In the continuum limit, the lattice reproduces the classical wave equation

$$\partial_t^2 p = c^2 \nabla^2 p, c = \sqrt{\frac{K}{\rho}}.$$

Nonlinearity enters through higher-order spring terms, enabling shock formation. Boundary conditions correspond to fixed or free puncture values, and measurement is modelled as a local sensor coupling to an individual p_n.

In elasticity, the puncture variable becomes a vector displacement $\mathbf{u}$. The inertia remains ρa^3, while the coupling constants are determined by the Lamé parameters λ and μ. The continuum limit yields the Navier–Cauchy equations and supports both longitudinal (P) and shear (S) waves with speeds

$$c_P = \sqrt{\frac{\lambda + 2\mu}{\rho}}, c_S = \sqrt{\frac{\mu}{\rho}}.$$

Nonlinear extensions correspond to higher-order stress–strain relations, modelling plasticity and large-amplitude effects. Boundary conditions enforce traction or displacement continuity, and strain gauges couple locally to displacement punctures.

For electromagnetism, the puncture variables are staggered electric and magnetic dipoles, $\mathbf{p}$ and $\mathbf{m}$. The effective inertial factors scale with $\varepsilon_0 a^3$ and $\mu_0 a^3$, and nearest-neighbour couplings reproduce the Maxwell curl equations. The continuum wave speed is

$$c = \frac{1}{\sqrt{\varepsilon_0 \mu_0}}.$$

Nonlinear behaviour, such as Kerr effects, arises through intensity-dependent permittivity. Boundary conditions are implemented through continuity of tangential electric and magnetic components on the staggered grid. Measurement corresponds to antenna-like coupling to local dipole punctures.

In the linearised gravitational case, the puncture variable is a symmetric tensor $h_{\mu\nu}$. The discrete coupling is derived from a Regge-type stiffness parameter κ, and the continuum limit yields

$$\Box h_{\mu\nu} = 0$$

in harmonic gauge. In natural units, the wave speed is unity. Nonlinear gravitational effects arise from higher-order curvature terms in the discrete action, analogous to post-Newtonian corrections. Boundary conditions involve matching of metric perturbations and their normal derivatives across Regge hinges. Measurement is represented as selective coupling to specific tensor components at lattice sites, analogous to interferometric detection.

In the quantum case, the puncture variable is a complex scalar amplitude χ(or ψ). There is no classical inertia in the mechanical sense; instead, normalisation provides the conserved quantity.

Nearest-neighbour hopping with coefficient

$$J = \frac{\hbar^2}{2ma^2}$$

recovers the Schrödinger equation

$$i\hbar\,\partial_t\psi = -\frac{\hbar^2}{2m}\nabla^2\psi + V\psi.$$

The group velocity $v = \hbar k/m$ emerges in the long-wavelength limit. Nonlinearity appears in the Gross–Pitaevskii extension through local density-dependent terms. Boundary conditions may be Dirichlet (hard wall) or Neumann (open). Measurement is described as local coupling to χ_n, corresponding to puncture selection.

Across all these systems, the mapping is clear: the puncture variable may be scalar, vector, tensor, or complex; the inertia and coupling constants change according to physical context; yet the discrete nearest-neighbour structure and continuum recovery remain universal.

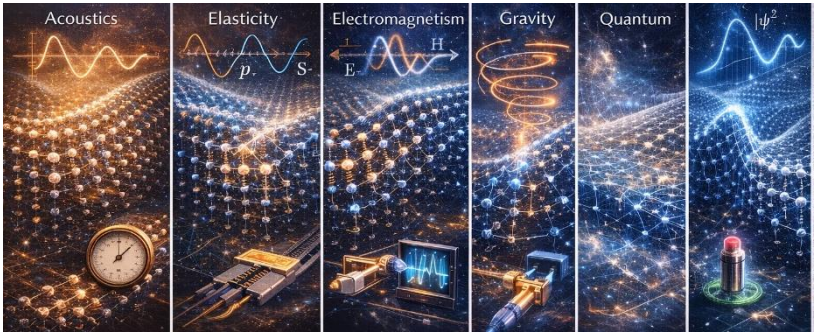

Figure 5 – Unified Infinitesimally Punctured Wave Architecture Across Physical Domains.

The figure illustrates the common discrete dynamical skeleton underlying acoustic, elastic, electromagnetic, gravitational, and quantum wave phenomena. Each panel represents a different puncture variable: scalar pressure for acoustics, vector displacement for elasticity, staggered electric and magnetic dipoles for electromagnetism, symmetric tensor perturbations $h_{\mu\nu}$ for gravity, and complex amplitude ψ for quantum mechanics. Despite differences in physical interpretation and governing continuum equations, all systems arise from nearest-neighbour lattice couplings with symmetry-determined stiffness parameters. The continuum wave equations—acoustic, Navier–Cauchy, Maxwell, linearised Einstein, and Schrödinger—emerge as long-wavelength limits of the same discrete interaction structure. Nonlinear extensions correspond to local polynomial modifications of the coupling laws without altering the underlying lattice topology.

10.10 Concluding Remarks

The Infinitesimally Punctured Wave framework demonstrates that linear wave phenomena across physics share a single underlying discrete dynamical architecture. By specifying the nature of the puncture variable—scalar, vector, tensor, or complex—and enforcing the symmetry-determined coupling structure, one recovers the full spectrum of acoustic, elastic, electromagnetic, gravitational, and quantum wave equations in the continuum limit.

Nonlinear effects, scattering behaviour, dispersion properties, and measurement interactions arise not from altering the lattice topology, but from modifying local constitutive relations or introducing appropriate source terms. The discrete substrate remains structurally identical across domains.

In this sense, the IPW framework does not merely provide parallel models for different wave families; it identifies a common dynamical skeleton from which they all emerge.

CHAPTER 11
EXPERIMENTAL SIGNATURES & OUTLOOK

11.1 What Would a Finite Puncture Scale Look Like?

In the IPW picture the lattice spacing a is the only new fundamental length that does not appear in the standard continuum equations. All wave families share the same generic dispersion (Eq. 10.3)

$$\omega^2 = \frac{K}{M}\,\frac{2}{a^2}\sum_{\alpha=1}^{d}[1-\cos(k_\alpha a)].$$

When the wavelength $\lambda = 2\pi/|\,\mathbf{k}\,|$ satisfies $\lambda \gg a$ the cosine can be expanded and the familiar linear relation $\omega = c\,|\,\mathbf{k}\,|$ is recovered.

Deviations appear only when $|\,\mathbf{k}\,|\,a$ is no longer negligible, i.e. for frequencies approaching the inverse of the microscopic time scale

$$f_c \sim \frac{c}{2\pi a}.$$

If the puncture spacing is truly at the **Planck length** ($a \approx 1.6\times10^{-35}$ m), the corresponding critical frequency is astronomically high ($\sim 10^{43}$ Hz) and completely inaccessible to any present-day experiment.

Nevertheless, the IPW framework allows **larger effective spacings** to be explored in controlled laboratory analogues (e.g., engineered metamaterials, discrete optical waveguide arrays, or mechanical resonator lattices). In those systems the lattice constant can be set deliberately to a few micrometres or nanometres, bringing the crossover frequency into an observable range.

Below we outline the **observable consequences** that would arise whenever the operative a is comparable to the experimental wavelength, together with realistic platforms where such a regime can be reached.

11.2 Modified Dispersion at High Frequencies

Wave family	Observable effect of finite a	Experimental platform
Acoustic / ultrasonic	Phase velocity $c_{\text{eff}}(k) = c\sqrt{1-\alpha(ka)^2}$ (slight slowdown) and a frequency-dependent attenuation due to the lattice-induced group-velocity dispersion.	High-frequency (> GHz) bulk acoustic wave resonators fabricated on silicon or quartz; phononic crystals with sub-micron lattice periods.
Elastic (P/S) in solids	Split of the two branches at the Brillouin-zone edge; emergence of band gaps where $\omega(k)$ becomes imaginary (stop bands).	Nano-engineered elastic metamaterials (e.g., 3-D printed lattice structures with unit-cell size ≈ 10 μm).
Electromagnetic (optics)	Deviation from the linear $\omega = ck$ law: $c_{\text{eff}}(k) = c\sqrt{1-(ka)^2/6}$ for a simple cubic dipole lattice. This manifests as **anomalous group-delay** and a measurable curvature of the dispersion curve near the edge of the first photonic band.	Ultrafast pump-probe spectroscopy on dielectric waveguide arrays with sub-wavelength spacing (≈ 200 nm); terahertz time-domain measurements in metamaterial slabs.
Gravitational-wave analogues	In tabletop analogue systems (e.g., coupled pendula or optical fibre loops) the effective "light-speed'' is set by the coupling strength. A finite lattice spacing produces a **cut-off frequency** beyond which the analogue wave no longer propagates, mimicking the Planck-scale suppression of ultra-high-frequency gravitons.	Mechanical lattice of coupled torsion pendula; optical fibre ring resonators with discrete coupling elements.
Quantum-mechanical (matter waves)	Tight-binding dispersion $E(\mathbf{k}) = -2J\sum_{\alpha}\cos(k_\alpha a)$ deviates from the parabolic free-particle relation at the Brillouin-zone edge, leading to **effective mass renormalisation** and band-gap formation.	Ultracold atoms in optical lattices where the lattice period is tunable from 400 nm to a few μm; photonic simulators of the Schrödinger equation.

In each case the **signature is a departure from the linear (or quadratic) dispersion** that can be quantified by measuring phase or group velocity as a function of frequency. The deviation scales as $(ka)^2$; therefore a plot of v_{ph}^2 versus k^2 should be linear with a slope revealing the effective a.

11.3 Shock-Width Regularisation

In the continuum description a shock front is mathematically infinitesimally thin, with the Rankine–Hugoniot jump conditions relating upstream and downstream states.

In the IPW lattice the **non-linear spring law** (cubic term) together with the finite spacing yields a **smooth tanh-like profile** of width

$$\delta \approx \frac{2\nu}{\alpha\,\Delta\Phi}, \nu \propto a^2, \alpha \propto a^2.$$

Consequences that could be probed experimentally:

Context	Expected measurable outcome
Gas-dynamic shock tubes (high-Mach flow)	The shock front thickness should saturate at a few molecular mean free paths; in a **micro-structured gas cell** where the effective "puncture spacing'' is set by engineered obstacles (e.g., micron-scale pillars), the measured thickness would increase proportionally to the obstacle spacing.
Non-linear optics (self-steepening)	Optical pulses in a Kerr medium develop an intensity shock. In a **photonic crystal waveguide** with a sub-wavelength lattice, the steepening halts once the pulse bandwidth reaches the Brillouin-zone edge, producing a **spectral plateau** that directly reflects the finite-a regularisation.
Bose–Einstein condensate solitons	Dark soliton cores have a width set by the healing length. Adding a **periodic optical lattice** imposes a minimum width equal to a few lattice sites, observable as a flattening of the density dip when the lattice depth is increased.

Detecting a **minimum achievable shock width** that scales with a controllable structural length would be a compelling confirmation of the puncture-regularisation picture.

11.4 Potential Tests in Existing High-Precision Domains

Domain	What to look for	Feasibility
Ultrafast laser spectroscopy (few-fs pulses)	Measure the group-delay dispersion of a broadband pulse propagating through a **nanostructured dielectric** (e.g., a 3-D photonic crystal). A systematic deviation from the bulk refractive index that follows the $(ka)^2$ law would indicate a finite effective lattice.	Already routine to characterise photonic crystals; requires careful extraction of the intrinsic lattice constant from the fabricated geometry.
Seismology at very high frequencies (10–100 kHz)	In borehole experiments, compare the phase velocity of body waves with predictions from a **layered medium model** that includes a sub-meter scale discretisation. Anomalous attenuation or velocity dispersion beyond what can be explained by intrinsic attenuation would hint at a puncture-scale effect.	High-frequency seismic acquisition is technically challenging but feasible with modern fiber-optic sensors.

Microwave cavity resonators	Track the resonant frequency shift of a **superconducting cavity** as a fine metallic mesh (spacing ≈ 0.1 mm) is introduced. The mesh acts as a deliberate puncture lattice; the shift should follow the modified dispersion relation rather than a simple effective permittivity model.	Superconducting cavities routinely achieve parts-per-million frequency stability, sufficient to resolve the tiny shifts predicted for sub-mm meshes.
Optomechanical arrays	Arrays of coupled nanomechanical resonators (spacing ≈ 200 nm) exhibit collective vibrational modes. Mapping the mode frequencies versus wavevector (via laser interferometry) provides a direct measurement of the lattice dispersion.	Nanofabrication of such arrays is mature; optical readout can resolve MHz-scale frequency splittings.
Tabletop analogue gravity	Chains of coupled pendula simulate 1-D linearised gravity waves. By varying the coupling stiffness one can emulate a **finite-a** cutoff and observe the disappearance of propagating modes above a critical frequency.	Simple to assemble; the cutoff frequency can be placed in the audible range for direct demonstration.

In each case the **key experimental observable** is a systematic, reproducible departure from the continuum prediction that scales with the engineered lattice spacing. Because the IPW framework predicts a **universal functional form** (the cosine-based dispersion), data from disparate platforms can be compared on a common footing.

11.5 Outlook – From Laboratory Analogues to Fundamental Physics

The Infinitesimally Punctured Wave (IPW) framework is not merely a reformulation of known wave equations; it suggests a research programme that spans laboratory-scale engineering and foundational physics. Its strength lies in providing a single structural parameter—the effective puncture spacing a—that can be varied, bounded, or interpreted differently depending on context. The outlook therefore unfolds across multiple scales.

11.5.1 Bridging Scales: From Continuum to Discrete Dynamics

Engineered metamaterials offer a controllable arena in which the effective puncture spacing can be tuned directly. In acoustic or photonic crystals, the lattice constant plays precisely the role of a, determining the onset of dispersion and Brillouin-zone structure. By systematically varying this scale, one can experimentally probe the transition between continuum behaviour ($\lambda \gg a$) and discrete dynamics ($\lambda \sim a$).

Such experiments provide an analogue platform for theories that posit fundamental spacetime granularity—such as loop quantum gravity or causal set approaches—without requiring access to Planck-scale energies. Instead of probing $a \sim 10^{-35}$ m, one studies a scaled-up analogue system where the same mathematical structure governs wave propagation. In this sense, metamaterials become laboratories for discrete geometry.

11.5.2 Quantum Simulation of Lattice Dynamics

Ultracold atoms in optical lattices already realise tight-binding Hamiltonians of the type discussed in Chapter 9. These systems naturally implement nearest-neighbour hopping with tunable coupling strength, interaction terms, and external potentials. Extending such platforms to include synthetic gauge fields, long-range interactions, or engineered anisotropies opens the possibility of simulating more complex puncture dynamics.

In particular, discrete curvature couplings inspired by Regge calculus could, in principle, be emulated in carefully designed optical lattice geometries. While a full tensorial simulation of linearised gravity remains ambitious, analogue graviton-like excitations—collective modes with tensorial structure—may become experimentally accessible. This would provide a rare opportunity to probe discrete geometric dynamics in a controlled tabletop setting.

11.5.3 Multiphysics Metamaterials

One of the most practical implications of the IPW framework is its demonstration that acoustic, elastic, electromagnetic, and even quantum matter waves share an identical discrete dynamical skeleton. The distinction lies only in the nature of the puncture variable and coupling coefficients.

This insight invites the design of multifunctional metamaterials capable of manipulating several wave types simultaneously. For example, a structured medium could be engineered to exhibit aligned band gaps for acoustic and elastic waves while simultaneously guiding electromagnetic radiation. Extending this concept further, hybrid platforms might couple photonic and phononic modes within a single puncture lattice, enabling cross-domain energy transfer or enhanced sensing.

Such multiphysics metamaterials would not merely be technological achievements; they would constitute direct physical realisations of the unified IPW architecture.

11.5.4 Precision Tests of Lorentz Invariance

Any finite lattice spacing introduces a microscopic length scale and, generically, a preferred frame. Even if rotational symmetry is approximately restored at long wavelengths, subtle anisotropic dispersion can remain at high frequencies. Precision tests of Lorentz invariance therefore provide indirect probes of an effective puncture scale.

Resonant cavity experiments, Michelson–Morley and Kennedy–Thorndike–type tests, and astrophysical observations of photon propagation place stringent bounds on anisotropic dispersion in the electromagnetic sector. Within the IPW framework, these bounds translate into upper limits on the effective lattice spacing a. Comparing such limits across different wave sectors—electromagnetic, gravitational, or even condensed-matter analogues—offers a powerful internal consistency check of the unified picture.

11.5.5 Towards a Quantum Gravity Phenomenology

If the puncture spacing corresponds to a truly fundamental scale—potentially near the Planck length—direct detection is unlikely. However, cumulative propagation effects may leave observable signatures. For instance, small deviations in dispersion could produce energy-dependent arrival times for photons from gamma-ray bursts, stochastic phase fluctuations in gravitational waves, or measurable decoherence in pulsar timing arrays.

The IPW framework supplies explicit modified dispersion relations that can be inserted into such analyses. Rather than treating each messenger—photons, gravitons, matter waves—independently, the theory provides a unified phenomenological parameter: the effective puncture spacing a. This allows observational constraints from different astrophysical channels to be compared within a single mathematical model.

11.5.6 Software and Computational Infrastructure

Finally, the structural universality of the IPW update rule suggests a practical step forward: the development of a shared open-source simulation infrastructure. Because all linear wave families reduce to the same discrete evolution scheme (with different puncture variables and coupling constants), a unified computational library could serve acousticians, photonic engineers, seismologists, and quantum physicists alike.

Such a platform would accelerate cross-disciplinary collaboration and enable systematic exploration of parameter space. Importantly, it would also provide a standardised environment for testing experimental proposals aimed at detecting finite-a effects. By lowering computational barriers, the software ecosystem would transform the IPW framework from a conceptual unifier into an operational research tool.

11.6 Key Take-aways

Concept	Experimental implication
Cosine-based dispersion	Look for curvature of $\omega(k)$ near the Brillouin-zone edge; the curvature coefficient directly yields the effective lattice spacing a.
Shock regularisation	Minimum observable shock thickness proportional to a; can be probed in engineered media (micro-structured gases, photonic crystals).
Band-gap formation	Presence of stop bands at frequencies where $\omega(k)$ becomes imaginary; measurable in phononic, photonic, or elastic metamaterials.
Universal scaling	All wave families share the same $(ka)^2$ correction; cross-checking results from acoustics, optics, and mechanics strengthens the evidence.
Upper bounds on a	High-precision dispersion measurements currently constrain a to be **much smaller than the smallest engineered lattice** (sub-nanometre) in the electromagnetic sector; analogous bounds can be inferred for acoustic and elastic waves.
Analogue gravity	Coupled pendulum or optical-loop arrays can emulate a finite-a cutoff for "gravitational" waves, providing a pedagogical demonstration of the concept.

11.7 Final Perspective

The Infinitesimally Punctured Wave framework proposes that the diverse family of classical and quantum wave phenomena can be understood as manifestations of a single discrete dynamical paradigm. By varying only the nature of the puncture variable—scalar, vector, tensor, or complex—and the symmetry-constrained coupling constants, one recovers the governing equations of acoustics, elasticity, electromagnetism, gravity, and quantum mechanics in the continuum limit.

Whether the puncture spacing $a$corresponds to a fundamental scale of nature or serves as an effective modelling parameter depends on physical context.

If a is indeed of Planckian order, direct detection would lie far beyond present experimental reach. Nevertheless, the framework remains empirically meaningful: engineered systems allow the construction of effective puncture lattices many orders of magnitude larger than any hypothetical fundamental scale. These systems provide controlled environments in which discrete wave dynamics can be studied directly.

Exploration of such effective lattices enables several concrete advances. First, it allows validation of the universal lattice dispersion relation across different wave sectors, testing whether the predicted $(ka)^2$-type corrections appear consistently in acoustic, elastic, electromagnetic, and quantum analogues. Second, it makes possible direct observation of shock-width regularisation and Brillouin-zone band-gap formation—phenomena that arise inevitably from finite lattice spacing. Third, it supports the design of multiphysics metamaterials that exploit the shared mathematical backbone of all wave families, enabling coordinated manipulation of sound, light, and mechanical vibrations within a single structured medium. Finally, it provides a coherent phenomenological framework within which to constrain any theory proposing a granular spacetime structure.

Looking forward, progress will likely emerge along three complementary fronts. Precision metrology—using optical cavities, microwave resonators, and high-frequency acoustic systems—can place increasingly stringent bounds on anomalous dispersion. Quantum simulation platforms, including optical lattices and superconducting qubit arrays, offer programmable discrete substrates in which puncture-like dynamics can be engineered and observed directly. Large-scale analogue experiments, from seismic monitoring networks to tabletop gravitational analogues, extend the accessible baseline over which cumulative discrete effects might manifest.

As fabrication techniques reach ever smaller length scales and measurement technologies approach ever higher frequencies, the separation between continuum modelling and discrete microstructure continues to narrow. Whether the ultimate outcome is detection of a fundamental puncture scale or the establishment of increasingly tight upper bounds, the investigation itself sharpens our understanding of wave physics at its deepest level. In this sense, the IPW framework does not claim to provide a final theory. Rather, it offers a unifying structure—conceptually economical and experimentally testable—that links continuum equations to discrete dynamics across all known wave phenomena.

CONCLUSION

A Unified Vision of Waves Through Infinitesimal Punctures

Across the ten chapters of this volume we have traced a single, remarkably simple idea to its most far-reaching consequences: **every wave—acoustic, elastic, electromagnetic, gravitational, quantum, or hybrid—can be regarded as the emergent, long-wavelength limit of an ultra-dense lattice of infinitesimal "punctures."**

- **Chapters 1–2** laid the conceptual groundwork, showing how a discrete network of point-like degrees of freedom, linked by linear (or weakly non-linear) springs, reproduces the familiar continuum partial-differential equations when the lattice spacing a tends to zero. The mathematics is elementary—finite-difference Laplacians, discrete curls, Regge-type hinge angles—yet the resulting continuum limits are the celebrated wave, Navier–Cauchy, Maxwell, and linearised Einstein equations.
- **Chapters 3–5** applied the generic formalism to concrete families of classical waves. Acoustic and surface-gravity waves emerged from scalar pressure and elevation punctures; elastic P- and S-waves followed from vector displacement punctures with Lamé-parameter springs; seismic propagation, shock regularisation, and attenuation arose naturally when the spring constants were allowed to fluctuate randomly. In each case the **Rankine–Hugoniot jump conditions**, **dispersion relations**, and **mode-conversion rules** appeared automatically as consequences of the underlying lattice dynamics.
- **Chapter 6** demonstrated that a modest non-linear term in the spring law regularises shock fronts, replacing the mathematical discontinuity with a smooth tanh profile whose width is set by the puncture spacing. This provides a physically transparent resolution of the classic paradox of infinitely thin discontinuities.

- **Chapter 7** showed that the staggered Yee-type arrangement of electric and magnetic dipole punctures reproduces Maxwell's curl equations, and that the speed of light follows directly from the product $\varepsilon_0\mu_0$ of the electric and magnetic puncture stiffnesses. Metamaterial designs become a matter of engineering spatial variations of those stiffnesses.
- **Chapter 8** lifted the construction to spacetime itself. By assigning a symmetric-tensor metric perturbation to each vertex of a four-dimensional Regge lattice, the linearised Einstein wave equation emerged, and the familiar transverse-traceless polarisations appeared as collective oscillations of the tensor punctures. If the spacing is identified with the Planck length, the lattice furnishes a natural ultraviolet regulator for quantum-gravity considerations.
- **Chapter 9** recast the Schrödinger equation as a tight-binding model of complex scalar punctures. The hopping amplitude reproduces the kinetic term, on-site energies encode external potentials, and a cubic on-site interaction yields the Gross–Pitaevskii non-linearity. Measurement is interpreted as a **puncture-selection event**: a strong local coupling to a detector collapses the wavefunction onto a single puncture, reproducing the Born rule without invoking an extraneous projection postulate.
- **Chapter 10** distilled the common structure of all these examples into a single discrete evolution equation, highlighted the symmetry principles (translation, rotation, gauge, diffeomorphism, U(1) phase) that dictate the form of the coupling tensors, and presented a universal dispersion relation that unifies the various characteristic speeds.
- **Chapter 11** turned the theoretical edifice toward experiment. Whenever the effective lattice spacing is brought into the range of the probing wavelength—by fabricating acoustic, elastic, photonic, or matter-wave metamaterials—observable signatures appear: curvature of the dispersion curve, band-gap formation, minimum shock widths, and frequency-dependent attenuation. These effects provide concrete, testable predictions that can validate (or tightly bound) the puncture-scale hypothesis in laboratory analogues, and they also furnish a phenomenological framework for interpreting high-precision astrophysical observations that might betray Planck-scale departures from perfect Lorentz invariance.

Why the IPW Framework Matters

1. **Conceptual Unity** – It dissolves the historical compartmentalisation of wave physics into separate disciplines. The same lattice skeleton underlies sound, light, seismic tremors, gravitational ripples, and quantum probability amplitudes.
2. **Computational Economy** – A single, modular code base that implements the generic update rule (Eq. 10.1) can simulate any of the wave families simply by swapping in the appropriate puncture variable and coupling tensor. This opens the door to multi-physics simulations that were previously fragmented across disparate software ecosystems.
3. **Design Freedom** – By prescribing spatial maps of the puncture parameters one can engineer bespoke dispersion, anisotropy, non-reciprocity, and topological protection across acoustic, elastic, electromagnetic, and even quantum platforms. The IPW view thus provides a universal language for modern metamaterial science.
4. **Foundational Insight** – The lattice furnishes a concrete, mathematically well-posed regularisation of singularities (point charges, shock fronts, curvature divergences) and offers a tangible model for how a fundamentally discrete spacetime could give rise to the smooth relativistic field theories we observe.
5. **Experimental Accessibility** – Although a true Planck-scale puncture spacing is beyond direct reach, the framework predicts **universal $(ka)^2$ corrections** that can be amplified in engineered nanostructures, photonic crystals, optical lattices, and mechanical resonator arrays. Measuring these corrections would constitute the first empirical foothold on the idea that space-time (and all media) possess an underlying granular architecture.

Looking Forward

The journey begun here invites many extensions:

- **Beyond Linearisation** – Incorporating full non-linear general relativity into a Regge-type puncture network, or exploring strong-field quantum-mechanical dynamics with higher-order hopping terms.

- **Quantum-Gravity Phenomenology** – Embedding the IPW lattice in path-integral or spin-foam formulations to study how puncture-scale discreteness influences vacuum fluctuations, black-hole entropy, or early-Universe cosmology.
- **Hybrid Analogue Experiments** – Building tabletop platforms that simultaneously host acoustic, elastic, and electromagnetic puncture lattices, thereby allowing direct observation of cross-wave mode conversion in a single engineered medium.
- **Machine-Learning Assisted Inverse Design** – Using differentiable simulations of the puncture lattice to discover optimal spatial distributions of K_{nm} that achieve target wave functionalities (perfect lenses, cloaks, topological edge channels).

In closing, the **Infinitesimally Punctured Wave** perspective offers a parsimonious yet powerful lens through which the diversity of wave phenomena can be understood, simulated, and engineered. By recognizing that the continuous fields of our textbooks are merely the macroscopic shadows of an underlying sea of infinitesimal punctures, we gain both a deeper appreciation of the unity of physics and a practical toolkit for shaping waves across the full spectrum of nature.

OPEN PROBLEMS AND RESEARCH DIRECTIONS

The Infinitesimally Punctured Wave (IPW) framework opens a broad and ambitious research landscape spanning theoretical physics, applied mathematics, engineering, and experimental science. What follows is a structured overview of key challenges whose resolution would strengthen the theory's foundations, expand its applicability, and provide decisive experimental tests.

1. Foundational and Theoretical Structure

A central open challenge is the derivation of a fully covariant, background-independent IPW action that recovers Regge calculus in the classical limit and yields a discrete Schrödinger-type dynamics for matter fields. While Chapter 8 develops the linearised gravitational case, a genuine quantum-gravitational formulation remains to be constructed. Promising directions include path integrals over puncture configurations, spin-foam-inspired constructions adapted to the puncture lattice, and possible supersymmetric extensions.

Equally important is a rigorous proof of convergence. The discrete evolution equations must be shown—mathematically—to converge to the corresponding continuum partial differential equations for sufficiently smooth initial data, including nonlinear regimes. Techniques from numerical analysis (consistency and stability implying convergence), Γ-convergence of discrete functionals, and homogenisation theory provide a natural starting point.

Another theoretical frontier concerns the relationship between puncture-induced ultraviolet cutoffs and renormalisation in quantum field theory. It remains to be explored whether the lattice spacing can function as a physically meaningful regulator that renders loop integrals finite without traditional counterterms. Direct computation of simple loop diagrams on the discrete lattice and comparison with Pauli–Villars or dimensional regularisation schemes could clarify this issue.

Finally, extending the puncture lattice to curved manifolds—toroidal, spherical, or more general topologies—would generalise the framework beyond flat space.

Discrete exterior calculus on simplicial complexes and Regge triangulations on curved backgrounds could reveal how curvature modifies dispersion and mode structure.

2. Mathematical Structure of the Discrete Medium

Several problems concern the internal mechanics of the lattice itself.

One is the optimisation of lattice geometry for anisotropic media. For elastic, electromagnetic, or gravitational systems with anisotropic tensors, the choice of lattice (e.g., body-centred cubic versus hexagonal) affects dispersion errors. Spectral analysis of discrete dispersion relations, variational optimisation, and even machine-learning-assisted topology searches may help identify optimal geometries.

Another direction involves systematically extending the coupling beyond nearest neighbours. Higher-order neighbour interactions introduce controlled dispersion, anisotropy, and effective nonlocality. A perturbative expansion of the discrete dispersion relation could classify regimes where such terms dominate, with direct comparison to photonic and phononic crystal experiments.

Thermal fluctuations also require incorporation. Introducing stochastic forces consistent with the fluctuation–dissipation theorem would connect the deterministic IPW framework to realistic environments. Langevin dynamics on the lattice, spectral density calculations, and temperature-dependent attenuation experiments would clarify how puncture noise influences effective quality factors and quantum decoherence.

Finally, the statistical mechanics of large puncture ensembles remains unexplored. Deriving entropy, specific heat, and phase transitions—such as stiff-bond percolation corresponding to melting or glass formation—would bridge microscopic puncture dynamics with macroscopic material behaviour. Monte Carlo sampling and mean-field theory offer natural tools.

3. Nonlinearity and Shock Physics

Chapter 6 introduces shock regularisation through finite puncture spacing, but quantitative scaling laws remain to be derived. In particular, the minimal shock thickness should depend jointly on the lattice spacing $a$and nonlinear coupling coefficients. Asymptotic analysis of travelling-wave solutions, high-resolution simulations in gas dynamics and nonlinear optics, and microstructured shock-tube experiments could establish measurable scaling relations.

Similarly, extending the electromagnetic puncture model to include second- and third-order nonlinearities ($\chi^{(2)}$, $\chi^{(3)}$) would allow investigation of harmonic generation, optical bistability, and soliton formation directly within the lattice formalism. Intensity-dependent permittivity terms and discrete coupled-mode equations provide a concrete starting point.

4. Quantum Measurement and Hybrid Dynamics

The interpretation of quantum measurement as puncture selection requires a detailed dynamical model. A Hamiltonian treatment of detector–puncture interactions should reproduce decoherence, pointer-state formation, and Born-rule probabilities without external collapse postulates. Open quantum system master equations, stochastic Schrödinger formulations, and comparisons with continuous-measurement theory are natural tools.

Hybrid quantum–classical puncture models also merit investigation. Systems where some punctures obey classical dynamics (e.g., elastic) and others quantum dynamics (e.g., matter waves) are relevant to optomechanics and cavity QED. Coupled Hamiltonians combining Poisson brackets and quantum commutators, alongside semiclassical Wigner simulations, could illuminate back-action effects.

5. Metamaterials and Topological Phenomena

The IPW framework suggests a unified methodology for multiphysics metamaterials capable of simultaneously controlling acoustic, elastic, and electromagnetic waves through a single puncture-parameter map. Multi-objective optimisation of lattice parameters and additive manufacturing of hierarchical lattices could realise this vision experimentally.

Breaking coupling symmetry intentionally—so that $K_{nm} \neq K_{mn}$—offers a route to nonreciprocal wave propagation across wave families. Floquet engineering, spatiotemporal modulation of stiffness or permittivity, and topological band theory analysis provide promising directions.

Topological phases themselves can be reformulated within the puncture lattice. Nontrivial winding of coupling phases (via Peierls substitutions or synthetic gauge fields) may yield protected edge states in acoustic, elastic, and photonic systems. Calculation of Berry curvature and Chern numbers from the discrete Bloch Hamiltonian would formalise this connection.

6. Experimental Tests and Bounds

A decisive priority is establishing experimental bounds on the effective puncture spacing. Cross-disciplinary campaigns—ultrafast optics, GHz acoustics, and gravitational analogues—could place quantitative upper limits on a. Precision cavity frequency shifts, Brillouin-zone spectroscopy in photonic crystals, and high-frequency seismic attenuation studies, combined with Bayesian inference, offer concrete methodologies.

Gravitational-wave analogue experiments represent another compelling direction. Mechanical pendulum arrays or optical fibre loops with discrete phase shifters could reproduce Regge-type dispersion and allow direct observation of lattice-induced cutoffs near the Brillouin edge.

A particularly clear experimental test would be demonstration of puncture-induced band-gap tuning. A phononic crystal with temperature-responsive stiffness, mapped via laser Doppler vibrometry before and after heating, could confirm the predicted universal $(ka)^2$ dispersion correction.

Finally, information-theoretic limits imposed by finite spacing deserve study. The lattice dispersion relation constrains mode density and therefore channel capacity. Applying Shannon–Hartley bounds within the Brillouin zone could connect wave physics directly to communication theory.

7. Computational Acceleration

Large-scale lattice simulations are computationally demanding. Machine-learning surrogate models—particularly graph neural networks respecting lattice connectivity—could dramatically accelerate multiphysics design cycles. Physics-informed loss functions enforcing energy conservation and transfer learning across wave families represent promising avenues.

How to Use This Research Agenda

The problems above naturally cluster by emphasis. Foundational theorists may gravitate toward quantum gravity, convergence proofs, and renormalisation. Engineers and materials scientists may focus on metamaterials, nonreciprocity, and band-gap tuning. Computational researchers can contribute through surrogate modelling and large-scale Monte Carlo methods. Several proposals—especially those involving dispersion measurements and analogue gravity setups—are immediately testable with current laboratory capabilities.

SELECTED BIBLIOGRAPHY

I. Mathematical Foundations & Numerical Analysis

[1] Courant, R., Friedrichs, K. O., & Lewy, H. (1928). Über die partiellen Differenzengleichungen der mathematischen Physik. *Mathematische Annalen, 100*, 32–74. https://doi.org/10.1007/BF01448839

[2] Courant, R., & Hilbert, D. (1989). *Methods of mathematical physics*. Wiley-. DOI:10.1002/9783527617210

[3] LeVeque, R. J. (2002). *Finite volume methods for hyperbolic problems*. Cambridge University Press.

[4] https://doi.org/10.1017/CBO9780511791253

[5] Whitham, G. B. (1999). *Linear and nonlinear waves*. Wiley. DOI:10.1002/9781118032954

[6] Shannon, C. E. (1948). A mathematical theory of communication. *Bell System Technical Journal, 27*, 379–423, 623–656. https://doi.org/10.1002/j.1538-7305.1948.tb01338.x

II. Acoustics, Elasticity & Seismology

[7] Achenbach, J. D. (1973). *Wave propagation in elastic solids*. North-Holland.

[8] Aki, K., & Richards, P. G. (2002). *Quantitative seismology* (2nd ed.). University Science Books.

[9] Graff, K. F. (1975). *Wave motion in elastic solids*. Clarendon Press.

[10] Landau, L. D., & Lifshitz, E. M. (1986). *Theory of elasticity* (3rd ed.). Elsevier. Translated from the fourth edition of *Teoria uprogosti "Nauka"*, Moscow, 1986. First published in English by Pergamon Press pic 1959.

[11] Landau, L. D., & Lifshitz, E. M. (1987). *Fluid mechanics* (2nd ed., Vol. 6, Course of theoretical physics; J. B. Sykes & W. H. Reid, Trans.). Pergamon Press.

[12] Morse, P. M., & Ingard, K. U. (1986). *Theoretical acoustics*. Princeton University Press.

[13] Stein, S., & Wysession, M. (1991). *An introduction to seismology, earthquakes, and earth structure*. Wiley-Blackwell.

III. Solid State Physics & Periodic Media

[14] Ashcroft, N. W., & Mermin, N. D. (1976). *Solid state physics*. Saunders College Publishing.

[15] Born, M. Wave Propagation in Periodic Structures. *Nature* 158, 926 (1946). https://doi.org/10.1038/158926a0

[16] Kittel, C. (2004). *Introduction to solid state physics* (8th ed.). Wiley.

[17] Milton, G. W. (2009). *The theory of composites*. Cambridge University Press. https://doi.org/10.1017/CBO9780511613357

IV. Electromagnetism & Photonic Crystals

[18] Griffiths, D. J. (2013). *Introduction to electrodynamics* (4th ed.). Pearson Education.

[19] Joannopoulos, John D., et al. *Photonic Crystals: Molding the Flow of Light - Second Edition*. REV-Revised, 2, Princeton University Press, 2008. *JSTOR*, https://doi.org/10.2307/j.ctvcm4gz9

[20] Engheta, N., & Ziolkowski, R. W. (Eds.). (2006). *Metamaterials: Physics and engineering explorations*. Institute of Electrical and Electronics Engineers. DOI:10.1002/0471784192

[21] Pendry, J. B. (2000). Negative refraction makes a perfect lens. *Physical Review Letters, 85*, 3966–3969. https://doi.org/10.1103/PhysRevLett.85.3966

[22] Smith, D. R., Pendry, J. B., & Wiltshire, M. C. K. (2004). Metamaterials and negative refractive index. *Science, 305*, 788–792. https://doi.org/10.1126/science.1096796

V. Metamaterials & Multiphysics Control

[23] Cummer, S. A., Christensen, J., & Alù, A. (2016). Controlling sound with acoustic metamaterials. *Nature Reviews Materials, 1*, 16001. https://doi.org/10.1038/natrevmats.2016.1

[24] Liu, Z., Zhang, X., Mao, Y., Zhu, Y. Y., Yang, Z., Chan, C. T., & Sheng, P. (2000). Locally resonant sonic materials. *Science, 289*, 1734–1736. https://doi.org/10.1126/science.289.5485.1734

VI. Nonlinear Waves & Solitons

[25] Dauxois, T., & Peyrard, M. (2006). *Physics of solitons*. Cambridge University Press.

VII. Quantum Mechanics & Quantum Field Theory

[26] Born, M. (1926). Zur Quantenmechanik der Stoßvorgänge. *Zeitschrift für Physik, 37*, 863–867. https://doi.org/10.1007/BF01397477

[27] Schrödinger, E. (1926). Quantisierung als Eigenwertproblem. *Annalen der Physik, 79*, 361–376. https://doi.org/10.1002/andp.19263840404

[28] Sterman, G. (1993). *An Introduction to Quantum Field Theory*. Cambridge: Cambridge University Press. https://doi.org/10.1017/CBO9780511622618

[29] Zurek, W. H. (2003). Decoherence, einselection, and the quantum origins of the classical. *Reviews of Modern Physics, 75*, 715–775. https://doi.org/10.1103/RevModPhys.75.715

[30] de Ronde, C. (2020). Measuring quantum superpositions. *arXiv*. https://doi.org/10.48550/arXiv.2007.01146

[31] Beige, A., Bukhari, A., Hodgson, D. J. M., Kanzi, S., & Purdy, R. H. (2025). Enhancing wave–particle duality. *arXiv*. https://doi.org/10.48550/arXiv.2503.20077

VIII. Quantum Simulation & Optical Lattices

[32] Bloch, I., Dalibard, J., & Zwerger, W. (2008). Many-body physics with ultracold gases. *Reviews of Modern Physics, 80*, 885–964. https://doi.org/10.1103/RevModPhys.80.885

[33] Georgescu, I. M., Ashhab, S., & Nori, F. (2014). Quantum simulation. *Reviews of Modern Physics, 86*, 153–185. https://doi.org/10.1103/RevModPhys.86.153

[34] Jaksch, D., & Zoller, P. (2005). The cold atom Hubbard toolbox. *Annals of Physics, 315*, 52–79. https://doi.org/10.1016/j.aop.2004.09.010

IX. General Relativity & Regge Calculus

[35] Einstein, A. (1916). Näherungsweise Integration der Feldgleichungen der Gravitation. *Sitzungsberichte der Königlich Preußischen Akademie der Wissenschaften*, 688–696.

[36] Regge, T. (1961). General relativity without coordinates. *Il Nuovo Cimento, 19*, 558–571. https://doi.org/10.1007/BF02733251

[37] Rovelli, C. (2007). *Quantum gravity*. In *Handbook of the Philosophy of Science*, Editor(s): Jeremy Butterfield, John Earman, North-Holland, https://doi.org/10.1016/B978-044451560-5/50015-4

X. Analogue Gravity & Discrete Spacetime

[38] Barceló, C., Liberati, S., & Visser, M. (2005). Analogue gravity. *Living Reviews in Relativity, 8*(12). https://doi.org/10.12942/lrr-2005-12

[39] Bombelli, L., Lee, J., Meyer, D., & Sorkin, R. D. (1987). Space-time as a causal set. *Physical Review Letters, 59*, 521–524. https://doi.org/10.1103/PhysRevLett.59.521

[40] Sorkin, R. D. (2003). Causal sets: Discrete gravity. https://arxiv.org/abs/gr-qc/0309009

XI. Lorentz Invariance & Precision Tests

[41] Herrmann, S., et al. (2009). Rotating optical cavity experiment testing Lorentz invariance. *Physical Review D, 80*, 105011. https://doi.org/10.1103/PhysRevD.80.105011

[42] Kostelecký, V. A., & Russell, N. (2011). Data tables for Lorentz and CPT violation. *Reviews of Modern Physics, 83*, 11–31. https://doi.org/10.1103/RevModPhys.83.11

[43] Will, C. M. (2014). The confrontation between general relativity and experiment. *Living Reviews in Relativity, 17*, 4. https://doi.org/10.12942/lrr-2014-4

XII. Quantum Gravity Phenomenology

[44] Amelino-Camelia, G. (2010). Doubly-Special Relativity: Facts, Myths and Some Key Open Issues. *Symmetry*, *2*(1), 230-271. https://doi.org/10.3390/sym2010230

[45] Jacobson, T., Liberati, S., & Mattingly, D. (2006). Lorentz violation at high energy: Concepts, phenomena, and astrophysical constraints. *Annals of Physics, 321*, 150–196. https://doi.org/10.1016/j.aop.2005.06.004

XIII. Neutrosophy & IPW-Related Works

[46] Smarandache, F. (1998). *Neutrosophy: Neutrosophic probability, set, and logic*. American Research Press. https://fs.unm.edu/eBook-Neutrosophics6.pdf

[47] Smarandache, F. (2019). Wave–particle duality as an infinite decimally punctured wave. In *Nidus Idearum* (Vol. 4). https://fs.unm.edu/NidusIdearum4.pdf

[48] Smarandache, F. (2022). Introduction to the n SuperHypergraph – the most general form of graph today. *Neutrosophic Sets and Systems, 48*, 483–485. https://doi.org/10.5281/zenodo.6096894

[49] Smarandache, F. (2026a). The infinitesimally punctured wave: A corpuscular visualization of wave–particle duality. *Neutrosophic Sets and Systems, 97*, 704–708. https://fs.unm.edu/NSS/39Infinitesimally.pdf

[50] Smarandache, F. (2026b). Comparisons of infinitesimally punctured wave with Copenhagen and de Broglie–Bohm interpretations. *Neutrosophic Sets and Systems, 98*, 85–92. https://fs.unm.edu/NSS/6InfinitesimallyPunctured.pdf

INDEX TERMS

A
Acoustic waves
Adiabatic bulk modulus (K)
Anisotropic lattice

B
Band gap (metamaterials)
Brillouin zone

C
Causality (dispersion relations)
Cubic spring law (nonlinear)

D
Deficit angle (Regge calculus)
Discrete curl (electromagnetism)
Discrete Laplacian

E
Effective mass (puncture inertia)
Elastic waves (P-waves and S-waves)

F
Finite-difference time-domain (FDTD)
Fourier analysis (dispersion relations)

G
Gravitational waves (linearised general relativity)

H
Hamiltonian (tight-binding formulation)

I
Impulse response (shock regularisation)

J
Jump conditions (Rankine–Hugoniot)

K
Lamé parameters (λ, μ)

L
Lattice spacing (a)
Linearised Einstein equations

M
Mass density (ρ)
Metamaterial design (puncture parameters)

N
Nonlinear Schrödinger equation (Gross–Pitaevskii form)

O
Operator formalism (discrete Hamiltonian)

P
Phase velocity (dispersion)
Puncture (infinitesimal lattice element)
Puncture selection (measurement mechanism)

Q
Quality factor (Q-factor)

R
Regge calculus (spacetime lattice formulation)

S
Shear modulus (μ)
Shock wave regularisation
Speed of sound (c)

T
Tight-binding model

U
Uniform lattice (cubic structure)

V
Velocity dispersion (group velocity)

W
Wave–particle duality (puncture interpretation)

Z
Zoeppritz equations (mode conversion)

APPENDIX A
ANALYTICAL BACKGROUND FOR INFINITESIMALLY PUNCTURED WAVES

This appendix collects the mathematical tools underlying the constructions presented in the main text. It is designed to be self-contained: readers with an undergraduate background in calculus, linear algebra, and introductory physics can follow the derivations, while specialists will find compact formulations suitable for further developments such as homogenisation theory, renormalisation analysis, or quantum field theoretic extensions.

The material is organised into eight sections corresponding to the core analytical ingredients of the Infinitesimally Punctured Wave (IPW) framework.

A.1 Discrete Differential Operators on Regular Lattices

Consider a simple cubic lattice in d spatial dimensions with spacing a. Lattice sites are indexed by integer vectors

$$\mathbf{n} = (n_1, \dots, n_d),$$

with physical coordinates

$$\mathbf{r}_\mathbf{n} = a\,\mathbf{n}.$$

For a scalar field $\phi_\mathbf{n}$ defined on lattice sites, define forward and backward difference operators in the α-direction:

$$\Delta_\alpha^+ \phi_\mathbf{n} = \frac{\phi_{\mathbf{n}+\hat{e}_\alpha} - \phi_\mathbf{n}}{a}, \Delta_\alpha^- \phi_\mathbf{n} = \frac{\phi_\mathbf{n} - \phi_{\mathbf{n}-\hat{e}_\alpha}}{a},$$

where $\hat{e}_\alpha$ is the unit lattice vector along axis α.

The centered second difference (discrete Laplacian) is

$$\Delta_2 \phi_\mathbf{n} = \sum_{\alpha=1}^{d} \frac{\phi_{\mathbf{n}+\hat{e}_\alpha} - 2\phi_\mathbf{n} + \phi_{\mathbf{n}-\hat{e}_\alpha}}{a^2}.$$

For vector fields $\mathbf{u_n}$, the discrete curl is most naturally formulated on a staggered (Yee-type) grid. Placing components on cell faces, the curl at the cell centre reads

$$(\nabla \times \mathbf{u})^{\alpha}_{\mathbf{n}} = \varepsilon_{\alpha\beta\gamma}\, \Delta^{+}_{\beta} u^{\gamma}_{\mathbf{n}},$$

where $\varepsilon_{\alpha\beta\gamma}$ is the Levi–Civita symbol.

The centered discrete divergence is

$$\left(\nabla \cdot \mathbf{u})_{\mathbf{n}} = \sum_{\alpha=1}^{d} \frac{u^{\alpha}_{\mathbf{n}+\hat{e}_\alpha} - u^{\alpha}_{\mathbf{n}-\hat{e}_\alpha}}{2a}. \right.$$

Up to $\mathcal{O}(a^2)$ truncation errors, the discrete operators satisfy the vector identities

$$\nabla \cdot (\nabla \times \mathbf{u}) = 0, \nabla \times (\nabla f) = 0,$$

ensuring preservation of solenoidal constraints in the electromagnetic IPW model.

A.2 Continuum Limit via Taylor Expansion

Let $\Phi_{\mathbf{n}} = \Phi(\mathbf{r_n})$ be the restriction of a smooth continuum field to lattice sites. Expanding about $\mathbf{r_n}$,

$$\Phi_{\mathbf{n}\pm\hat{e}_\alpha} = \Phi \pm a\ \partial_\alpha \Phi + \frac{a^2}{2}\partial^2_\alpha \Phi \pm \frac{a^3}{6}\partial^3_\alpha \Phi + \frac{a^4}{24}\partial^4_\alpha \Phi + \cdots .$$

Substituting into the discrete Laplacian yields

$$\Delta_2 \Phi_{\mathbf{n}} = \nabla^2 \Phi(\mathbf{r_n}) + \frac{a^2}{12}\nabla^4 \Phi(\mathbf{r_n}) + \mathcal{O}(a^4),$$

where $\nabla^4 = \sum_\alpha \partial^4_\alpha$.

Thus the leading continuum equation is recovered as $a \to 0$, while the a^2 correction generates the characteristic $(ka)^2$ lattice dispersion curvature.

The same expansion applies componentwise for vector and tensor fields.

A.3 Lattice Dispersion Relations

Consider a linear scalar IPW lattice:

$$M\ddot{\phi}_{\mathbf{n}} = Ka^2 \Delta_2 \phi_{\mathbf{n}}.$$

Assume plane-wave solutions

$$\phi_{\mathbf{n}}(t) = \phi_0 e^{i(\mathbf{k}\cdot\mathbf{r}_{\mathbf{n}} - \omega t)}.$$

Using the discrete Laplacian,

$$\Delta_2 \phi_{\mathbf{n}} = \frac{2}{a^2} \sum_{\alpha=1}^{d} [\cos(k_\alpha a) - 1] \phi_{\mathbf{n}}.$$

The exact lattice dispersion relation becomes

$$\omega^2(\mathbf{k}) = \frac{2K}{M} \sum_{\alpha=1}^{d} [1 - \cos(k_\alpha a)].$$

For $|\mathbf{k}|\, a \ll 1$,

$$\omega^2 = c^2 |\mathbf{k}|^2 - \frac{c^2 a^2}{12} |\mathbf{k}|^4 + \mathcal{O}(a^4), c = \sqrt{\frac{K}{M}}.$$

The group velocity is

$$v_g = \frac{\partial \omega}{\partial |\mathbf{k}|} = c\left(1 - \frac{a^2}{6} |\mathbf{k}|^2 + \mathcal{O}(a^4)\right).$$

This universal $(ka)^2$ correction underpins the experimental signatures discussed in Chapter 11.

A.4 Energy Conservation and Hamiltonian Structure

For a linear, lossless IPW lattice, the discrete Hamiltonian is

$$H = \sum_{\mathbf{n}} \left[\frac{1}{2} M \dot{\Phi}_{\mathbf{n}}^2 + \frac{1}{4} \sum_{\mathbf{m} \in N(\mathbf{n})} K_{\mathbf{nm}} (\Phi_{\mathbf{m}} - \Phi_{\mathbf{n}})^2 \right].$$

The factor ¼ avoids double-counting bonds. Differentiating H and using the equations of motion gives $\dot{H} = 0$, confirming exact discrete energy conservation.

In electromagnetism, the Hamiltonian separates into electric and magnetic contributions:

$$H_{\text{EM}} = \frac{1}{2} \sum_{\mathbf{n}} [\varepsilon_0 |\mathbf{p}_{\mathbf{n}}|^2 + \mu_0^{-1} |\mathbf{m}_{\mathbf{n}}|^2].$$

The discrete Maxwell equations correspond precisely to Hamiltonian flow generated by H_{EM}.

A.5 Nonlinear Extensions and Shock Regularisation

With a cubic spring law,

$$F_{\mathbf{nm}} = K\Delta\Phi_{\mathbf{nm}} + K_2(\Delta\Phi_{\mathbf{nm}})^2 + K_3(\Delta\Phi_{\mathbf{nm}})^3,$$

where $\Delta\Phi_{\mathbf{nm}} = \Phi_{\mathbf{m}} - \Phi_{\mathbf{n}}$,

the continuum limit yields a Burgers-type equation:

$$\partial_t\Phi + \alpha\Phi\,\partial_x\Phi = \nu\,\partial_x^2\Phi, \alpha = \frac{K_2a^2}{M}, \nu = \frac{Ka^2}{M}.$$

The travelling shock solution is

$$\Phi(x,t) = \Phi_L + \frac{\Phi_R - \Phi_L}{2}\left[1 + \tanh\left(\frac{x - St}{\delta}\right)\right], \delta = \frac{2\nu}{\alpha(\Phi_R - \Phi_L)}.$$

Thus $\delta \propto a^2$, demonstrating finite-width shock regularisation.

A.6 Regge Calculus Primer

In Regge calculus, spacetime is discretised into simplices. Associate a symmetric perturbation $h_{\mu\nu}^{(\mathbf{n})}$ with each vertex.

The deficit angle at a hinge is

$$\Theta_{\mu\nu}^{(\mathbf{n})} = 2\pi - \sum_{\text{incident dihedrals}} \phi_{\mu\nu}^{(\mathbf{n})}.$$

Linearisation yields

$$\Theta_{\mu\nu} \approx a^2\left(\partial_\mu\,\partial_\nu h_a{}^a - \partial_\alpha\,\partial^\alpha h_{\mu\nu}\right).$$

The Regge action

$$S_{\text{Regge}} = \frac{1}{16\pi G}\sum_{\mathbf{n},\mu<\nu} \Theta_{\mu\nu}^{(\mathbf{n})}\,A_{\mu\nu}^{(\mathbf{n})}$$

reduces in the continuum limit to the linearised Einstein operator.

A.7 Statistical Treatment of Disorder

For random puncture parameters, the ensemble-averaged Green's function satisfies

$$\langle G\rangle = G_0 + G_0\Sigma\langle G\rangle.$$

In the Born approximation,

$$\Sigma(\mathbf{k},\omega) \approx \frac{\langle |\, \delta K(\mathbf{q})\, |^2 \rangle}{M^2} \frac{1}{\omega^2 - \Omega^2(\mathbf{k}-\mathbf{q}) + i0^+}.$$

The attenuation coefficient is

$$\alpha(\omega) = \frac{1}{2 v_g(\omega)} \operatorname{Im}\, \Sigma.$$

Identifying $\alpha = \pi f/(Qv)$ gives the quality factor $Q(\omega)$.

A.8 Numerical Stability and the CFL Condition

For explicit integration of

$$M \ddot{\Phi}_{\mathbf{n}} = K a^2 \Delta_2 \Phi_{\mathbf{n}},$$

the CFL stability bound is

$$\Delta t \le \frac{a}{c\sqrt{d}}, c = \sqrt{\frac{K}{M}}.$$

The factor $\sqrt{d}$ arises from the maximum eigenvalue of the discrete Laplacian.

For nonlinear systems, the effective wave speed may increase locally. In practice, one monitors the maximum characteristic speed and adapts Δt accordingly.

APPENDIX B
EXERCISES & THOUGHT EXPERIMENTS

This appendix provides analytical exercises, computational tasks, and conceptual thought experiments designed to deepen understanding of the Infinitesimally Punctured Wave (IPW) framework. The problems range from direct derivations to open-ended explorations suitable for research projects.

Readers are encouraged to attempt analytical problems symbolically before resorting to numerical simulation.

B.1 Discrete–Continuum Correspondence

Exercise 1 – Taylor Expansion of the Discrete Laplacian

Starting from the definition of the discrete Laplacian on a cubic lattice, perform a Taylor expansion to order a^4 and explicitly derive the $a^2\nabla^4$ correction term.

Question: How does this correction modify the dispersion relation at high wavenumber?

Exercise 2 – Anisotropic Lattice

Consider a rectangular lattice with spacings $a_x \neq a_y \neq a_z$.

1. Derive the modified discrete Laplacian.
2. Compute the dispersion relation.
3. Determine under what conditions the long-wavelength limit becomes isotropic.

B.2 Lattice Dispersion and Group Velocity

Exercise 3 – Exact Brillouin Zone Edge

Using the exact dispersion relation

$$\omega^2(\mathbf{k}) = \frac{2K}{M}\sum_{\alpha}[1 - \cos(k_\alpha a)],$$

compute:

1. The maximum attainable frequency.
2. The group velocity near the Brillouin zone boundary.
3. The physical interpretation of vanishing group velocity at the zone edge.

Thought Experiment – High-Frequency Signal Transmission

Suppose you design a metamaterial with lattice spacing $a = 1$mm and launch acoustic waves at wavelengths comparable to $2a$.

What qualitative distortions would you expect?
How would these distortions differ from viscous attenuation?

B.3 Energy and Hamiltonian Structure

Exercise 4 – Discrete Energy Conservation

Starting from the discrete Hamiltonian

$$H = \sum_n \left[\frac{1}{2} M \dot{\Phi}_n^2 + \frac{1}{4} \sum_{m \in N(n)} K_{nm} (\Phi_m - \Phi_n)^2 \right],$$

show explicitly that $\dot{H} = 0$using the equations of motion.

Exercise 5 – Nonlinear Energy

Extend the Hamiltonian to include a cubic spring term.

Derive the modified conserved energy and identify the additional nonlinear potential term.

B.4 Shock Regularisation

Exercise 6 – Shock Width Scaling

Starting from the Burgers-type equation derived in Appendix A, show that the shock thickness satisfies $\delta \propto a^2$.

Question: What happens to δif the quadratic nonlinearity is removed?

Thought Experiment – Microscopic View of a Shock

Imagine placing a microscopic probe capable of resolving individual punctures inside a propagating shock.

Would it observe a discontinuity?

How would the measurement depend on probe resolution relative to a?

B.5 Electromagnetic Punctures

Exercise 7 – Discrete Curl Identities

Verify numerically (or analytically) that

$$\nabla \cdot (\nabla \times \mathbf{u}) = 0$$

holds on the staggered lattice up to truncation error.

Exercise 8 – CFL Stability Bound

Derive the Courant stability condition for the 3D electromagnetic puncture lattice and explain why the factor $\sqrt{3}$ appears.

B.6 Quantum Punctures

Exercise 9 – Discrete Schrödinger Dispersion

Derive the exact dispersion relation for the tight-binding Hamiltonian

$$E(\mathbf{k}) = 2J \sum_{\alpha} [1 - \cos(k_\alpha a)].$$

Show that for $ka \ll 1$ this reduces to

$$E = \frac{\hbar^2 k^2}{2m}.$$

Exercise 10 – Norm Conservation

Using the leapfrog scheme provided in Chapter 9, prove that the discrete L^2 norm is conserved up to second-order truncation error.

Thought Experiment – Measurement as Puncture Selection

Consider a detector that couples to a single lattice site χ_n.

If the wavefunction is delocalised over many sites, how does the probability of detection scale with lattice spacing?

How does the continuum Born rule emerge?

B.7 Gravitational Punctures

Exercise 11 – Linearised Regge Operator

Starting from the linearised deficit angle expression, show that the continuum limit yields the wave operator acting on $h_{\mu\nu}$.

Thought Experiment – Detecting Lattice Spacetime

Assume a fundamental puncture spacing at the Planck scale.

1. Estimate the cumulative phase shift for a photon travelling one gigaparsec.
2. Would such a shift be detectable with current interferometry?

B.8 Disorder and Attenuation

Exercise 12 – Born Approximation

Starting from the Dyson equation, derive the expression for the attenuation coefficient in the weak-disorder limit.

Thought Experiment – Correlated Disorder

How would the attenuation spectrum change if the stiffness fluctuations had a finite correlation length ξ?

Would long-wavelength waves be more or less sensitive to such correlations?

B.9 Research-Level Explorations

These problems are intentionally open-ended and suitable for graduate projects:

1. Design a multiphysics metamaterial whose acoustic and electromagnetic band gaps coincide.
2. Construct a discrete model exhibiting topologically protected edge states within the IPW framework.
3. Explore whether a renormalisation-group flow can be defined directly on the puncture lattice.
4. Investigate whether nonlinear gravitational punctures admit soliton-like solutions.

The exercises above are not merely technical drills; they are intended to illuminate how a single discrete dynamical structure can generate the full diversity of wave phenomena. The IPW framework invites readers to move fluidly between analysis, simulation, and conceptual reasoning — from microscopic punctures to macroscopic waves.

INFINITESIMAL PUNCTURES series

Foundational books:

1 INFINITESIMALLY PUNCTURED GEOMETRY

2 INFINITESIMALLY PUNCTURED PHYSICS

3 INFINITESIMALLY PUNCTURED STRUCTURES

Companion books:

4 INFINITESIMALLY PUNCTURED PHYSICS
USED IN EXTENDED NONSTANDARD ANALYSIS

5 INFINITESIMALLY PUNCTURED WAVES

ISBN 978-1-59973-870-3

For more than a century, singularities and ultraviolet divergences have stood at the frontiers of modern theoretical physics, marking points where our most successful theories cease to be mathematically well defined.

Infinitesimal Punctures proposes a structural shift in perspective: instead of inserting point-like sources into smooth manifolds, matter and physical attributes are interpreted as intrinsic geometric defects—measure-zero punctures—within spacetime itself. In this framework, curvature, charge, and quantum behavior arise not as external additions but as distributionally supported features of geometry.

The Infinitesimally Punctured Wave (IPW), Infinitesimally Punctured Surface (IPSu), Infinitesimally Punctured Space (IPSp), Infinitesimally Punctured Manifold (IPM), and in general Infinitesimally Punctured Quantum Physics (IPQP) were introduced and developed by Florentin Smarandache in 2019 and respectively in 2025-2026.

The 'infinitesimal distance' (which is virtual and theoretical) was later extended by the author to a 'very tiny real distance' (which is practical), allowing a wave to be 'broken' in a real sense at any point.

Waves are among the most fundamental phenomena in nature. From sound in air and light in vacuum to seismic tremors and quantum matter waves, their mathematical descriptions are traditionally expressed through continuum field equations. Yet every measurement of a wave ultimately yields discrete outcomes.

Infinitesimally Punctured Waves proposes a unifying framework in which this apparent tension between continuity and discreteness is resolved at a structural level. The Infinitesimally Punctured Wave (IPW) approach models a wavefield as the macroscopic limit of an ultra-dense lattice of interacting "punctures"—elementary carriers of physical quantities coupled through local dynamical rules. In the limit of vanishing lattice spacing, the familiar partial differential equations of acoustics, elasticity, electromagnetism, gravity, and quantum mechanics emerge. For finite spacing, the same formalism predicts systematic corrections, controlled dispersion, and experimentally testable deviations.